Bird fluxes, flight- and avoidance behaviour of birds in offshore wind farm Luchterduinen

J.J. Leemans
R.S.A. van Bemmelen
R.P. Middelveld
J. Kraal
E.L. Bravo Rebolledo
D. Beuker
K. Kuiper
A. Gyimesi

Bureau Waardenburg
Ecologie & Landschap

Bureau Waardenburg
Ecology & Landscape

Bird fluxes, flight- and avoidance behaviour of birds in offshore wind farm Luchterduinen

J.J. Leemans
R.S.A. van Bemmelen
R.P. Middelveld
J.J. Kraal
E.L. Bravo Rebolledo
D. Beuker
K. Kuiper
A. Gyimesi

Commissioned by: Rijkswaterstaat WVL

1 November 2022
report nr 22-078

Bird fluxes, flight- and avoidance behaviour of birds in offshore wind farm Luchterduinen

J.J. Leemans *MSc.*, dr. R.S.A. van Bemmelen, R.P. Middelveld *MSc.*, J. Kraal *MSc,* E.L. Bravo Rebolledo *MSc.,* D. Beuker, K. Kuiper *MSc.*, dr. A. Gyimesi

Status: final version

Report nr:	22-078
Project nr:	18-0178
Date of publication:	1 November 2022
Photo credits cover page:	D. Beuker & E.L. Bravo Rebolledo
Project manager:	dr. A. Gyimesi
Second reader:	R.C. Fijn, *MSc*.
Name & address client:	Rijkswaterstaat Water, Verkeer en Leefomgeving Lange Kleiweg 34 2288 GK Rijswijk
Reference client:	RWS-2018/20121 zaaknummer 31140364
Signed for publication:	Team Manager Bureau Waardenburg bv R.C. Fijn, *MSc*.
Signature:	

Please cite as: Leemans, J.J., R.S.A. van Bemmelen, R.P. Middelveld, J. Kraal, E.L. Bravo Rebolledo, D. Beuker, K. Kuiper & A. Gyimesi, 2022. Bird fluxes, flight- and avoidance behaviour of birds in offshore wind farm Luchterduinen. Bureau Waardenburg Report 22-078. Bureau Waardenburg, Culemborg.

Keywords: bird radar, wind turbine, macro-avoidance, meso-avoidance, flight height, flight speed, flight intensity, laser range finder, visual observations, North Sea, seabirds

Bureau Waardenburg
Ecology & Landscape

Bureau Waardenburg, Varkensmarkt 9, 4101 CK Culemborg, the Netherlands
0031 (0) 345 512 710, info@waardenburg.eco, https://waardenburg.eco

Preface

The Dutch governmental Wozep (Offshore Wind Ecological Programme) avian research in and around offshore windfarm Luchterduinen (LUD) concentrated on gaining insight in species-specific fluxes, avoidance- and flight behaviour of birds. This main document details measurements of the bird radars from 22 February 2019 – 31 December 2021 and field observations conducted in the wind farm during the same period.

In order to put the measured avoidance rates of northern gannets in perspective and make it readily available for collision risk models in wind farm assessments, we compiled a literature review of studies at the latitude of the Dutch coastline, comprising of Dutch, Belgian and south English wind farms. The resulting memo is enclosed as an appendix to the main report, providing advice on the avoidance rate for northern gannet in wind farms in the southern regions of the North Sea, far from breeding colonies.

Parallel to our study, the Danish Hydraulic Institute (DHI) conducted similar research within the MEP-LUD under the license obligation of Eneco, the owner of Luchterduinen. The results of the two projects are integrated in a separate report to provide better understanding of macro-, meso- and micro-avoidance in Luchterduinen wind farm and how this translates into overall avoidance rates. This report is also appended to the main report.

The work is commissioned by Rijkswaterstaat (RWS). Jos de Visser has coordinated the project with input from Martine Graafland and earlier from Suzanne Lubbe. Together with Sytske van den Akker (formerly Eneco) they also provided useful comments on the setup of the research and arranging permits for the fieldwork. Later, Marin van Regteren from Eneco provided valuable support to arrange the field observations. Joris Diehl (RWS-CIV) and Roelant Snoek (Waterproof) assisted and gave advice around technical issues with the bird radars. Rene Somer, Silvester Heijnen and Meije Kentson (Robin Radar Systems) provided support from the radar manufacturer. The study profited from fruitful discussions with Judy Shamoun-Baranes, Maja Bradaric and Jens van Erp (all University of Amsterdam). The authors also thank all staff members of Eneco and Vestas who helped us during the fieldwork. Aonghais Cook (British Trust for Ornithology), Karen Krijgsveld (Wageningen Environmental Research), Roel May (Norwegian Institute for Nature Research), Jos de Visser and Maarten Platteeuw (both RWS) gave valuable comments on an earlier version of this report.

The fieldwork team from Bureau Waardenburg consisted of Elisa Bravo Rebolledo, Daniel Beuker, Robert Jan Jonkvorst, Jacco Leemans, Koen Kuiper, Rob van Bemmelen, Abel Gyimesi, Mark Collier and Ruben Fijn, whose tremendous efforts made the collection of all the data possible. Data analysis was carried out by Jacco Leemans, Jente Kraal, Rob van Bemmelen and Robert Middelveld. Abel Gyimesi had the overall responsibility as project manager, Ruben Fijn conducted the quality control, while Maarten Japink and Riny van Beurden assisted with the management of the vast amount of radar data. Job de Jong and Paul de Gier dealt with the organization of the data of the field observations. We thank them all for their contribution.

Bureau Waardenburg has a quality assurance system that is certified in accordance with ISO 9001: 2015. In this guideline it is underlined that the quality of our products is ensured in an intern review, carried out by a recognized expert on the subject matter.

Summary

Aim and scope

The main aim of this project was to improve measurements on input parameters of collision risk models. The focus of our project laid on carrying out measurements on the parameters empirical meso- and macro-avoidance and species-specific fluxes. In addition, also measurements on the variables flight height and flight speeds were highlighted as necessary to improve collision risk models. Besides these main research questions, we aimed to bring the understanding further on which factors determine the number, species composition and spatial distribution of birds in and around wind farm Luchterduinen. To answer these research questions radar measurements and visual observation were used.

Species composition

A total of 6,778 individual birds were seen in and around the wind farm of Luchterduinen between the start of the study period in February 2019 and the end of 2021. Of the various bird species in the wind farm, lesser black-backed gulls was the most abundant one, with a total of 1,609 individuals. Other frequently observed seabird species were great cormorant (n = 1,005), black-legged kittiwake (n = 858) and northern gannet (n = 257). A few big groups of starlings led to the large total number of 1,148 individuals and thus starling was the migratory bird species with the highest number of individuals recorded.

General flux patterns

The current report presents the results of nearly three years of radar measurements. From the 22nd of February 2019 to the 31st of December 2021, on average 65 bird targets per km per hour were recorded by the vertical radar in and around wind farm Luchterduinen. Exceptionally high fluxes of more than 500 bird targets per km per hour were recorded in 222 out of 16,209 hours in total (1.4%). The temporal variation in the hourly average number of tracks per km shows a roughly similar pattern each year, with peak fluxes in early spring (*i.e.* late February and March) and autumn (*i.e.* October and November). A (slight) increase in the number of tracks recorded in July can be distinguished in all three years, with a notably large peak at the end of July 2019.

The fluxes in and around wind farm Luchterduinen during the study period seem to be in the range of the ones measured earlier in wind farm OWEZ (Krijgsveld *et al.* 2011). Also, the pattern in fluxes throughout the year (*i.e.* highest fluxes during migration in March and October) and seasonal patterns throughout the day are in line with the pattern in fluxes measured in OWEZ. On the other hand, the number of hours with a mean traffic rate of more than 500 birds per hour seems to be somewhat higher in Luchterduinen than in OWEZ. High numbers of radar tracks in the lowest three altitude meters indicate that the radar database is likely heavily contaminated by wave clutter. However, filtering these completely out would have led to a loss of actual bird tracks. These and all other relevant filter steps we had to apply imply that the unfiltered radar data is not yet directly applicable to produce direct MTR estimates for collision risk models. Our current estimates, however, indicate that the fluxes calculated in the collision risk model of Band (2012) based on observed densities could be an overestimation of reality.

Effect of weather on fluxes

Bird flux at rotor height was higher in autumn than in spring, with both lower or stronger winds and during north(western) winds in spring or with northeastern winds in autumn. This agrees with the expectation that birds preferably migrate with light tailwinds. Wind speed had a particularly strong and consistent effect on bird flux at rotor height, with least flux recorded between approximately 13-15 m/s (6-7 Bft). Less clear relations for the flux at rotor height were found with the time since sunrise and sunset and between day and night.

Flight height

The highest number of bird tracks was measured at altitudes below 5 meters, while another peak is found at the altitude range of 30-40 meters and a smaller one around 120. Above altitudes of 120 meters, the number of detected tracks steadily decreased with altitude. On average 48% of the total flux measured by the radar occurred at the height of the rotor-swept zone. Furthermore, the proportion of tracks above the rotor-swept zone indicated that in the migration periods in spring and autumn a relatively higher proportion of birds pass by at higher altitudes than in the summer and winter.

Furthermore, we determined species-specific flight height distributions based on a combination of visual observations and radar measurements. Based on this combined dataset, most of the birds (39%) were recorded between 25 and 50 meters followed by the height class between 10 and 25 meters (24%) and between 50 and 100 meters (17%). These species-specific flight height distributions are limited to the proportion of birds in certain height bands up to an altitude of 200 m, as we assumed that at altitudes higher than 200 m visual observers cannot provide reliable species compositions. The number of observations for each species was not sufficient to calculate flight height distributions in height bands of 1 meter. This lowers the usability of the presented flight height distributions in the extended Band collision risk model, but the distributions can still be useful in for example the basic Band model height.

Flight speed

Flight speed of different bird species in and around the wind farm is automatically measured by the radar. Here, flight speed refers to the ground speed, which is the speed of a flying bird relative to the ground and is therefore not corrected for wind. The eleven most tagged species were used in this analysis. Results showed higher flight speeds for cormorants (16.49 m/s), Sandwich terns (14.90 m/s) and northern gannets (13.90 m/s), compared to gull species. Interestingly, all gull species showed very similar flight speeds. The most abundant bird species, the lesser black-backed gull, had an average flight speed of 12.25 m/s. Especially for species without available GPS-logger data in the literature, our measurements can provide valuable information for collision risk models.

Nocturnal activity

Carrying out species-specific measurements on the main research question of avoidance behaviour and flux rates is currently impossible during the night. However, we could show that the relative percentage of tracks during day and night shows a clear pattern with an increasing proportion of night-time tracks during spring and autumn peaking in the months March and October, indicating nocturnal migration. Outside these migration periods, in

January, June, July, August and December, more than 63-73% of the tracks were detected during daytime. Using several rough assumptions, these results could suggest that 1) local birds together show a maximum nocturnal activity between 27-37%, and 2) on average roughly 52,000-65,500 birds migrate per km through Luchterduinen in March during the night, while in October this could be 56,000-73,000 birds.

Macro-avoidance

Macro-avoidance was tested using two different methods. First of all, the number of field observations of several bird species inside and outside the wind farm were used to statistically test macro-avoidance per bird species. Of these bird species, great cormorant was observed to be more often inside the wind farm than outside. In contrast, northern gannets, razorbill/guillemot, common guillemot and Sandwich tern were observed significantly more often outside the wind farm than inside, indicating macro-avoidance of the wind farm by these species. Interestingly, no gull species was found to be significantly affected by the wind farm. Macro-avoidance was also estimated by comparing flux between the northwestern (outside the OWF) and southeastern (inside the OWF) beams of the vertical radar. The flux outside and inside the OWF interacted with season, resulting in avoidance of 29% in spring, and apparent attraction in both autumn and winter of 36%. These avoidance rates represent values in a post-construction situation and hence less relevant for collision risk models that conventionally rely on pre-construction measurements on bird numbers upon which macro-avoidance rates are applied.

Meso-avoidance

Horizontal meso-avoidance was estimated by comparing fluxes between line segments in the turbine zone and outside the turbine zones using data from the horizontal radar. In all seasons, flux was ca. 60% lower close to the turbine than further away, indicating meso-avoidance. There were indications of vertical avoidance, but the effects were small and not clear in all seasons. These general meso-avoidance values will be further specified to species level in a future part of the project.

Influence of fishing vessels

We did not detect an increase in bird flux when potential fishing vessels were near the offshore wind farm, but our analysis was greatly impacted by the very large uncertainty in the classification of active fishing vessels. Therefore, this analysis should ideally be repeated using fishing vessel (VMS) data, which can provide a much higher certainty regarding fishing vessel presence and activity.

Table of contents

1 Introduction

1.1 Background

The construction of wind farms in the North Sea has various consequences for seabirds. Research has indicated three main types of effects, namely:

1. Collision mortality: Direct mortality due to birds colliding with turbines and associated infrastructure (Desholm & Kahlert 2005);
2. Displacement and attraction: Displacement of birds resulting in a functional loss of available habitat within the wind farm (Furness *et al.* 2013). Turbines serving as a platform for roosting birds, or the base acting as an artificial reef resulting in increased food availability and thus increased numbers of foraging seabirds is seen as attraction (Dierschke *et al.* 2016);
3. Barrier effects: wind farms may form a physical barrier for birds that alter flight paths when commuting between colonies and foraging areas or during migration (Masden *et al.* 2010).

Determining the species-specific risk of collision between birds and turbines is therefore one of the key issues in the planning processes of offshore wind farms (Brabant & Vanermen 2020; Odinga *et al.* 2021; Potiek *et al.* 2022). Predictions of collision risk have led to projects either being withdrawn from the planning process or being denied planning consent. However, the data on which species-specific collision risk is assessed, is extremely limited and assessments rely on models that can be highly sensitive to assumptions, notably about bird flight- and avoidance behaviour (Cook *et al.* 2018).

However, direct measurements on collision mortality in the marine environment are challenging, as it is almost impossible to collect corpses or conduct long-term observations on collision events at sea. As more detailed information of collision rates is absent, Collision Risk Models (CRM) are used to predict the risk posed by offshore wind farms to seabird populations (Masden & Cook 2016; Brabant & Vanermen 2020; Potiek *et al.* 2022). Different CRMs are available, but at their core most of them calculate the probability of a bird colliding, based on the likelihood of the bird occupying the same space as a turbine blade at the same instant (Masden & Cook 2016). The collision risk of an individual bird is then scaled up, based on the total number of birds of a certain species likely to fly through the rotor-swept area of a wind farm over a given period of time. Before calculating the actual number of predicted casualties, an avoidance rate is applied, which takes into account the proportion of birds likely taking action to avoid a collision (Masden & Cook 2016; for more details see §1.2).

Recent research in the Ecology and Cumulation Framework (KEC (Rijkswaterstaat 2015, 2019)) and the EIAs of various offshore wind farms aimed at delivering estimations on species-specific numbers of collision victims. During these studies, the numbers of collision victims were calculated with the Band model (Band 2012), at that time the most sophisticated model for wind farms at sea (Masden & Cook 2016), and later the stochastic Collision Risk Model (sCRM; Marine Scotland 2018). This latter model is also based on the

Band model but allows more detailed input data to be used, specifically in relation to modelling variability around certain parameters (Marine Scotland 2018). The results of these calculations showed that substantial numbers of collision casualties with offshore wind turbines could be expected among a number of species of seabirds (for example northern gannet, black-legged kittiwake, lesser black-backed gull, great black-backed gull and herring gull) and migratory birds. Some of these species are sensitive to additional mortality on top of their natural mortality, due to their small natural populations, or because the Dutch North Sea forms an important habitat for a significant proportion of their population, or because a large proportion of the flyway-population migrates in concentrated flyways through the North Sea.

However, the outcomes of CRMs are known to be highly sensitive to the assumptions made about the behaviour of the species concerned (Masden 2015). Hence, for species with high expected casualty rates in offshore wind farms, it is important to use the best-available assumptions in collision modelling (Thaxter *et al.* 2018), in order to avoid under- or overestimations of the numbers of casualties. However, data on avoidance behaviour, fluxes, flight speeds and flight altitudes are scarce and could be highly location-specific (Piggott *et al.* 2021). Therefore, more detailed studies in offshore wind farms are required. For this, data collected by specialized bird radars, camera recordings and visual observations are currently the best available methods.

To achieve this goal, RWS has purchased a 3D fixed Robin Radar system, consisting of a horizontal and vertical radar (in short: RWS bird radars). This system was installed in offshore wind farm Luchterduinen in August 2018. Rijkswaterstaat contracted Bureau Waardenburg to carry out analyses of the bird radars and additional field observations to estimate species-specific fluxes, avoidance- and flight behaviour of birds in and around offshore wind farm Luchterduinen.

1.2 Aim and scope

The main aim of this project was to improve measurements on input parameters of collision risk models, such as the Band model (Band 2012). The focus of our project laid on carrying out measurements on the parameters empirical meso- and macro-avoidance and **species-specific fluxes**. We assessed how birds respond to wind farm Luchterduinen at two different scales (figure 1.2.1), based on the same definitions as used in the ORJIP study (Skov *et al.* 2018):

1. **Macro-avoidance**: avoidance of the wind farm as a whole, within an area of 3 km distance from the wind farm up to the rotor-swept zone (and a 10 m buffer around it) of the outermost line of wind turbines;
2. **Meso-avoidance**: anticipatory or impulsive evasion of rows of turbines within the wind farm up to the rotor-swept zone and a 10 m buffer around it.

The last component of avoidance behaviour, *micro-avoidance* (*i.e.* last-second action to avoid collision with the turbine blades within the rotor-swept-zone and a 10 m buffer around it) is not part of the current study and will be measured within the MEP-LUD research conducted by DHI, under the license obligation of Eneco, the owner of Luchterduinen. The two projects will be integrated in a later phase to provide a complete understanding of bird fluxes, number of collisions and macro-, meso- and micro-avoidance in the Luchterduinen wind farm.

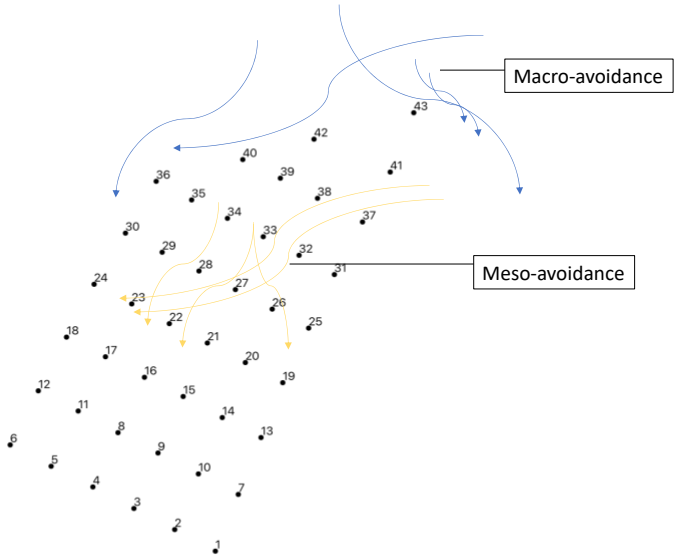

Figure 1.2.1 *Theoretical examples of avoidance behaviour of Luchterduinen. Turbines are indicated by black dots, macro-avoidance as blue arrows and meso as yellow arrows.*

In addition, also measurements on the variables flight height and flight speeds were highlighted as necessary to further improve collision risk models. Besides these main research questions, we aimed to bring the understanding further on which factors determine the number, species composition and spatial distribution of birds in and around wind farm Luchterduinen.

To answer these research questions radar measurements and visual observation were used. Bird radars are capable of simultaneously tracking multiple birds in a relatively large area, which cameras or visual observers cannot achieve. The radar database relied mainly on automatic filtering of the bird radar itself, but also post-processing took place in order to approach actual bird flight intensities. However, radars do not provide species-specific information. Therefore, besides monitoring and analysing the radar data, we also collected species-specific data in Luchterduinen, by carrying out visual observations.

2 Data collection

2.1 Radar measurements

2.1.1 Radar specifications

The RWS bird radars were installed on the railing of WTG42 of offshore wind farm Luchterduinen (figure 2.1.1), at approximately 23 m above mean sea level. The installation was carried out in August 2018 and Robin Radar carried out the calibration in September 2018. Access to the radar images was obtained by Bureau Waardenburg on the 27th of September 2018. The installed bird radars are a so-called Robin 3D Fixed System, consisting of a horizontal Furuno magnetron-based S-band radar and a fixed vertical Furuno magnetron-based pulse X-band radar. The aim of the horizontal radar is to detect and measure the spatial flight patterns and flight speeds of birds, while the aim of the vertical radar is to detect birds and estimate fluxes and flight heights. The horizontal radar radiates in theory 360 degrees round, but in order to protect the wind turbine from radiation damage, a blank sector is created towards the turbine (figure 2.1.2), The blank sector ranges from 275° to 346°, thus in total 71°, *i.e.* 19.4% of the complete circle around the radar.

The vertical radar works in a similar way to the horizontal radar but tilted 90 degrees, resulting in a rotation of the radar in the vertical plane. Emission of the vertical radar is blanked downwards to prevent superfluent clutter (*i.e.* unwanted back-scattered signal), reflection from the water and the turbine components beneath the radar. The vertical beam is rather narrow, and hence the radiation field resembles a 'bow-tie' shape when viewed from above. Radar tracks detected by both the horizontal and vertical radar are combined by the radar software into a 3D track, containing information both on the horizontal position in space and the altitude.

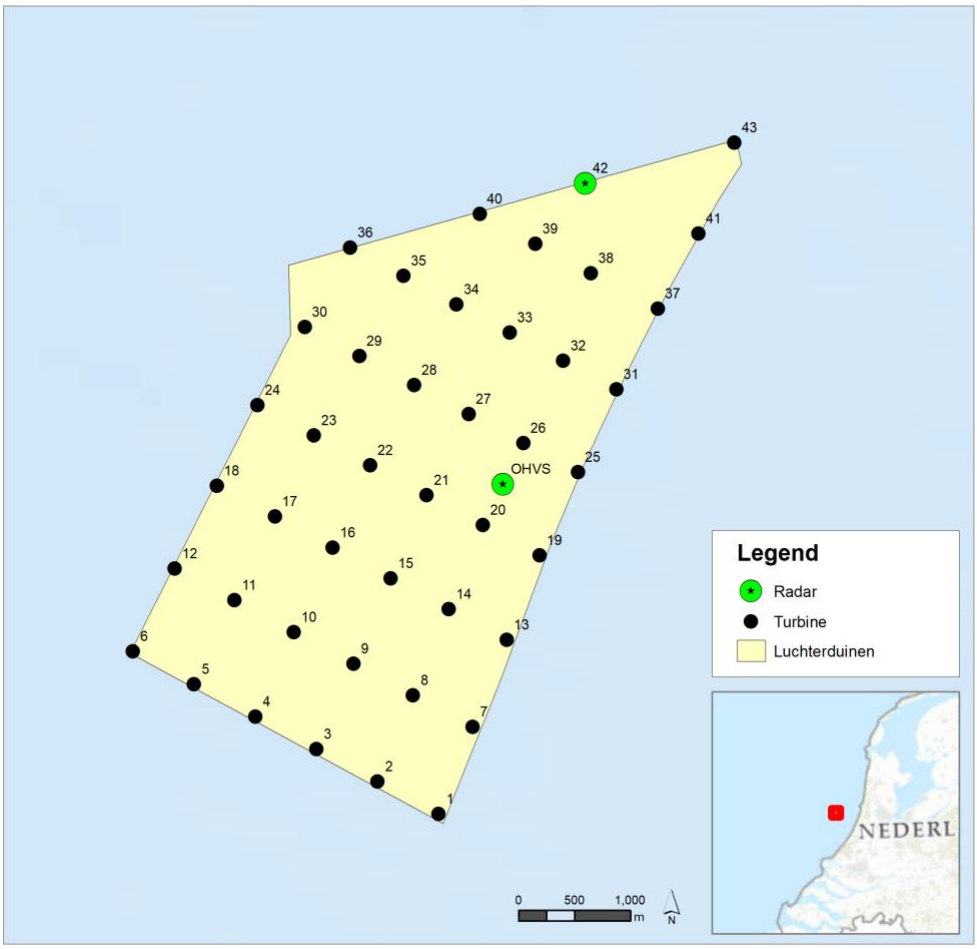

Figure 2.1.1 *Location of the bird radar systems on wind turbine 42 within Luchterduinen. At the OHVS station another radar is located from the DHI-Eneco project.*

2.1.2 Radar validation and software updates

Validation Luchterduinen radars

The scanning range of the horizontal radar was indicated by the manufacturer to be 6 km and that of the vertical radar 1.5 km. The bird radar system in wind farm Luchterduinen was validated during controlled observations in autumn 2018 and spring and summer 2019 from turbines located at 0.7 km, 1.1 km and 1.5 km from the radar (Skov 2019). The validation results regarded the accuracy of flight height measurements made by the vertical radar, false negative bird detections by the horizontal radar, false positive bird detections by the horizontal radar and detection probability of the horizontal radar. For details on these measurements, we refer to the report by Skov (2019), but we summarize the results here below. Based on the results of the validation, in practice the horizontal radar rarely seems to detect bird echoes farther than 5.5 km away and most of the observations occur up to 3-4 km (figure 2.1.2). The altitude range of the vertical radar could not be validated by visual observations. However, based on images of all the detected vertical radar tracks, the radar

seems to readily measure tracks up to approximately 3 km (Gyimesi *et al.* 2020) with a maximum altitude of 5.5 km, thus higher than originally indicated.

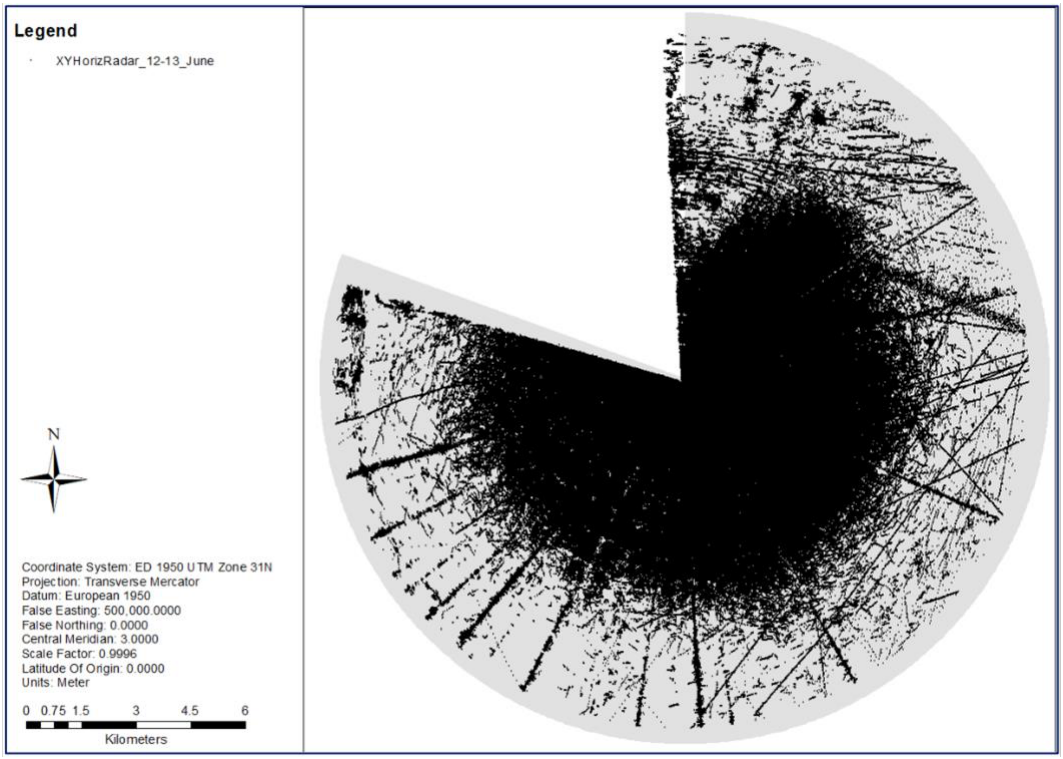

Figure 2.1.2 *Visualisation of the effective horizontal radar range. Plot shows all horizontal radar echoes of 12-13 June 2019. Figure adapted from Skov 2019.*

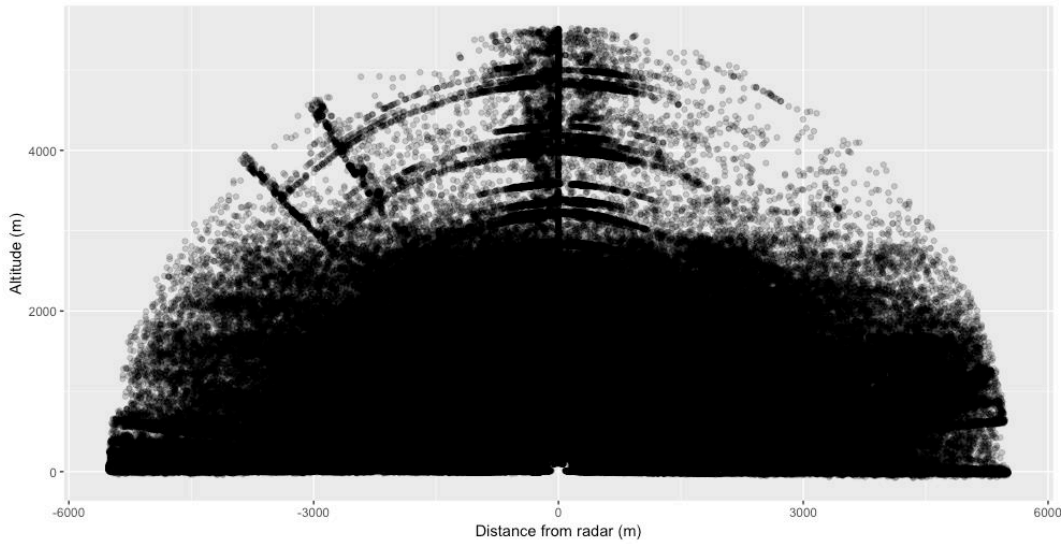

Figure 2.1.3 *Scatterplot of all vertical radar tracks from 21 February 2019 to 30 November 2019. Distance from the radar (in meters) is depicted on the x-axis and altitude on the y-axis (in meters). Negative distances correspond with the vertical radar beam to the northwest and positive values to the southeast. Source: Gyimesi et al. 2020.*

The flight height measurements of the vertical radar were validated by direct comparisons with the height estimates obtained from parallel recordings by a laser rangefinder. With the exception of the great black-backed gull, the correspondence between the radar and rangefinder recordings was reasonable.

The observations to quantify false negative recordings by the horizontal radar revealed that during windy conditions a clearly lower proportion of seabird tracks was recorded by the radar than by visual observers: during calm conditions a false negative rate of 10.83 % was estimated, during moderate conditions the rate increased to 40.00 % and during windy conditions it increased further to 73.17 %.

The mean number of recorded tracks by the radar and by the observers during the validation measurements did not reflect a clear relationship between the number of false positive recordings and wind speed. The false positive detection rates for the horizontal radar showed an overall rate of 31.27%.

Software updates

On the 21st of February 2019, the bird detection software of the Robin Fixed radars in Luchterduinen was updated to version 3.04, with the aim to reduce the amount of clutter (*i.e.* unwanted radar noise) that entered the database. Namely, from the moment of installation of the radars in Luchterduinen until that point, the radars were classifying a large number of wave tracks as birds. Consequently, even in periods with relatively low wave heights (*i.e.* ±75 cm), the database was filled with clutter identified as birds by the radar. After the update, the number of tracks per day was significantly reduced, indicating that the software was more effectively filtering clutter (figure 2.1.4).

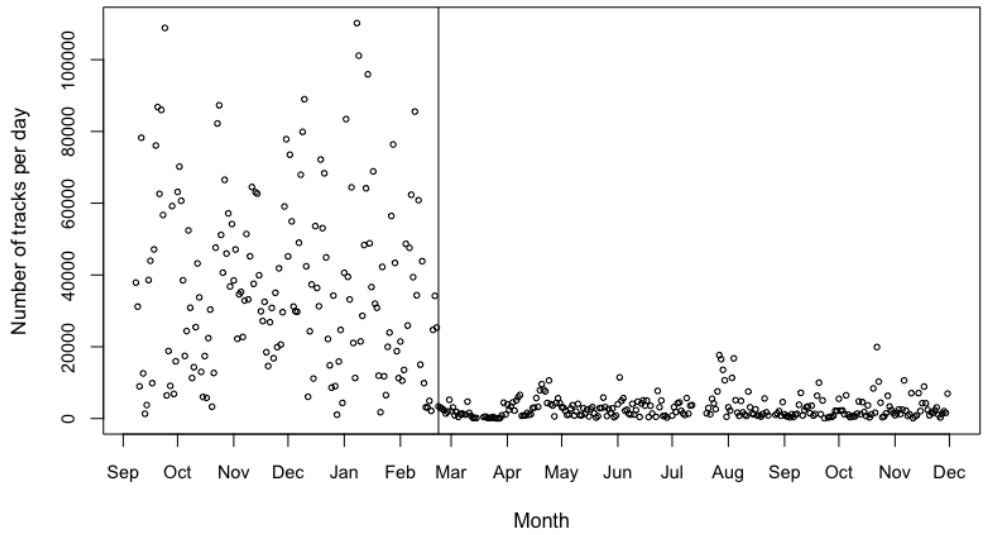

Figure 2.1.4 *Number of tracks registered by the radars per day from the 1st of September 2018 until the 30th of November 2019. The vertical line indicates the date on which the radar software was updated.*

This version was implemented until the 22nd of July 2021, when the radar software was updated to version 20.07. In this version the dynamic range configuration was corrected to improve the size estimates of the targets, mainly within 1km from the radar. Also the sea clutter filter was further improved.

Validation of identical radar systems

The radar system in Luchterduinen was not validated again after the software updates, but another, identical system in wind farm Borssele was, in order to evaluate the performance of the radars after the software updates. The results of this latter radar validation showed that the false negative rate of the radars was after the software update comparable to the false negative rate before the software update. Patterns in the detection of the horizontal radar also strongly suggested that most tracks detected in periods with higher waves are a result of wave clutter. The results of this validation study showed that the number of tracks with negative altitudes was clearly reduced after the software update.

2.1.3 Data filtering

Prior to the analyses of the data collected by the radar, several steps were taken to filter the dataset to prevent as much as possible any non-bird tracks entering the calculations. First of all, the choice was made for this report to exclude data from the period before the 22nd of February 2019, to prevent a large number of wave clutter contaminating the dataset (see §2.1.2). Some of the further filtering steps were only applied to the data of one of the radars, as the two radars differ in their sensitivity for different clutter sources. Namely, the different radar types and the different wavelengths mean that the sensitivity to clutter induced by waves and precipitation also differs significantly between the two radar types. All filter steps are outlined in this paragraph, where we indicate between brackets to which radar dataset we applied the described steps. For the horizontal radar, most filter steps were in line with van Erp *et al.* (2021), who examined the same (horizontal) dataset in their paper. Due to time limitations, we decided not to apply the step of filtering all tracks with an airspeed <5 m/s, as done by van Erp *et al.* (2021), as this would require substantial effort while affecting just a small proportion of all tracks.

Rain showers (vertical radar)

During monitoring of the radar performance, it became obvious that in certain periods the vertical radar still registered rain as bird targets. During these periods, rain showers introduced large amounts of clutter into the database in short periods of time (figure 2.1.5). Possibly, these rain showers developed too fast to activate the dynamic radar filters on time. If so, the radar usually classified these showers as bird flocks and small birds. The large number of tracks in the database created by rain showers could severely distort the flux calculations. Therefore, we filtered out all hours of which we had any indication that it could be raining in Luchterduinen.

For this purpose, we used data from the radar database that indicate the percentage of each radar image where rain filtering was active. We determined per minute how many radar images were more than 5% affected by the rain filter. If this threshold applied to more than half of the radar images in a minute, then this minute was marked as a ‘rain minute’.

If one hour consisted of more than 9 ‘rain minutes’, then this hour was marked as ‘rain hour’. Subsequently, all ‘rain hours’ were filtered out from the dataset. On top of that, we applied an additional rain filtering based on measurements of the Royal Netherlands Meteorological Institute (KNMI) done at the nearest weather station, which is located near the shore of Zandvoort. If the data from this location indicated any precipitation during an hour, then this hour was also precautionarily removed from the dataset.

After these data were filtered out, a visual control indicated that some hours in the remaining dataset still contained many tracks caused by rain showers. Therefore, we applied additional filtering based on the properties of each track, which are assigned to each track by the radar software. We first identified a sample of hours with rain showers and hours with bird migration by expert judgement through visually inspecting the radar images of those hours. Subsequently, an exploration of the properties of rain showers indicated that such tracks were often assigned the property ‘in blob formation’, which is a property that is assigned by the radar software to targets with multiple reflection centres, assumed to originate from different tracks that are detected at (very) close distance to each other but distinguishable by the tracker of the radar as individual tracks. On the contrary, in hours with intensive bird migration, the property ‘in blob formation’ occurred considerably less often. Therefore, we filtered out all hours in which more than 100 tracks were assigned as ‘in blob formation’ and at least 15% of all tracks during that hour were assigned as such. By carrying out these steps, we could effectively filter out the hours with the most intensive rain showers.

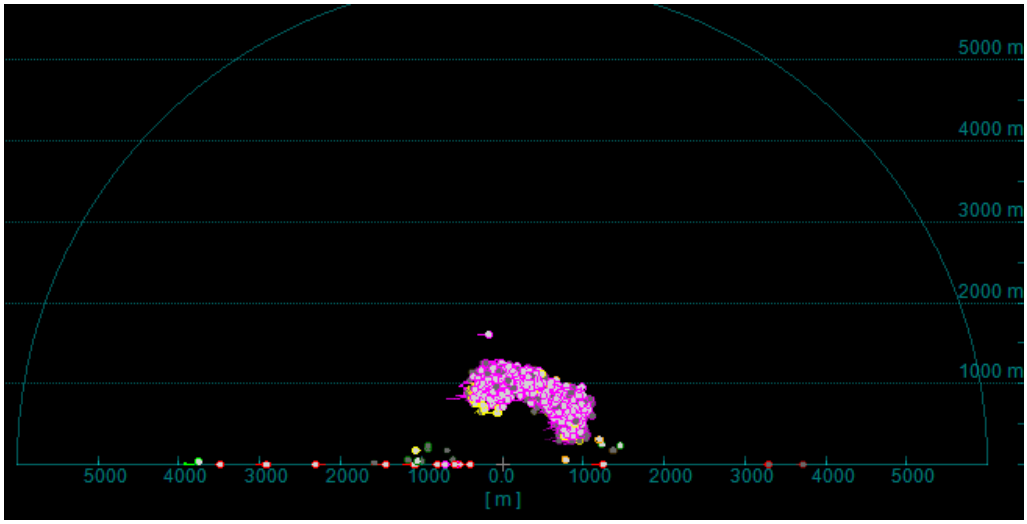

Figure 2.1.5 *Typical example of a rain shower registered by the vertical radar as bird flocks (purple tracks) and small birds (yellow tracks).*

Wave clutter (horizontal radar)

In a similar way to rain, sea clutter may in theory also contaminate the radar dataset with non-bird targets, while at the same time, a high filter activity caused by waves may also hamper the detection of birds (Mateos-Rodriquez 2009). For example, Krijgsveld *et al*. (2011) showed that birds could not be recorded by the bird radar at wave heights more than 1.80 m (corresponding to 3 Bft. wind from the west). Due to their smaller size and corresponding smaller radar signal strength, songbirds are expected to suffer earlier from

being lost in sea clutter than larger birds. Therefore, in order to prevent the calculation of unrealistic bird fluxes due to superfluous filtering or a high number of sea clutter entering the database as birds, we removed all hours with an average 'land mask' filtering above 0.24 (van Erp *et al.* 2021). This value indicates the percentage of each radar image on which filtering is active due to, for example, wave clutter.

For the vertical radar, we found no evidence of a relationship between the number of tracks at low altitudes and wave height. Hence, the decision was made not to determine any wave clutter threshold for the vertical radar data. The vertical radar, however, sometimes registers tracks at negative altitudes, which would mean that birds fly beneath sea level. These negative altitudes occurred nearly always among the so-called combined tracks, *i.e.* tracks that were registered both by the horizontal and vertical radar. These measurements being obviously erroneous, Robin Radar investigated the case and determined that it must have been caused by false reflections, but the issue should only consider tracks with negative altitudes, and tracks with positive altitudes could be trusted. Therefore, we removed all vertical tracks with an average negative altitude from the dataset. This issue of negative altitudes was corrected in a software update in 2021.

Stationary clutter (horizontal radar)
Reflections of the radar beam on stationary objects like wind turbines or ships may induce stationary clutter that could be classified as birds. These clutter tracks have a stationary character, *i.e.* the track moves only a limited distance in a relatively long period. Therefore, we calculated for each track its straight-line displacement over time (*i.e.* distance between start of track and end of track divided by the duration of the track), and subsequently filtered out all tracks within the lowest 0.1% percentile of straight-line displacement over time (van Erp *et al.* 2021)

Classification (both radars)
The radar software classifies each track, based on certain echo characteristics. Tracks could, for example, be classified as small bird, medium bird, or large bird or as a bird flock. Likewise, airplanes or boats detected by the radar enter the database with their own classification. Plausibly, we only considered bird tracks in the calculations.

Periods without radar coverage (both radars)
Alongside all periods that we filtered out of the dataset, the radars in Luchterduinen were not operational during certain periods, for example due to maintenance. The hours in which the radars were (partially) not operational were identified for both radars separately and subsequently filtered out.

Table 2.1.1 provides an overview of the percentage of hours in each month of the study period (after the software update on 21 February 2019) that remained in the database after all filter steps were applied.

Table 2.1.1 *Overview of the percentage of hours in each month of the study period (after the software update on 21 February 2019) that remained in the database after all filter steps were applied.*

	2019		2020		2021	
month	**HR**	**VR**	**HR**	**VR**	**HR**	**VR**
January	-	-	24.1	82.8	25.5	59.1
February	77.4	73.2	9.6	66.5	46.0	79.2
March	21.2	65.1	16.0	68.3	51.2	84.1
April	71.4	83.9	65.0	90.3	44.2	80.0
May	54.0	82.7	32.9	53.0	60.1	56.5
June	51.8	64.7	65.7	84.3	62.5	70.0
July	66.7	82.4	54.7	80.4	54.8	65.1
August	30.1	64.7	64.8	77.3	22.3	50.4
September	31.1	63.1	27.9	14.9	66.0	57.5
October	17.2	55.0	12.8	58.5	14.0	65.2
November	28.6	63.2	29.0	67.9	24.3	51.4
December	23.5	62.3	27.4	60.3	30.1	33.6

2.2 Field observations

2.2.1 Study period

Visual observations in Luchterduinen stretched over a period of almost three years. The first field visit was carried out on the 1st of February 2019 and the final visit was carried out on the 14th of December 2021. Originally, visual observations in Luchterduinen were planned to be carried out twice a month from the beginning of 2019. However, due to Covid regulations in 2020, weather circumstances, and the availability of boats this schedule of twice a month could not be met completely. The final fieldwork schedule, ultimately aiming to collect field data four times in each month is provided in table 2.2.1. Altogether 47 of 48 planned field trips were carried out, the last field day on 14 December 2021 was cancelled upon arrival to the wind farm due to too high waves to enter the wind turbine. Furthermore, two October counts were carried out just outside the month, one on 28 September and one on 1 November.

*Table 2.2.1. Date, weather conditions and turbine location of the visual observations of the study. *) no observations were done this day, as the weather circumstances on-site did not allow to enter the wind turbine.*

Date	Turbine(s)	Wind direction	Wind speed (Bft)	Temperature (°C)
01-02-2019	41	E	3	1
13-02-2019	41	SW	5	6
22-03-2019	42	SW	3	11
29-03-2019	41	SW	0-1	9
03-04-2019	41	S/SW	3-4	8
18-04-2019	41	NE	4	11
02-05-2019	41	W/NW	3-4	10
13-05-2019	41	NE	2	12
22-05-2019	39	W/SW	2-3	14
07-06-2019	41	E	4	14
18-06-2019	33	NW	1-2	16
03-07-2019	41	N	3-4	15
16-07-2019	41	W/NW	2	17
09-08-2019	41	E/SE	5	18
26-08-2019	39, 41	E/NE	2	28
10-09-2019	39	E/NE	1	16
23-09-2019	39	S/SW	4	16
30-10-2019	39	E	4	8
01-11-2019	41	S/SW	4	8
05-11-2019	39	S	3	10
14-11-2019	41	S/SE	5	8
17-12-2019	41	S	4-5	9
18-12-2019	33, 39	S/SW	4	8
21-01-2020	39	SW	3-4	4
22-01-2020	33	N/NE	1-2	5
23-01-2020	41	S/SE	1-2	5
24-01-2020	41	S/SW	3-4	4
06-02-2020	41	W	2-3	7
22-06-2020	41	W	2-3	20
15-07-2020	33	W	2-3	18
23-07-2020	41	SW	5	17
03-08-2020	39	SW	2-3	14
10-09-2020	41	N/NE	1-2	17
16-09-2020	39	N	4-5	19
28-09-2020	41	N	4	15
15-12-2020	33	SW	4	10
26-02-2021	41	NW	3	7
02-03-2021	39	E	3	6
25-03-2021	41	SW	3-4	7
21-04-2021	33	N	5	9
30-04-2021	41	W/NW	3	10
07-05-2021	39	W/NW	4-5	7
14-06-2021	41	W/SW	3	16
03-08-2021	33	NE	2	16
08-10-2021	41	E	2	8
10-11-2021	39	S/SW	3-4	11
24-11-2021	41	S	3-4	8
14-12-2021	*	SW	5	9

2.2.2 Location

The bird radars are installed on wind turbine 42 (WTG42), and hence field observations could potentially be carried out from this turbine. However, these observations come with several disadvantages. First of all, the safe working area outside the radar beams are limited to the northwest quadrant of the turbine, and hence bird observations could not be carried out in all wind directions. In addition, the highest chance of clutter formation in the radar images is in close proximity to the radars. However, at larger distances, the radar measurements suffer from detection loss. Therefore, observations were ideally conducted close to the bird radars, but not from the turbine where the radars were installed.

Hence, most of the observations were carried out from wind turbine 41 (WTG41). This turbine is one of the closest ones to WTG42 and has a clear view on the space around the radars. In addition, being located at the north-eastern edge of the wind farm, WTG41 is suitable for measurements on bird movements both inside and outside the wind farm. Furthermore, WTG41 lies not only in the range of the horizontal radar but is the only turbine directly in the beam of the vertical radar. In addition, wind turbines 39 and 33 (WTG39 and WTG33) were also used to collect measurements on bird movements further inside the wind farm. On two occasions, we carried out observations from two different wind turbines within the same day, to be able to directly compare the differences in species composition within the wind farm. These results of these field days and further comparisons of within wind farm observations were reported earlier in a separate note (Gyimesi 2020).

2.2.3 Field measurements

The general purpose of this project was to obtain data on species composition, fluxes, flight altitudes, flight speeds and macro- and meso avoidance in the Luchterduinen wind farm. Among these general project goals, the visual observations explicitly aimed to measure species composition and flight altitudes by standardized observations and tag as many radar tracks as possible to collect data on species-specific flight speeds, macro- and meso-avoidance. The visual observations did not intend to measure species-specific fluxes. Instead, the project was set up to provide fluxes by the radar and subsequently define species-specific fluxes based on the species composition measured in the field. To do so, observers carried out both visual observations on numbers and species of birds inside and outside the wind farm, as well as tagging of radar tracks to record bird species, number of birds involved and their flight behaviour. If possible, all measurements were carried out with a laser rangefinder (LRF, SAFRAN Vectronix - Vector 21 Aero), but otherwise (*e.g.* high humidity disturbing the LRF measurements) binoculars and telescopes were used. The LRF data can provide accurate recordings of position, angle, height and distance from the radar (Borkenhagen *et al.* 2018). The LRF was calibrated on site and synchronised with the clock of the radar computer. The observation data were directly entered into a field tablet that is connected to the LRF via a Bluetooth connection.

<u>Measuring species composition and flight height</u>

In order to determine species composition and flight height, the observers followed a point count survey methodology, *i.e.* a point-based recording of activity. The field protocol was

designed to collect measurements on the bird species at different altitudes inside and outside the wind farm and on their displayed behaviour.

Observations from WTG41 at the edge of the wind farm were carried out towards inside and outside the wind farm, with each round in a specific direction consisting of 30 minutes of observations. From WTG 33 and WTG 39, only measurements inside the wind farm were carried out. In order to collect data at different distances and flight heights, observations in each direction consisted of three rounds of 10 minutes, during which the horizon was alternately positioned:

1) upper end of the field of view (1/8);
2) halfway of the field of view (1/2);
3) lower end of the field of view (7/8).

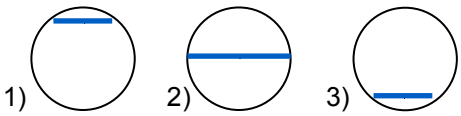

Most importantly, species name, flight altitude and number of individuals were recorded. Registering flight direction and additional information (plumage, age, distance) were secondary. If possible, bird targets were measured by the LRF, providing exact information regarding flight height and distance to the observer, otherwise these parameters were visually estimated.

The priority of these measurements was to collect proper species information and not to register all birds that flew in the scope of the observer. Namely, the estimation of the density of bird movements relied on the radar measurements. During the field measurements, notes were made whether all birds were recorded or only a subsample whenever numbers of birds present were too high to register them all. This latter rarely occurred, as bird densities were in most cases not as high, but if so, very first bird passing by formed the next observation, no selection on size or distance took place, and hence we assume to have collected a representative sample of species composition.

Measuring flight height and -speed

Essentially, the horizontal radar records measurements on flight speed of birds, while the vertical radar also provides information on the flight altitude of birds. However, the radar measurements lack species information, and hence part of the field observations (especially from WTG41 lying in the coverage of the vertical beam) were oriented to couple species information to the tracks measured by the radars. These observations were carried out in rounds of 30 minutes. From WTG41, observations were carried out for 30 minutes towards WTG42 (*i.e.* towards NW) and for 30 minutes long towards SE, both within the beam of the vertical radar. If possible, birds that were coupled to tracks were also measured with the LRF. Data were directly entered into the mobile application of the radar (*i.e.* Visualizer or Mobile Viewer), when necessary annotated by the id of the LRF measurement.

Measurements on macro- and meso-avoidance

Defining species-specific avoidance behaviour relied partly on species composition measured during visual observation inside and outside the wind farm (macro-avoidance), as well as on analysing radar tracks inside and outside the wind farm (macro-avoidance) or entering the wind farm but avoiding individual turbines (meso-avoidance). As the radar measurements lack species information, during field observations time was allocated to

add species information to radar tracks. From WTG41 at the edge of the wind farm, separate observations were oriented towards the wind farm and outside of the wind farm. In addition, observations were also carried out from turbines deeper within the wind farm (see §2.2.2). If possible, observations were done with the LRF, otherwise with binoculars and telescopes. Data were directly entered into the mobile application of the radar (*i.e.* Visualizer or Mobile Viewer), when necessary annotated by the id of the LRF measurement.

Camera measurements

In order to collect more information on species composition and flight height of birds in and around Luchterduinen than by visual observations twice a month, the project intended to make use of a pan-tilt rugged daylight camera being integrated with the RWS bird radar through the MUSE system to record videos of flying birds. The installation of the camera took place in September 2020, but shortly afterwards the camera turned out be broken down. In October 2021 a new, better camera was installed next to the radar. After new problems with the image quality and tests with turning off the radar, the conclusion was drawn that the horizontal radar is interfering with the camera. Therefore, the camera was turned off and is moved to another wind turbine to avoid interference with the radar. However, as this occurred after finalizing the analyses for this report, no camera recordings were currently available to support the visual observations.

3 Species composition

3.1 Methods

3.1.1 Visual observations

In this chapter, data are presented on the species composition that was observed in and around wind farm Luchterduinen during the visual observations that were carried out from February 2019 until the end of 2021. The presence of each species in and around the wind farm was calculated in two different ways, based either on the number of individuals or the number of observations, and expressed per month. As the presence of a few large groups of individuals of a certain species would dominate the species composition on a certain date, and ultimately the species composition of that month, we used the species compositions based on the number of observations per species to calculate species-specific fluxes (§4).

Birds were divided into the categories 'seabirds' and 'migratory birds'. We considered species as seabirds when they use the area to forage, rest or as daily commute between breeding/resting places and foraging areas (such as gulls). In contrast, we considered species as migratory birds when they only visit the study area on their seasonal migration routes in spring and autumn (such as passerines, waders, ducks and geese).

3.1.2 Tagged radar tracks

During field observations, radar tracks were tagged to couple species information to these radar tracks (see §2.2.3 for methods). In paragraph 3.2.2 below we provide an overview of the number of radar tracks that were tagged per species.

3.2 Results

3.2.1 Visual observations

Number of individuals

A total of 6,778 individual birds have been observed in the study period between February 2019 and the end of 2021 (numbers per hour of seabirds in table 3.2.1 and numbers per hour of migratory birds in table 3.2.2). Based on the number of individuals, most birds were present in the area in November, although this is mainly the result of large groups of migrating starlings. For all the other months, seabirds accounted for the majority of the observations (table 3.2.1). Lesser black-backed gull was observed most with a total of 1,609 individuals, followed by 1,148 starlings and 1,005 great cormorants. Other numerous species were the kittiwake (n = 858), northern gannet (n = 257) and great black-backed gull (n = 185). Finally, also common scoters (n = 168) seemed to occur in high numbers but this entails mainly one group consisting of 150 individuals in February 2019.

Local seabirds were seen all year round, but seasonal differences were observed within species. High numbers of species such as lesser black-backed gulls and great cormorants were especially seen in the summer (June-August), contrasting the frequent presence of species such as great black-backed gull, black-legged kittiwake, razorbill and common guillemot in autumn and winter. The highest number of birds observed per hour in one month were 54.8 lesser black-backed gulls per hour in August.

Migratory birds were mostly present in October. Several passerines were seen in March, April, September and November too. Only starlings could temporarily outnumber local seabirds, all other migratory bird numbers were generally low. Geese dominated the view of migratory birds in February, although this was largely affected by large groups of mainly brent and barnacle goose that were observed on the 1st of February in 2019.

Table 3.2.1 *Overview of the numbers of observations of seabirds in the Luchterduinen wind farm per hour and between brackets the number of individuals of seabirds per hour. Visual observations were done from February 2019 until the end of 2021.*

Species	Jan	Feb	Mar	Apr	May	Jun	Jul	Aug	Sep	Oct	Nov	Dec
Arctic skua	0	0	0	0	0	0	0	0	0	0	0.1 (0.1)	0
bl.-b. gull spec.	0	0	0.2 (0.2)	0	0	0	0.1 (0.3)	0	0.8 (0.8)	0	0.1 (0.1)	0
bl.-headed gull	0	0	0.3 (4.6)	0.2 (1.7)	0	0.1 (0.1)	0.3 (0.3)	0.3 (0.5)	1.4 (3.5)	2.6 (4.6)	0	0
bl.-legged kittiwake	2.4 (2.6)	2.3 (3.1)	1.5 (1.7)	0.1 (0.2)	0	0.1 (0.1)	0	0.1 (0.1)	0	15.1 (44.3)	8.7 (10.1)	30.7 (47.3)
common eider	0	0.1 (1.6)	0	0	0	0	0	0	0	0	0.1 (0.1)	0
com. guillemot	0.7 (1.1)	1 (1.3)	0.3 (0.5)	0	0	0	0	0	0.1 (0.1)	1.4 (4.6)	1.7 (2.1)	1.2 (1.2)
common gull	1.3 (1.6)	1.2 (1.3)	0.3 (0.3)	0.6 (0.9)	0.1 (0.1)	0.1 (0.9)	0.2 (0.2)	0.3 (0.3)	1.1 (1.1)	3.4 (3.9)	0.2 (0.2)	3.3 (3.5)
common scoter	0	0.1 (11.1)	0	0.1 (0.1)	0	0.1 (1.5)	0	0.1 (0.1)	0.1 (0.2)	0.1 (0.1)	0	0
common/arctic tern	0	0	0	0	0	0	0	0.1 (0.1)	0	0	0	0
great bl.-b. gull	0.7 (0.7)	0.6 (0.6)	0.6 (0.6)	0.2 (0.2)	0	0.2 (1.6)	0.3 (0.3)	0.1 (0.1)	4.5 (8.1)	3.1 (3.6)	0.6 (0.7)	1.7 (1.8)
great comorant	3.3 (3.6)	1.3 (1.4)	1.5 (2.8)	2.8 (4.5)	1.8 (2.1)	17.6 (31)	10.1 (24.4)	14.1 (23.9)	3.3 (4.2)	2.9 (3.6)	1.4 (1.6)	5.3 (7.8)
great skua	0	0	0	0	0	0	0	0	0	0	0.1 (0.1)	0
gull spec.	0.1 (0.1)	0.4 (0.8)	0.9 (2)	0.1 (0.1)	0	1.5 (2)	0.3 (0.3)	0.5 (0.5)	0.1 (0.3)	1 (1.4)	1.2 (1.2)	5.3 (7.8)
herring gull	1.9 (1.9)	0.6 (0.7)	1.2 (1.2)	0.2 (0.3)	0.3 (0.3)	0.5 (0.5)	0.2 (0.2)	0.1 (0.1)	0.6 (0.6)	0.3 (0.3)	0.4 (0.4)	0.8 (1)
large gull spec.	3 (3.3)	2.1 (2.5)	1.9 (2.3)	7.5 (12.3)	1.4 (1.6)	3.5 (3.8)	7.9 (9.9)	6 (10.4)	3.8 (5.8)	5.6 (8.1)	0.4 (0.5)	0.5 (0.7)
lesser bl.-b. gull	0	1.6 (2.3)	0.8 (0.8)	10.2 (13.5)	2.7 (3.1)	34.5 (47.2)	24 (29.4)	33.6 (54.8)	15.2 (18)	5.9 (6.9)	0.2 (0.2)	0
little gull	0	0	0	0.2 (5.5)	0	0	0	0.8 (0.9)	0	0	0	0
loon spec.	0	0	0	0	0	0	0	0	0	0	0	0.2 (0.5)
northern gannet	3.3 (3.7)	0.9 (1)	0.8 (0.8)	0.6 (0.8)	0.8 (0.9)	0	0.9 (1)	0.5 (0.5)	1.2 (1.2)	8.3 (9.4)	3.9 (4.2)	3 (3.2)
razorbill	0.3 (0.3)	0.1 (0.1)	0.1 (0.6)	0	0	0	0	0	0	2.1 (8.1)	0.8 (1.9)	0.7 (0.7)
razorb./guillemot	0.4 (0.4)	2.4 (3.5)	1.3 (2.6)	0.2 (0.2)	0	0	0	0	0	3.1 (15.7)	3.4 (6.2)	1.8 (2.7)
red-thr. diver	0	0	0	0	0	0	0	0	0	0	0	0.7 (0.7)
sandwich tern	0	0	0.1 (0.1)	0.3 (0.7)	2.6 (4.5)	0	0.2 (0.3)	0.3 (0.3)	0.2 (0.2)	0.1 (0.3)	0	0
sandw./comm. tern	0	0	0	0	0.1 (0.1)	0	0	0	0	0	0	0
small gull spec.	0	0	0.1 (0.1)	0.1 (0.2)	0	0	0.4 (0.4)	0.1 (0.1)	0	0.3 (1.7)	0.2 (0.2)	3 (8.2)
tern spec.	0	0	0	0.3 (0.5)	0	0.1 (0.1)	0	0.1 (0.4)	0.2 (0.5)	0	0	0
tern/gull spec.	0	0	0	0.4 (1.1)	0.1 (0.1)	0	0	0	0	0	0	0

Table 3.2.2 *Overview of the numbers of observations of migratory birds in the Luchterduinen wind farm per hour and between brackets the number of individuals of migratory birds per hour. Visual observations were done from February 2019 until the end of 2021.*

Species	Jan	Feb	Mar	Apr	May	Jun	Jul	Aug	Sep	Oct	Nov	Dec
barn swallow	0	0	0	0	0.1 (0.1)	0.2 (0.2)	0	0	0	0	0	0
barnacle goose	0	0.1 (3.7)	0	0	0	0.1 (0.1)	0	0	0	0	0	0
brent goose	0	0.1 (2.1)	0	0	0	0	0	0	0	0	0	0
Canada goose	0	0	0	0	0	0.1 (2.4)	0	0	0	0	0	0
common kestrel	0	0	0	0	0	0	0.1 (0.1)	0	0	0	0	0
common shelduck	0	0	0	0	0.1 (0.1)	0	0	0	0	0.1 (0.1)	0	0
common swift	0	0	0	0	0	0.5 (1.2)*	0	0	0	0	0	0
duck spec.	0	0	0.1 (0.1)	0	0	0	0	0	0	0.1 (0.1)	0	0
Eurasian skylark	0	0	0	0	0	0	0	0	0	0.1 (0.1)	0	0
gadwall	0	0	0	0	0	0	0	0	0	0.1 (0.3)	0	0
goose spec.	0	0.1 (1.9)	0.1 (0.2)	0	0	0	0	0	0.1 (0.2)	0	0.1 (0.3)	0
grey heron	0	0	0	0	0	0	0	0.3 (0.4)	0.1 (0.2)	0	0	0
greylag goose	0	0	0.1 (0.1)	0	0	0	0	0	0	0	0	0
hooded crow	0	0	0	0	0.1 (0.1)	0	0	0	0	0	0	0
jackdaw	0	0	0	0	0.1 (0.2)	0	0	0	0	0	0	0
large passerine spec.	0	0	0	0	0	0	0	0	0	0.1 (0.3)	0.1 (0.3)	0
meadow pipit	0	0	0	0.1 (0.2)	0	0	0	0	0	0.3 (0.4)	0	0
messenger pigeon	0	0	0	0	0	0	0	0.1 (0.1)	0	0.3 (0.3)	0	0
oystercatcher	0	0	0	0	0	0	0	0.1 (0.4)	0	0	0	0
peregrine	0	0.1 (0.1)	0	0	0	0	0	0	0	0.1 (0.1)	0	0
pigeon spec.	0	0	0	0	0	0	0	0	0	0.1 (0.1)	0	0
pintail	0	0	0	0	0	0	0	0	0	0.1 (0.1)	0	0
small grebe spec.	0	0	0	0	0	0	0	0	0.1 (0.2)	0	0	0
small passerine spec.	0	0	0	0.2 (0.2)	0.2 (0.2)	0	0	0	0.1 (0.7)	1.3 (1.7)	0.1 (0.1)	0
starling	0	0	0.2 (0.5)	0.1 (0.1)	0	0	0	0	0.1 (0.1)	1.9 (31.7)	1.2 (51.1)	0
wader spec.	0	0	0	0	0	0	0	0	0	0.1 (1.4)	0	0
waterbird spec.	0	0	0	0	0	0.1 (2.5)	0	0	0	0	0	0
white wagtail	0	0	0.1 (0.1)	0	0	0	0	0	0	0	0	0

* Possibly birds foraging in (the vicinity of) the wind farm area (c.f. Krijgsveld *et al.* 2011).

Number of observations

Large groups of birds can sometimes dominate the number of birds seen in the area. For instance, a total of 1,138 individual starlings were observed, but merely on 38 occasions. Another species with a high number of individuals in and around the wind farm was common scoter, but these individuals can be attributed to just six observations. In order to have an estimation of the frequency that a certain species occurs in the wind farm area and thus potentially recorded by the radar, we also expressed the observed species composition as the number of observations per species. This approach could correct for the momentary occurrence of a large number of migrating birds, while the rest of the observations considering local birds. This analysis revealed that the lesser black-backed gull was the most observed species (figure 3.2.1 and figure 3.2.2), with 1,199 recordings (30.9%), followed by great cormorants (n = 589; 15.2%), unidentified gulls (n = 574; 14.8%) and black-legged kittiwakes (n = 515, 13.3%). Table 3.2.3 presents the species composition separately for each month.

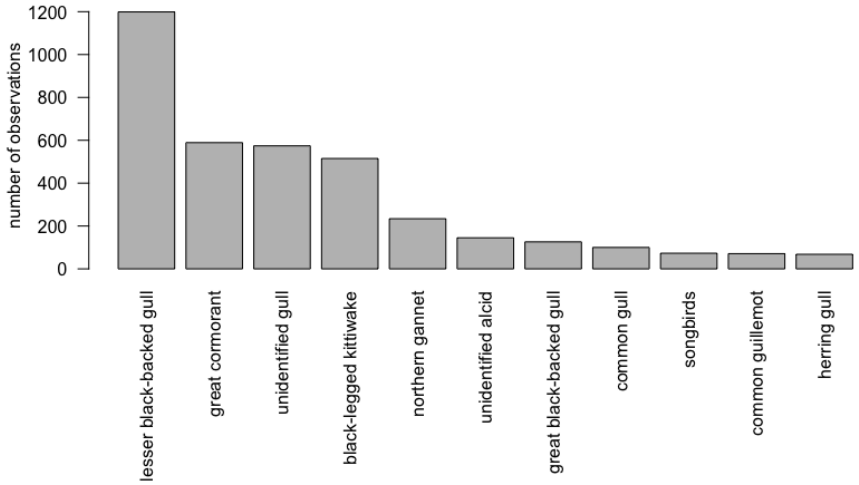

Figure 3.2.1 *Total number of observations per species for the species with at least 50 recordings. Species are ordered based on number of observations.*

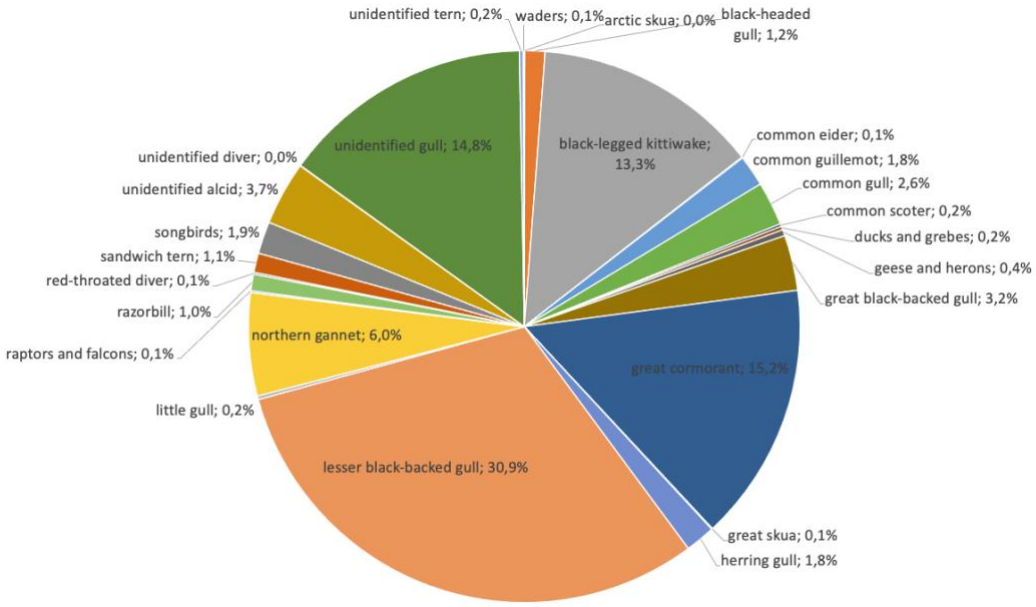

Figure 3.2.2 *Species composition based on the number of observations done during visual observations between February 2019 and the end of 2021.*

Table 3.2.3 *Overview of the monthly species compositions comprising of each species(group) observed in Luchterduinen wind farm.*

species	Jan	Feb	Mar	Apr	May	Jun	Jul	Aug	Sep	Oct	Nov	Dec
arctic skua											<1%	
black-headed gull			2%	1%		<1%	1%	<1%	4%	4%		
bl.-leg. kittiwake	14%	15%	12%	<1%		<1%		<1%		25%	35%	53%
common eider		<1%									<1%	
common guillemot	4%	7%	2%						<1%	2%	7%	2%
common gull	7%	8%	2%	2%	1%	<1%	<1%	<1%	3%	6%	1%	6%
common scoter		<1%		<1%		<1%		<1%	<1%	<1%		
great bl.-b. gull	4%	4%	5%	1%		<1%	1%	<1%	14%	5%	2%	3%
great cormorant	19%	9%	12%	11%	18%	30%	22%	24%	10%	5%	6%	9%
great skua											<1%	
herring gull	11%	4%	9%	1%	3%	1%	<1%	<1%	2%	<1%	2%	1%
lesser bl.-b. gull		11%	7%	42%	26%	58%	53%	58%	46%	10%	1%	
little gull				1%				1%				
northern gannet	19%	6%	7%	2%	8%		2%	1%	4%	14%	16%	5%
razorbill	2%	1%	1%							4%	3%	1%
red-throated diver												1%
Sandwich tern			1%	1%	25%		<1%	<1%	1%	<1%		
unidentified alcid	2%	16%	10%	1%						5%	14%	3%
unidentified diver												<1%
unidentified gull	18%	17%	25%	33%	15%	8%	20%	12%	14%	11%	8%	15%
unidentified tern				1%	1%	<1%		<1%	1%			
ducks/grebes			1%		1%	<1%			<1%	1%		
geese/herons		2%	1%			<1%		<1%	1%		<1%	
raptors/falcons		1%					<1%			<1%		
songbirds			2%	2%	4%	1%		<1%	1%	7%	5%	
waders								<1%		<1%		

3.2.2 Tagging of radar tracks

A total of 1,089 horizontal and vertical radar tracks were identified to species or species-group level (figure 3.2.3). From these, the majority of records (56%) concerned lesser-blacked gulls. Great cormorant represented 16% of the tagged tracks, followed by black-legged kittiwake (5%), common gull and herring gull (4%) and great black-backed gull (3%). Unidentified large gulls (*i.e.* either great black-backed gull, herring gull or lesser black-backed gull) formed 3% of tagged tracks, while 2% concerned black-headed gull and northern gannet, and 1% concerned Sandwich tern and unidentified gulls. Species with fewer than 1% of observations were not included in figure 3.2.3.

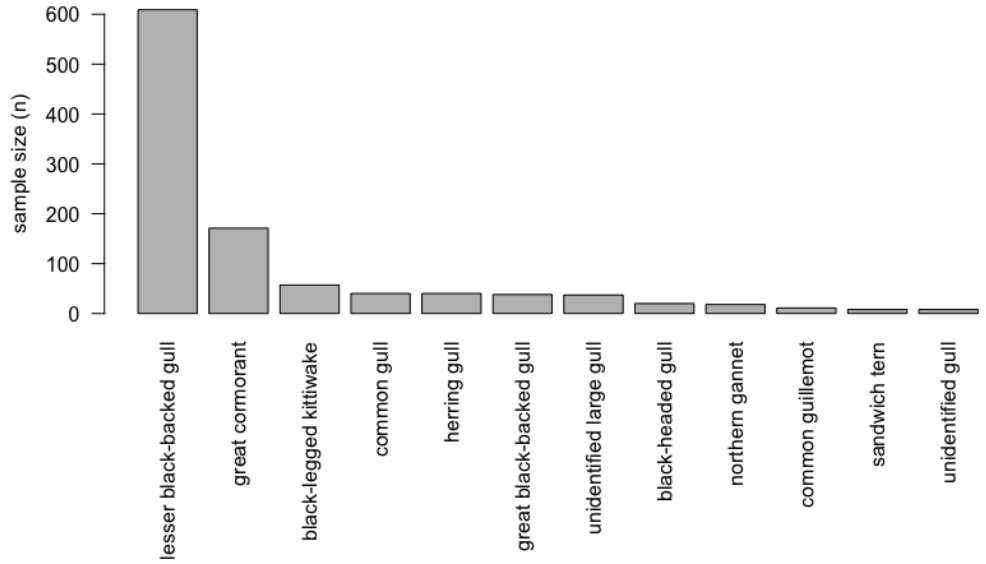

Figure 3.2.3 Number of tagged horizontal and vertical radar tracks per species(groups).

3.3 Discussion

We presented species compositions based on the number of observations of each species during visual observations in wind farm Luchterduinen between February 2019 and the end of 2021. Due to safety restrictions, field visits to Luchterduinen were only possible on days with relatively favourable weather circumstances. In addition, field visits were only carried out in daylight. Therefore, the presented species compositions are only representative for situations under favourable weather circumstances and during daylight. Moreover, be aware that the presented numbers are not expressed as fluxes (numbers per time interval in a specific area) but as absolute numbers of birds observed during our standardized protocols. Based on the combination of bird fluxes measured by the radar and the species compositions presented above, calculated species-specific fluxes are provided in chapter 4.2.

Large numbers of starlings were observed in Luchterduinen in the months of October and November. Interestingly, out of the 900 starlings in November, around 750 individuals were counted on the 10th of November in 2021. On liveatlas.nl, an overview of the counts of birds in the Netherlands can be found, which also shows high numbers of starlings in October and November. Similar numbers can be found in the coastal area of the Netherlands. According to trektellen.nl, high numbers of starlings were observed on the 10th of November in 2021 along the Dutch coast with a maximum of more than 43,000 starlings counted near The Hague. This day was the 9th best day of starling migration in the Netherlands in autumn 2021.

The species composition found in the Luchterduinen wind farm is very dependent on the days on which observations were done. The aim was to spread out the observation days

evenly over the month, as a human observer cannot be present in the wind farm every day. The migratory peak of starlings on the 10th of November 2021 indicates that if no observation day was planned within that day, these migrations might have been missed. This is also the case for bird migrations at night, which we can visualize through the radar, but are unable to specify as to which bird species are present on these nights of intense migration. Moreover, bird species composition at night is likely to be markedly different from that during daytime, since many species actually prefer migrating by night.

On an annual basis, lesser black-backed gull was the most numerous species in and around the wind farm, followed by great cormorant and black-legged kittiwake. The occurrence of large numbers of truly marine oriented species as the lesser black-backed gull and kittiwake is not surprising and was recorded already during the post-construction monitoring in the wind farm area (Heinänen & Skov 2018). The presence of relatively high numbers of cormorants 25 km from the coast is evidently a strong indication that such an offshore wind farm is attractive to this species. We also presented monthly species compositions, because species composition can reasonably vary between months as not all species are equally numerous throughout the year (table 3.2.3). However, note that these monthly species compositions are based on a sample size of four field visits per month. Carrying out offshore field observations from wind turbines and platforms is challenging and hence are generally scarce, meaning that our setup of collecting field observations on four days per month is scientifically very valuable, especially since our field observations were conducted year-round, as marine spatial planning should also aim to account for the year-round distribution and abundance of seabirds (Piggott *et al.* 2021). Nevertheless, circumstances offshore can substantially vary between days, and hence a sample size of four days per month always remains limited. The presented monthly species compositions therefore come with a significant uncertainty, especially in the case of migratory birds that can pass the area in large numbers but in a short period. Consequently, observations can occur by chance at moments when large numbers of migrants pass by and hence dominating the recorded species composition if we look at the total number of observed birds per species, while we have no species information of the passage of groups on days without field observations. In contrast, we trust that our field observations provide a good indication of the relative presence of seabird species that use the area for a longer period throughout the year.

4 General flux patterns

4.1 Methods

In this chapter, data are presented on the flux (*i.e.* flight intensity) of birds flying in and around wind farm Luchterduinen. The flux calculations were based on the filtered dataset of vertical radar data, also including the so-called combined tracks of the radar (see §2). In an earlier stage of the project these combined tracks were excluded from the analysis (Gyimesi *et al.* 2020). This led to an investigation by Robin Radar, assuring that combined tracks (except for the ones with negative altitudes) are reliable to include in the calculations. Using the vertical radar data provided the possibility of calculating fluxes at different altitude levels. Moreover, the vertical radar is – compared to the horizontal radar – on the one hand less contaminated with wave clutter and on the other hand suffering less from data loss due to heavy filtering (table 2.1.1). Based on the detection capabilities of the vertical radar, and in accordance with preliminary analyses of the University of Amsterdam (Bradarić 2022), flux lines were drawn from 500-1,500 meters from the radar at both the north-western and south-eastern side of the radar (Fijn *et al.* 2015), for the sake of using a balanced spatial coverage.

Fluxes were determined as the number of tracks per km per hour (also referred to as 'mean traffic rate' (MTR)). Hence, fluxes were calculated by summing all tracks per hour that intersected with the two flux lines of one kilometre, and subsequently dividing by two to get the average number of tracks per km per hour. Overall patterns of fluxes are described, which give an insight in the variations throughout the study period, including variation between months and at different times of day and night. Additionally, the fluxes were differentiated for different altitude levels as below, at and above rotor height (§6.2.1).

Species-specific fluxes were calculated for each month based on 1) the average flux per km per hour during daytime in that month, and 2) the monthly species compositions based on the number of observations during visual observations (see §3.2 and table 3.2.3). Note that the species-specific fluxes during night-time could not be determined, as the species compositions are only representing bird activity during daylight.

Lastly, we used a flux line 500-1,000 meters from the radar along the south-eastern radiation line of the vertical radar (thus inside the wind farm) to determine absolute monthly species-specific daylight fluxes per km inside the wind farm at rotor height. These monthly species-specific fluxes deviate from the hourly fluxes reported in other chapters, but are directly applicable in collision risk models. To calculate these fluxes, we summed all tracks per month at rotor height (25-137 meters) during daylight that intersected along the 500 m long flux line, and subsequently multiplied it by two to get the absolute fluxes inside the wind farm per km per month during daylight at rotor height. Furthermore, we determined seasonal species compositions inside the wind farm at rotor height based on the number of observations during visual observations. We applied these species compositions to the monthly fluxes at rotor height to determine absolute monthly species-specific daylight fluxes per km inside the wind farm at rotor height.

4.2 Results

In the study period from the 22nd of February 2019 to the 31st of December 2021, on average 65 bird targets per km per hour were recorded by the vertical radar in and around wind farm Luchterduinen. Relatively low fluxes were recorded during the majority of the hours. In more than 40% of the hours (6,801 out of 16,209 hours), the mean traffic rates (MTRs) measured by the vertical radar were lower than 25 bird targets per km per hour (figure 4.2.1). Exceptionally high fluxes of more than 500 bird targets per km per hour were recorded in 222 out of 16,209 hours in total (1.4%). The hours with MTRs of more than 500 bird targets mostly occurred during night in March, October and November (figure 4.2.2b). During the day, hours with MTRs of more than 500 bird targets occurred mostly in July 2019 and autumn 2021 (figure 4.2.2a). In total, most hours with MTRs of more than 500 bird targets were seen in 2021 (n = 92) compared to 2019 (n = 68) and 2020 (n = 62). The highest fluxes were measured during the autumn migration on the 13th of October 2020, when between 17:00 and 20:00 (GMT) respectively 2,753; 4,345 and 4,503 bird targets per km per hour were measured by the vertical radar.

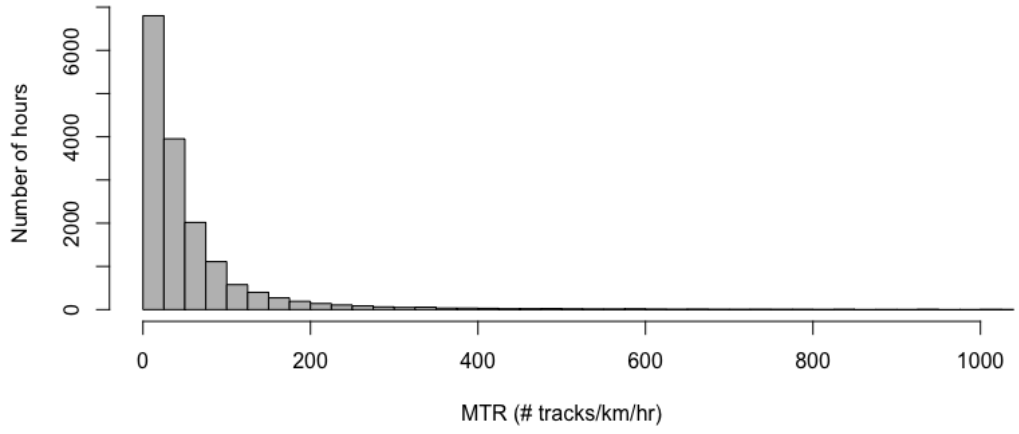

Figure 4.2.1 *Distribution of mean traffic rates (MTRs) in Luchterduinen throughout the study period, as measured by the vertical radar.*

Temporal variation in fluxes

The temporal variation in the hourly average number of tracks per km shows a roughly similar pattern each year (figure 4.2.3), with peak fluxes in early spring (*i.e.* late February and March) and autumn (*i.e.* October and November). In 2019, an early flux peak was detected on the 27th of February, while in 2020 and 2021 the peak fluxes in spring were recorded in March. However, the peak of the 27th of February 2019 is slightly inflated, as it is only based on an average of four hours at night (the radars were offline during the rest of the day). In autumn, the highest peaks were recorded in October 2019 and 2020 and November 2021. A (slight) increase in the number of tracks recorded in July can be distinguished in all three years, with a notably large peak at the end of July 2019.

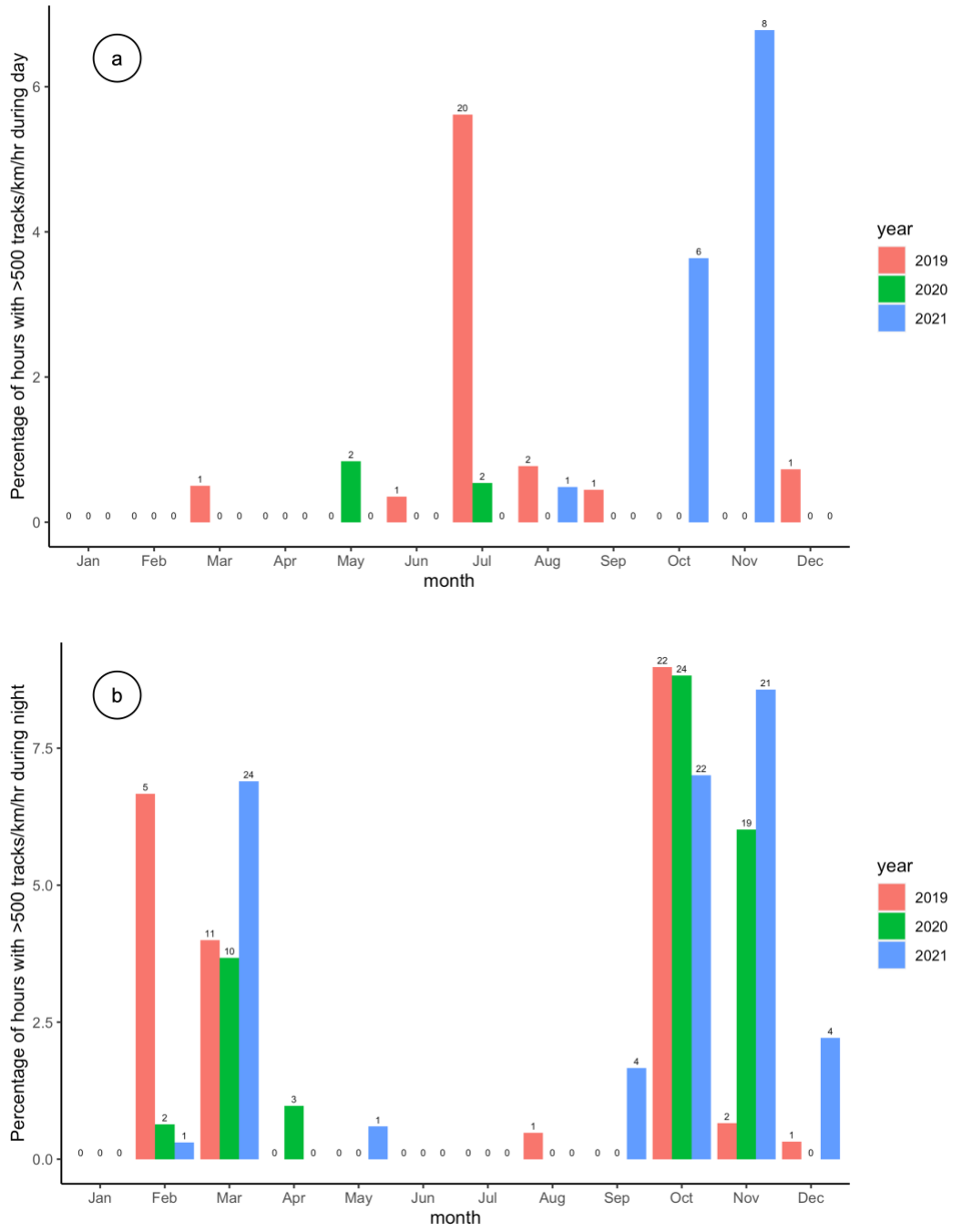

Figure 4.2.2 *The percentage of hours per month during day (a) and during night (b) for each year in which the vertical radar recorded fluxes of more than 500 tracks per km per hour. The total number of hours with >500 tracks/km/h per month during day and during night are given above each bar.*

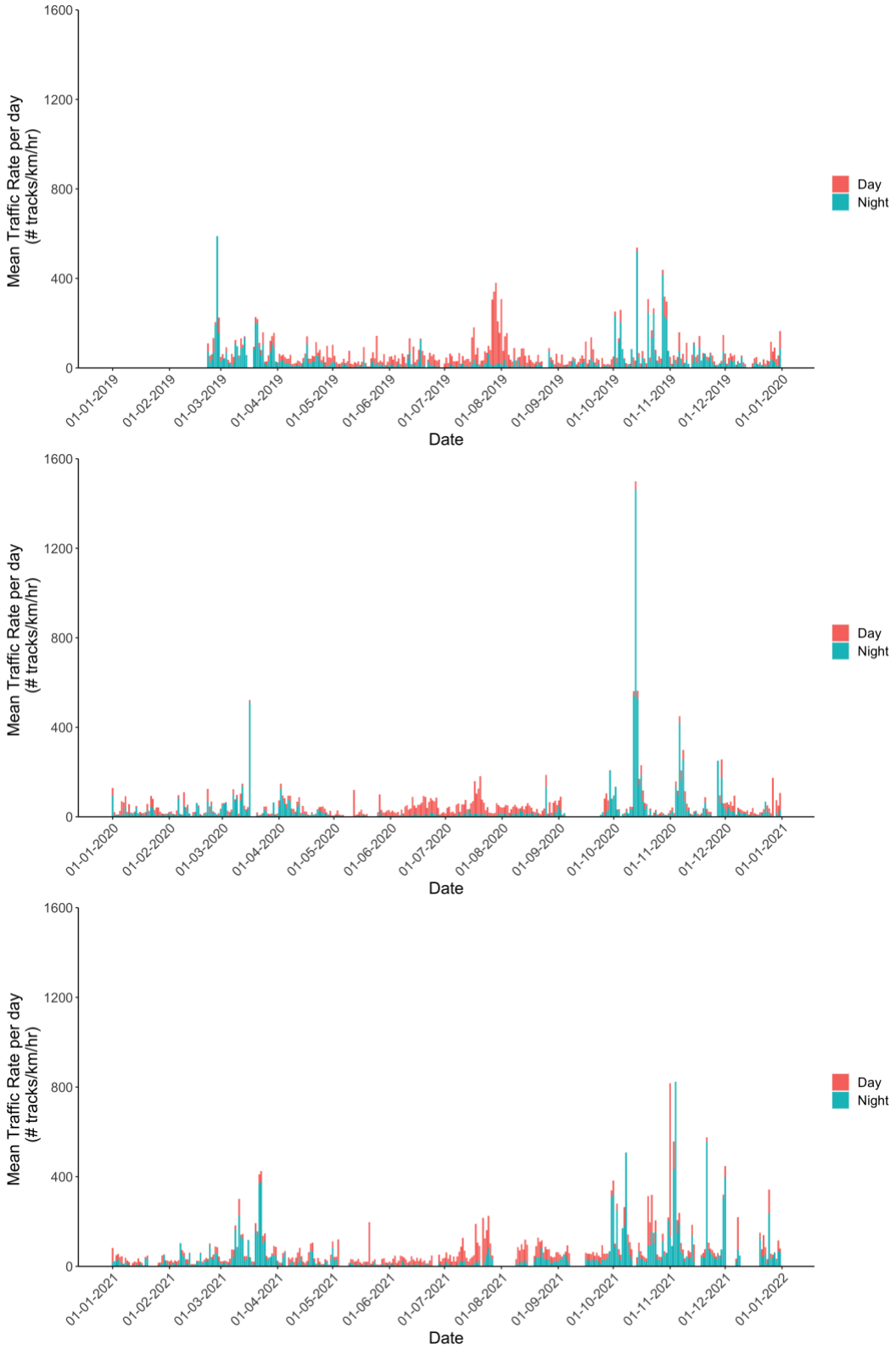

Figure 4.2.3 *Daily variation in the average MTR measured in Luchterduinen during daylight hours (red) and during night-time (blue) for 2019 (top), 2020 (middle), 2021 (bottom). Each bar indicates the average MTR during each day.*

Daily flux patterns

Flight activity around Luchterduinen was not constant during the day. From May to August, fluxes were on average higher in daylight than during night-time, while this pattern was reversed in the other months (figure 4.2.3). However, it must be noted that this pattern is also influenced by differences in daylength during the year (see also §8). It is nonetheless still notable that during most peaks of spring and autumn migration, MTRs were generally substantially higher during the night than during the day, indicating heavy nocturnal migration in these periods.

Considering the within-day variation in more detail, the radar measurements revealed that the number of birds passing through the area was peaking at the start of the night during the migration periods in spring and autumn (figure 4.2.4). During the night, the numbers steadily decreased to daytime levels. In winter and summer, such patterns are not observed. During these seasons, the numbers of birds are the highest during the daylight period.

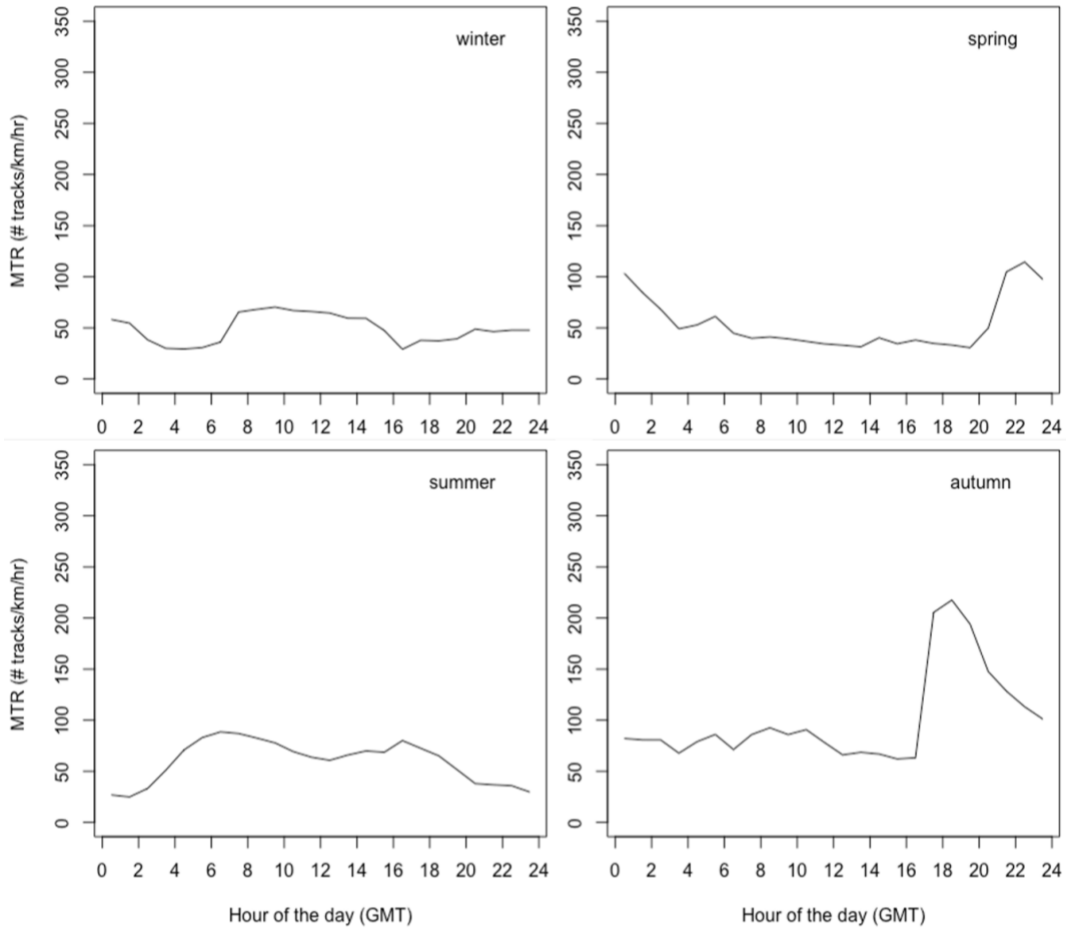

Figure 4.2.4 *Seasonal patterns of the variation in flight intensities during the day. Flight intensity is presented on the y-axis as the average MTR per hour.*

Species-specific fluxes

The highest fluxes during daylight are calculated for lesser black-backed gull with on average 49 birds per km per hour in July, closely followed by black-legged kittiwake with 48.81 birds per km per hour in December (table 4.2.1). Other species with on average more than 10 birds per km per hour in one month are great cormorant and northern gannet. Among the migrant species groups, songbirds are most numerous in October and November. Note, however, that migrants tend to largely fly during night-time, while these presented fluxes are merely based on the daylight hours.

Table 4.2.1 *Average species-specific fluxes per km per hour during daylight in each month based on vertical radar measurements and the monthly species composition measured during visual observations, for local birds (above line) and migrants (below line).*

species	Jan	Feb	Mar	Apr	May	Jun	Jul	Aug	Sep	Oct	Nov	Dec
arctic skua	0	0	0	0	0	0	0	0	0	0	0.2	0
black-headed gull	0	0	0.97	0.3	0	0.1	0.53	0.32	2.66	3.1	0	0
bl.-leg. kittiwake	7.24	6.02	5.51	0.15	0	0.1	0	0.16	0	18.28	31.91	48.81
common eider	0	0.19	0	0	0	0	0	0	0	0	0.2	0
common guillemot	2.13	2.72	0.97	0	0	0	0	0	0.16	1.72	6.3	1.86
common gull	3.83	3.11	0.97	0.89	0.28	0.1	0.36	0.32	2.03	4.14	0.61	5.31
common scoter	0	0.19	0	0.15	0	0.1	0	0.16	0.16	0.17	0	0
great bl.-b. gull	2.13	1.55	2.27	0.3	0	0.2	0.71	0.16	8.44	3.79	2.24	2.65
great cormorant	9.79	3.5	5.51	4.17	6.38	14.31	20.59	16.97	6.25	3.45	5.08	8.49
great skua	0	0	0	0	0	0	0	0	0	0	0.41	0
herring gull	5.53	1.55	4.21	0.3	1.11	0.41	0.36	0.16	1.09	0.34	1.42	1.33
lesser bl.-b. gull	0	4.28	2.92	15.19	9.44	28.01	49	40.35	28.61	7.07	0.81	0
little gull	0	0	0	0.3	0	0	0	0.96	0	0	0	0
northern gannet	9.79	2.33	2.92	0.89	2.78	0	1.78	0.64	2.19	10	14.23	4.77
razorbill	0.85	0.39	0.32	0	0	0	0	0	0	2.59	2.85	1.06
red-throated diver	0	0	0	0	0	0	0	0	0	0	0	1.06
Sandwich tern	0	0	0.32	0.45	9.16	0	0.36	0.32	0.31	0.17	0	0
ducks/grebes	0	0	0.32	0	0.28	0.1	0	0	0.16	0.69	0	0
geese/herons	0	0.78	0.65	0	0	0.2	0	0.32	0.31	0	0.41	0
raptors/falcons	0	0.39	0	0	0	0	0.18	0	0	0.17	0	0
songbirds	0	0	0.97	0.6	1.39	0.61	0	0.16	0.31	5	4.67	0
waders	0	0	0	0	0	0	0	0.16	0	0.17	0	0

Absolute species-specific fluxes inside wind farm at rotor height

The highest absolute monthly fluxes inside the perimeter of Luchterduinen wind farm at rotor height during daylight are calculated for lesser black-backed gull with up to 27,444 birds per km in July (table 4.2.2). Black-legged kittiwake had the second highest monthly maximum with 4,121 birds per km flying at rotor height in January. Other species with a maximum more than 1,000 birds per km at rotor height in one month were great black-backed gull and great cormorant. For several species, we did not observe any birds at rotor height, thus the calculated fluxes for these species were zero birds.

Table 4.2.2 *Absolute monthly species-specific fluxes per km inside the wind farm at rotor height during daylight based on vertical radar measurements and seasonal species compositions inside the wind farm at rotor height measured during visual observations.*

species	Jan	Feb	Mar	Apr	May	Jun	Jul	Aug	Sep	Oct	Nov	Dec
arctic skua	0	0	0	0	0	0	0	0	0	0	0	0
black-headed gull	0	0	0	0	0	0	0	0	96	150	110	0
bl.-leg. kittiwake	4,121	1,712	0	0	0	0	0	0	870	1,296	1,021	3,842
common eider	0	0	0	0	0	0	0	0	0	0	0	0
common guillemot	0	0	0	0	0	0	0	0	0	0	0	0
common gull	822	408	0	0	0	0	0	0	227	312	279	730
common scoter	0	0	0	0	0	113	237	124	0	0	0	0
great bl.-b. gull	647	372	51	86	66	0	0	0	668	1,111	732	545
great cormorant	276	88	180	312	227	1,112	2,299	1,213	87	108	113	272
great skua	0	0	0	0	0	0	0	0	0	0	0	0
herring gull	941	446	437	763	549	0	0	0	192	301	219	846
lesser bl.-b. gull	668	400	3,963	6,970	4,950	13,938	27,444	14,808	3,032	4,760	3,449	555
little gull	0	0	0	0	0	0	0	0	0	0	0	0
northern gannet	79	25	51	86	66	0	0	0	109	135	141	78
razorbill	0	0	0	0	0	0	0	0	0	0	0	0
red-throated diver	39	13	0	0	0	0	0	0	0	0	0	39
Sandwich tern	0	0	51	86	66	0	0	0	0	0	0	0

4.3 Discussion

One of the main objectives of the project was to determine species-specific fluxes in wind farm Luchterduinen based on measurements by the bird radars. The current report presents the results of nearly three years of radar measurements. The fluxes during the study period seem to be in the range of the ones measured earlier in wind farm OWEZ (Krijgsveld *et al.* 2011). Also, the pattern in fluxes throughout the year (*i.e.* highest fluxes during migration in March and October) and seasonal patterns throughout the day are in line with the pattern in fluxes measured in OWEZ. On the other hand, the number of hours with a mean traffic rate of more than 500 birds per hour seems to be somewhat higher in Luchterduinen than in OWEZ. Krijgsveld *et al.* (2015) reported 40 of such hours per year in OWEZ compared to 62-92 hours in Luchterduinen.

Nevertheless, it took a great effort to reach realistic numbers of radar measurements not being contaminated by a large amount of non-bird tracks in the dataset caused either by rain or by waves. The dataset of the X-band vertical radar turned out to contain a large amount of rain data. Rainy periods could result in an extremely high number of tracks in the dataset of the vertical radar, ranging from values such as 16,341 tracks in one hour on 12 July 2019 and 13,917 tracks in one hour on 15 June 2019. Visual inspection of the radar images from rainy periods revealed that especially at the boundaries of rainy periods a large number of tracks entered the database as small birds or flocks, as the dynamic rain filtering of the radar tends to be activated with a slight delay after rainfall starts. Several

tests to automatically differentiate rain tracks from bird tracks did not suffice, and hence we decided to use a precautionary approach and delete all hours that had any indications of rain contamination, either by relying on the values of the radar's own rain filter or on the nearest KNMI rain measurements from a location near the coast of Zandvoort. However, even with this precautionary approach we did not succeed to filter out all rain events. A visual sample of the radar images indicated that still some hours with large numbers of tracks caused by rain showers were present in the remaining dataset. Therefore, an additional filtering based on track properties was necessary (see §2.1.3), with which we could filter out the hours with the most intensive rain showers. However, even after all these filter steps, we cannot exclude that some rain showers were still present in our final dataset.

All the different steps of rain filtering led to deleting altogether 8,521 hours from the dataset, *i.e.* 34% of all measured hours. This feels to be an unrealistic high proportion of rainy hours, and hence a point of further investigation should be whether the rain filters can be improved, in order to prevent more data loss than necessary, especially considering that rain (and similar adverse weather circumstances with lower visibility) could lead to increased collision risk (Hüppop *et al.* 2006; Hüppop *et al.* 2016). For example, actual rain measurements at the radar location itself could already facilitate much more effective data filtering. Rain showers often occur very locally, which makes even the nearest KNMI rain measurements close to Zandvoort likely inaccurate for the purpose of filtering. On-site rain measurements would enable much more precise filtering of rainy periods.

All the filter steps we had to apply to come to realistic MTR estimates imply that the unfiltered radar data is not yet directly applicable to produce MTR estimates. This means that unfiltered data in periods of rain are not useful to assess bird fluxes, while it is during these rainy periods with limited visibility that birds tend to become more vulnerable to collisions (Marques *et al.* 2014; Aschwanden *et al.* 2018), although this theory needs field confirmation. More in-depth analyses of the characteristics of rain tracks (which was out of the scope of this project) may potentially enable filtering of rain tracks instead of filtering rainy periods as a whole. With this approach, bird fluxes may potentially be assessed even in rainy periods. However, the extent in which dynamic filtering of the radar as a response to rain may also filter out bird tracks should then also be quantified. Therefore, a reliable assessment of bird fluxes in rainy periods was currently not possible.

Despite the susceptibility of the vertical radar to detect rain showers, we still decided to calculate fluxes based on vertical radar data instead of the horizontal radar data. Compared to the horizontal radar, the vertical radar suffers less from data loss due to heavy filtering, as the horizontal is much more susceptible to wave clutter. Moreover, using data of the vertical radar provided the possibility of calculating fluxes at different altitude levels (see Chapter 6). One disadvantage of using vertical radar data is that we cannot change the orientation of the flux lines used to calculate the fluxes. The vertical radar beam covers areas to the northwest and the southeast from the radar, and hence also the flux lines lay in these directions. If the flux of birds goes in a perpendicular direction to these flux lines (*i.e.* towards southwest or northeast) the calculated fluxes per length of the flux lines are genuine. However, the length of the 'effective flux lines' decreases if the birds are mainly flying in different directions (figure 4.3.1). In such situations, fluxes per kilometre will be

underestimated (Kleyheeg-Hartman & Potiek 2020), which may also be the case with our reported fluxes. This effect might be small during autumn migration, as migrating birds mainly follow a northeast-southwest direction during their seasonal migration. In spring, the direction of migration over the North Sea often has a more easterly component (figure 4.3.2), when birds from the United Kingdom make the crossing (Bradarić *et al.* 2020). It is recommended for future studies to explore whether horizontal radar data and vertical radar data can be combined to correct flux calculations for the main flight direction of tracks.

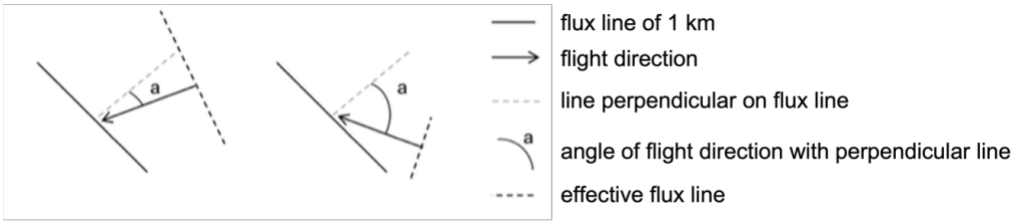

Figure 4.3.1 *The length of the 'effective flux line' will be smaller than 1 km if the bird's flight direction is not perpendicular to the flux line. The larger the angle of flight direction with the perpendicular line, the smaller the 'effective flux line' will be. Adjusted from Kleyheeg-Hartman & Potiek 2020.*

The underestimation caused by the above-mentioned issue may mostly be relevant for migratory birds that in large numbers cross the area in a certain direction in a short period of time. If that direction is not perpendicular to the radar orientation, large deviations in measured fluxes can occur (see figure 4.3.2). Local birds will not consistently cross the radar beam in a certain direction and hence the deviations will be on average smaller and more consistent throughout the year. Note that an individual local bird may cross the flux line multiple times, and hence fluxes must not be interpreted as the number of individuals present in the area. Multiple crossings of the same individual are, however, not likely for migrating birds that pass the area on their seasonal migration. Furthermore, the warning to infer species-specific fluxes based on radar measurements holds in a general sense, as the calculations also rely on tracks classified as 'flocks' by the radar, which indisputably means that more than one target was measured, but the exact number is not known.

As the vertical radar is less susceptible to wave clutter than the horizontal radar, we did not do any filtering of wave clutter. Nonetheless, it is clear that waves may also contaminate the dataset of the vertical radar, principally in the lowest altitude levels above the sea surface (see §6.2.1). However, several species of seabirds also prefer to fly at these low altitudes. Filtering out all tracks just above sea level may therefore reduce the contamination of wave clutter, but in the same time also lose the majority of tracks of some species. An exploratory analysis in which we filtered out the lowest three meters, showed that the remaining dataset contains 176 hours with an MTR above 500 birds/km/hour (compared to 222 hours including altitudes of 0-3m). Especially in the autumn of 2021, a lot of wave clutter could have entered the dataset, as after filtering out the lowest 3 m of dataset the MTR dropped in 36 different hours below 500 birds/km/hour. The presence of wave clutter in the dataset at low altitudes must therefore be considered when interpreting the presented results, and should eventually be improved in future radar filtering software.

The species-specific fluxes presented in this study are mainly meant to give an indication of the order of magnitude of the fluxes for each species in each month. As the fluxes are based on the total fluxes recorded by the vertical radar, they are directly related to the number of hours in each month that remained in the filtered dataset. On average 34% of all hours is filtered out (table 2.1.1), which means that the presented species-specific fluxes are likely to be an underestimation of the actual fluxes. However, we cannot assume that the actual fluxes are then on average 34% higher than those presented, as birds may show less flight activity during rainy weather. Furthermore, the calculated fluxes may undeniably contain overestimations if rain showers or wave clutter were still present in the filtered dataset. This implies that the species-specific fluxes presented in this study come with great uncertainty. On top of that comes the uncertainty involving the calculated monthly species compositions (see §3.3).

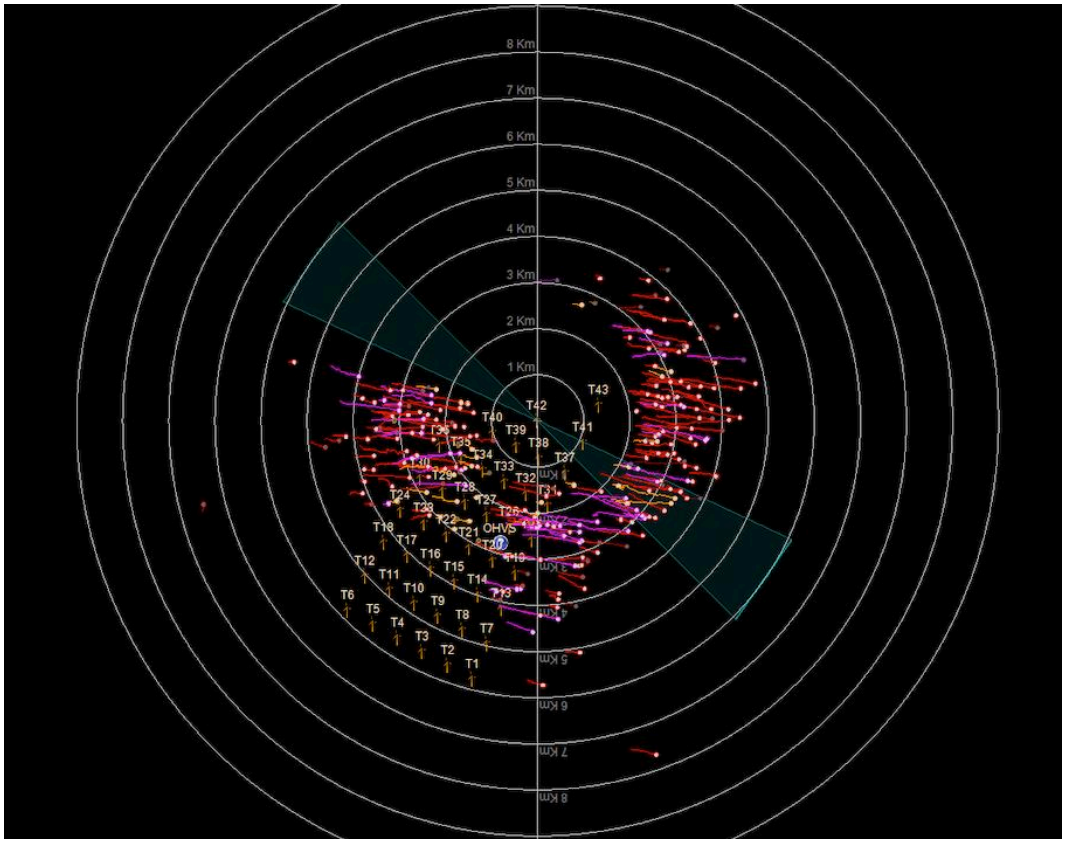

Figure 4.3.2 *Example of nocturnal spring migration with an easterly direction that is mainly recorded by the horizontal radar and much less by the vertical radar. This radar image is taken on 1st of April 2020 between 00h00 and 01h00. During this hour, an MTR of 80 birds per km per hour was calculated, which is clearly an underestimation of the actual flux.*

A comparison with species-species fluxes used for collision risk modelling for the study Kader Ecologie en Cumulatie (KEC 4.0; Potiek et al. 2022) shows some great deviations from the absolute annual fluxes calculated in this study based on the species composition as calculated in §3 (table 4.3.1). For all species, except arctic skua, lesser black-backed gull, northern gannet and Sandwich tern, the fluxes used in KEC 4.0 are higher than those

calculated in the current study, even considering that the KEC 4.0 results were corrected for macro-avoidance (table 4.3.1). If we exclude the lowest three meters from the fluxes found in this study, the fluxes decrease with values ranging from 5 (arctic skua) to 1,811 (lesser black-backed gull). However, the high flux rates of lesser black-backed gulls are also confirmed by the visual observations. Especially in the summer months (June-August) very high numbers of lesser black-backed gulls were seen. Together with the high fluxes rates of cormorants in the same period this could lead to the high fluxes measured by the radar in the summer months in all years but especially in 2019.

The fluxes used in KEC 4.0 are calculated by the stochastic Collision Risk Model (Marine Scotland 2018), based on interpolated two-monthly densities from long-term aerial- and ship surveys (ESAS/MTWL data). The calculation of fluxes in this model, as well as in the Band model (Band 2012) it builds upon, assumes that there is a constant flux of birds flying through the wind farm. It has been pointed out earlier that seabirds are more likely to move around tortuously (Patrick *et al.* 2014), and hence assuming constant straight fluxes can largely overestimate the number of birds flying through the wind farm in a given time period (Masden & Cook 2016), of which our results might give an indication. Our results highlight the need to further investigate the way the Band model calculates fluxes from densities, as the difference between the KEC fluxes and the fluxes of the current study based on field measurements indicate that the Band model may produce unrealistically high flux rates.

Table 4.3.1 *Absolute species-specific fluxes per km per year calculated in the current study and used for collision risk modelling in the KEC 4.0 study (Potiek et al. 2022). The latter are corrected for macro-avoidance.*

	Annual flux measured in Luchterduinen			
species	Current study	KEC 4.0	Difference	Macro-avoidance
arctic skua	31	0	-	80% ***
black-legged kittiwake	17,693	47,297	-62,6%	58% *
great black-backed gull	4,295	9,122	-52,9%	47% *
great skua	62	180	-65,5%	80% ***
herring gull	3,622	13,841	-73,8%	44% *
lesser black-backed gull	55,226	10,815	410,7%	64% *
little gull	374	17,688	-97,9%	80% **
northern gannet	9,652	7,725	25,0%	82% *
Sandwich tern	3,346	1,185	182,3%	70% **

* Skov *et al.* 2018

** Dierschke *et al.* 2016

*** Equal to northern fulmar in Dierschke *et al.* 2016

However, our analyses also shows how using different methods to determine species compositions may also affect calculated fluxes. For some species, the annual fluxes at rotor height as presented in Table 4.2.2 exceed the annual total fluxes as presented in Table 4.3.1. For the latter, we used the species composition as calculated in §3, which is based on all observations done during the visual observations thus including observations around the wind farm and without any altitude information. In contrast, we only included

data with altitude information and inside the wind farm to calculate species compositions at rotor height within the wind farm. Additionally, slightly different flux lines were used in both methods. The resulting differences in the calculated absolute annual flux through Luchterduinen using these two different methods stress the importance of taking uncertainties into account when interpreting the presented data.

5 Effect of weather on fluxes

Offshore wind farms (OWFs) are a potential threat to birds, causing increased mortality due to collisions. As collision rates will inevitably increase with intensity of bird movements, it is important to understand when events of intense migration can be expected, so that mitigation measures can be designed and successively taken. Intensity of bird migration and its direction are strongly dependent on the season (*e.g.*, pre- or post-breeding migrations) but also on weather conditions (wind direction and speed) (Newton 2010). In this chapter, we present the effects of wind speed and direction, visibility, and time relative to sunset and sunrise, on bird fluxes in Luchterduinen.

5.1 Methods

Weather data

Wind was measured using ultrasonic sensors type FT-702, located on top of the nacelle of turbine 41. Wind speed and direction were recorded at 20 s intervals. For our analysis, wind speed and direction were averaged per hour. Hourly records of visibility were obtained from the KNMI website (https://www.knmi.nl/nederland-nu/klimatologie/uurgegevens) for airfield De Kooy, Den Helder (52°55'N 4°46'E), being the nearest station collecting such data.

Data filtering

The fluxes calculated in this analysis were based on vertical radar data. As the purpose of this analysis was to investigate the effect of weather on fluxes and not to calculate general flux rates, the data were filtered in a slightly different way than what is described in §2.1.2, following the filtering steps used by the University of Amsterdam (Bradarić 2022), to produce comparable results. For this analysis, we applied rain filtering based on 5-minute interval KNMI weather data from a location near the shore of Zandvoort. If the data from this location indicated any precipitation during an interval of 5 minutes, then these minutes were removed from the dataset. Furthermore, only tracks classified by the radar as 'bird' below or equal to an average altitude of 300 meters were included in the analysis. This altitude is relevant for studying bird flight behaviour at rotor height, while wind conditions above 300 meters can be substantially different from lower altitudes and hence also influence migratory patterns (Kemp *et al.* 2013).

Data selection

Radar data were selected for whole hours (in UTC) during two spring and two autumn periods: 1) 15 August - 30 November 2019, 2) 15 February - 31 May 2020, 3) 15 August - 30 November 2020, 4) 15 February - 31 May 2021. For each hour, flux (# birds/km/h) was calculated as in §4.1. In addition, the time since sunset and since sunrise were recorded for the start of each hour; based on this, hourly records were categorized as day or night. Finally, weather data were coupled for each hour. Only data records (hours) where both flux and wind data were available were retained in the final data set.

Statistical analysis

The effects of weather and timing on bird fluxes were estimated using Bayesian Generalised Additive Models (GAMs), assuming a Poisson distribution of the response variable. Models were fitted using Integrated Nested Laplace Approximation (INLA) in the R-INLA package version 21.11.22 (Lindgren & Rue 2015) in R version 4.1.2 (R Core Team 2020). Models included visibility and season as linear fixed effects and random walk models of order 2, separately for each season, for wind speed and wind direction (as a circular variable). A random walk model of order 2 was also included for the time since sunset for nightly hours and sunrise for daytime hours. To deal with overdispersion, an observation-level random effect was included. These observational-level random intercepts were added to 'take up' any variance unexplained by the other model terms. This is a way to deal with overdispersion (a common problem with Poisson models) and makes it easy to assess the amount of unexplained variance. Before fitting the models, we standardized wind speed, time since sunset/sunrise so that their means were 0 and standard deviations were 1. Wind direction was scaled from -1 to 1, with 0 representing North. The importance of each covariate was interpreted from the effect sizes.

5.2 Results

Missing values and sample sizes

Following the filtering steps described above, approximately 60% of the wind speed data lacked flux measurements in Luchterduinen (figure 5.2.1). In addition, wind data were missing for substantial blocks of time (figure 5.2.1b). Although retaining only data where both flux and wind data were available left only 49% of the original data, the sample sizes for the analysis were still considerable (figure 5.2.2).

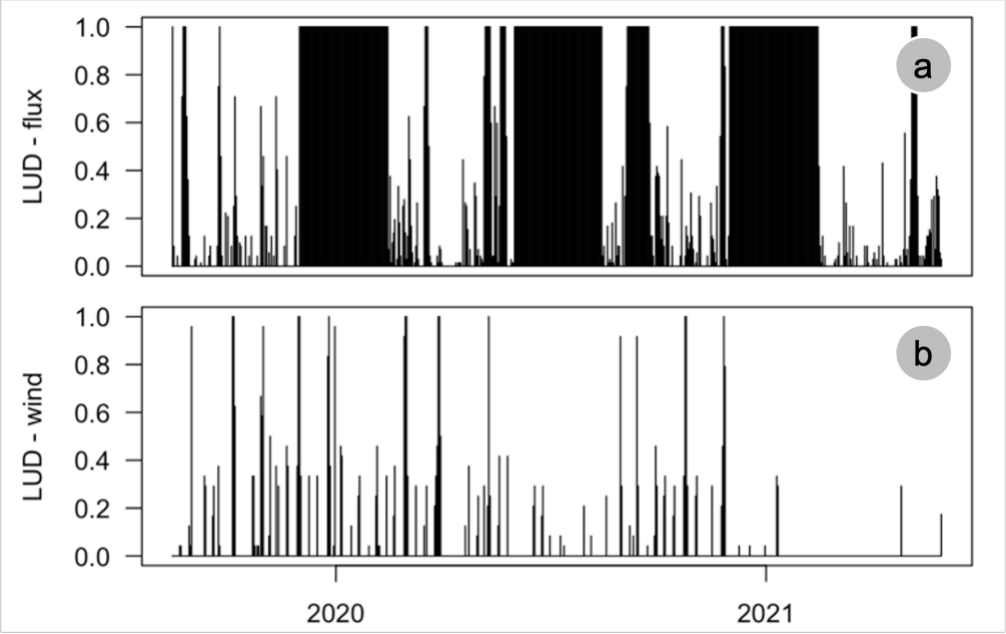

Figure 5.2.1 *Proportion of missing values per day of flux (a) and wind data (b). Note that no flux data were used (and therefore indicated as 'missing' here) for the periods between 30 November and 15 February and between 31 May and 15 August.*

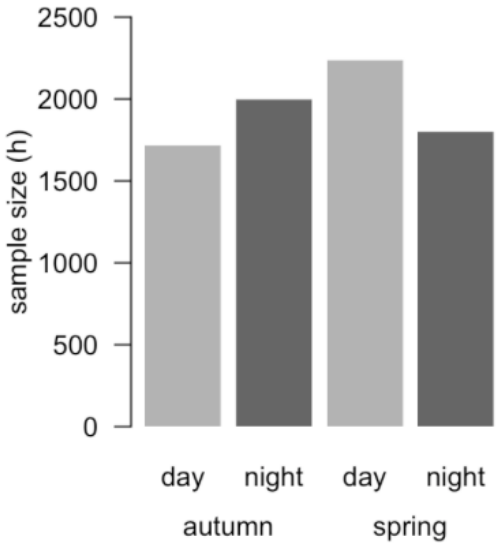

Figure 5.2.2 Number of hours with both radar and wind data for autumn (left) and spring (right).

Model results

Bird flux at rotor height was strongly affected by wind speed and direction (figure 5.2.3), with most intense flux at both low and high speeds, with a dip around 13-15 m/s (6-7 Bft) in both seasons (figure 5.2.4). In addition, bird fluxes were substantially higher in autumn than in spring (figure 5.2.5). In autumn, bird fluxes peaked with northeasterly winds, whereas in spring bird fluxes peaked with northwesterly winds. Fluxes at rotor height were similar between day and night, and also the time since sunset and sunrise had minor effects, with slightly higher fluxes during the first hours of the day, and lower fluxes during the first hours of the night.

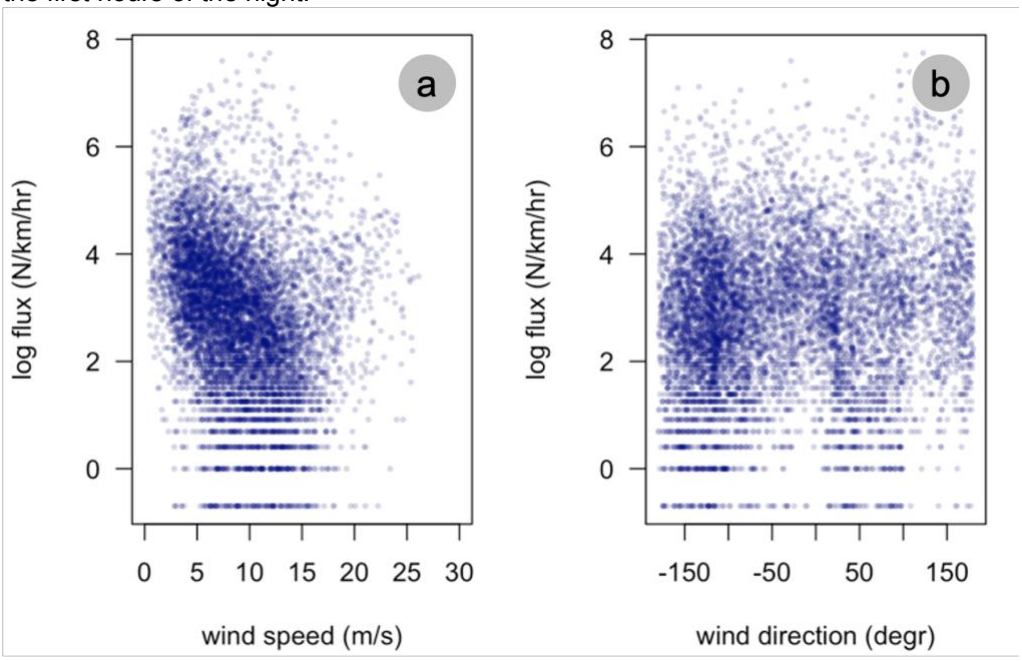

Figure 5.2.3 Flux as a function of wind speed (a) and wind direction (b).

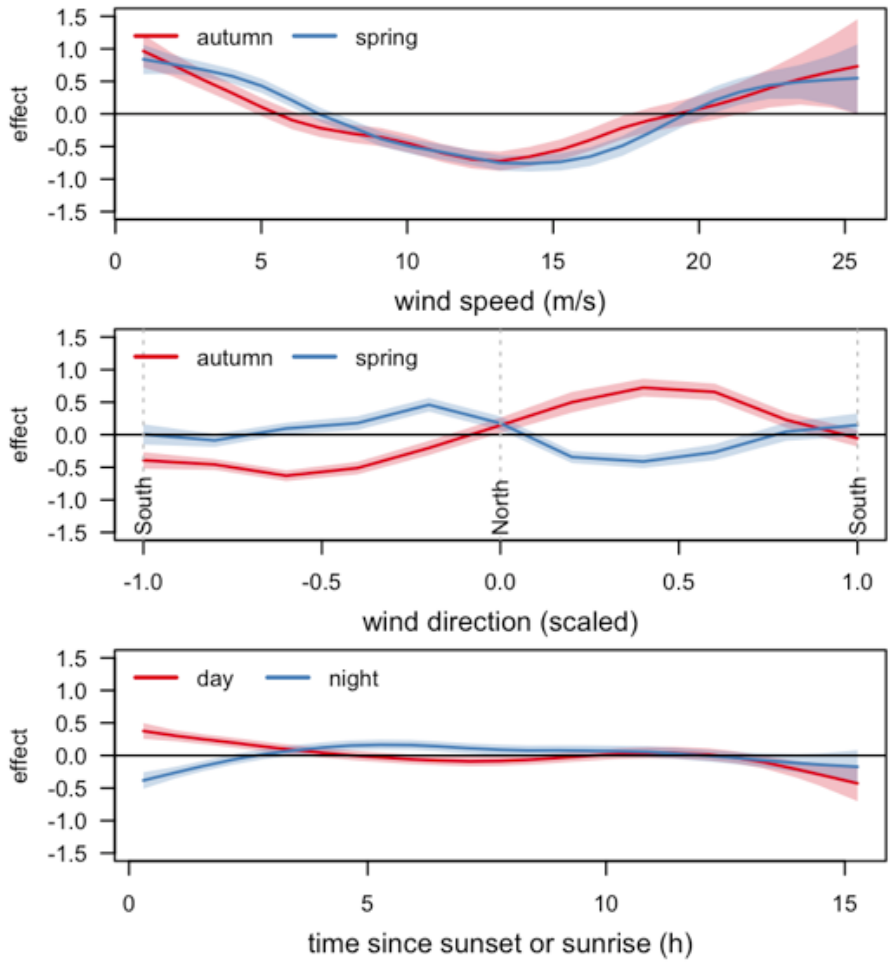

Figure 5.2.4 *Effects of wind speed, wind direction and hour of the day on bird flux in Luchterduinen. Wind directions are scaled from -1 to 1, with 0 representing North, negative values westerly directions and positive values easterly directions.*

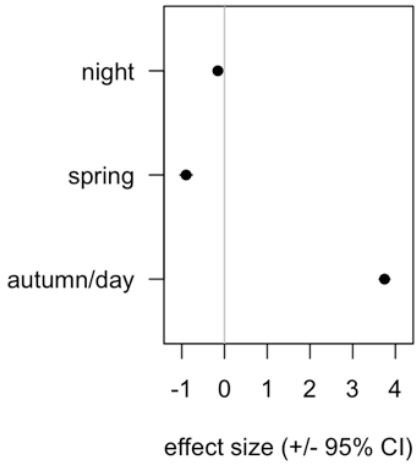

Figure 5.2.5 *Fixed effects parameter estimates, showing the relative effect of each variable. The base level for was autumn/day: effects for spring, day and visibility are relative to this base level.*

Predictive performance

Due to the addition of observational-level random intercepts, the fitted values perfectly follow the observations (figure 5.2.6c). The link between predicted values and observations was considerably weaker when leaving out the observational-level random intercepts (figure 5.2.6d), indicating that these were generally large compared to the other effects included in the model (figure 5.2.6b). Especially high flux values are poorly predicted by the model (figure 5.2.6d).

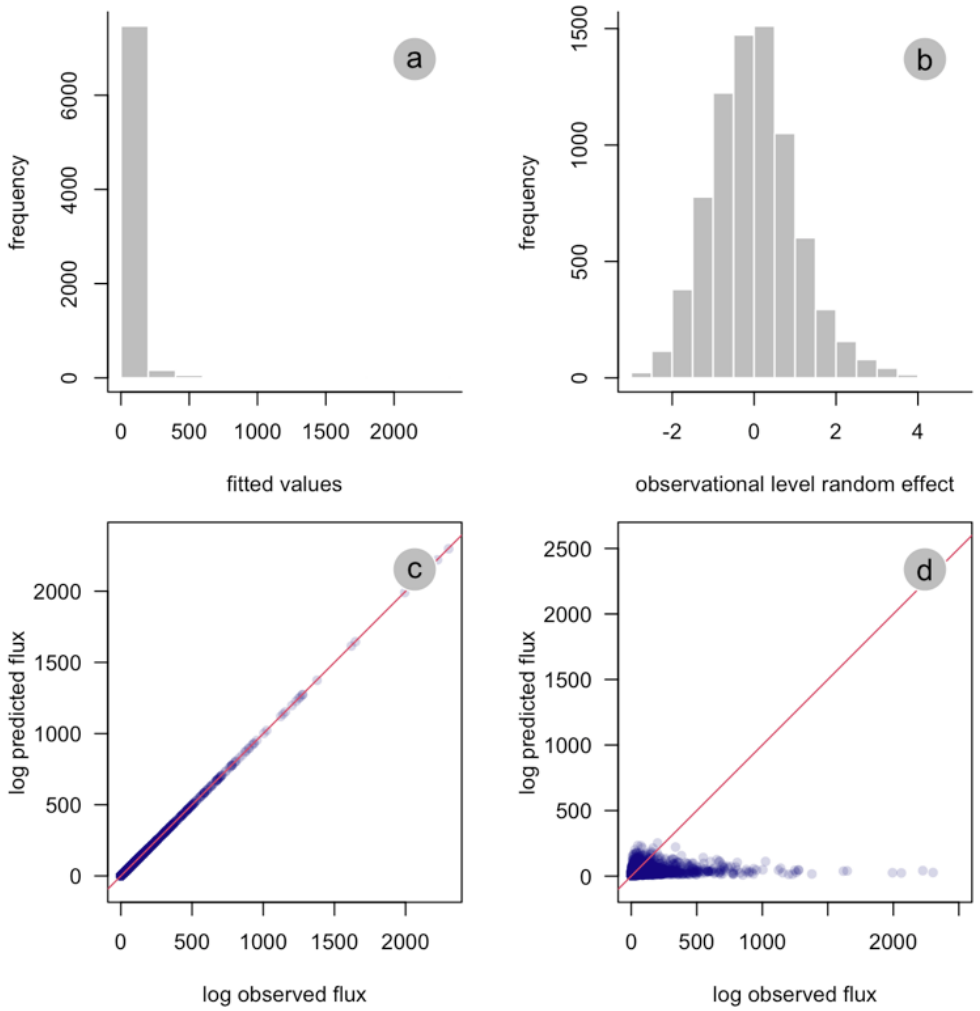

Figure 5.2.6 *a) Distribution of fitted values. b) Distribution of observation-level random intercepts on the scale of the linear predictor. c) Relation between observed and fitted values. d) Relation between observed and predicted values not considering the observation-level random intercepts.*

5.3 Discussion

Bird flux at rotor height was higher in autumn than in spring, and with both low or strong winds and during north(western) winds in spring or with northeastern winds in autumn. Wind speed had a particularly strong and consistent effect on bird flux at rotor height, with least flux recorded between approximately 13-15 m/s (6-7 Bft). Less clear relations for the

flux at rotor height were found with the time since sunrise and sunset and between day and night.

These patterns largely align with what can be expected for a coastal or nearshore site along the Dutch North Sea coast. The higher number of birds during autumn can be explained by larger population sizes just after the breeding season and mortality during the time until spring migration (Newton 2010; Dokter *et al.* 2018). Intense migration during northeastern winds in autumn and during northwesterly winds in spring fit the observation that many birds wait for light tailwind conditions to cross the North Sea; from Scandinavia to the Netherlands or from the Netherlands to the United Kingdom in autumn, or from the United Kingdom to the continent in spring (Newton 2010, Fijn *et al.* 2015, Bradarić *et al.* 2020). Passerines usually do not migrate during stronger winds, and hence the higher migration intensity during strong winds (>15 m/s; > 7 Bft) as suggested by the model, is surprising. Indeed, this pattern is not well supported by the raw data, with only few flux records at wind speeds exceeding 15 m/s to support this. Likely, these records pertain to clutter caused by high waves not well filtered out by the radar software.

Contrary to our expectations, fluxes did not show a clear pattern relative to the time since sunset or sunrise. The fluxes of nocturnal migrants, such as thrushes, usually show a peak just after sunset (Krijgsveld *et al.* 2011; Fijn *et al.* 2012; Welcker 2019). Likewise, diurnal migration usually peaks in the first few hours after sunrise (Krijgsveld *et al.* 2011; Fijn *et al.* 2012). Therefore, a peak of migrants was expected especially in autumn shortly after sunrise (*i.e.* given the distance from land to the OWF and the time it usually takes to cover this distance) when birds would depart from nearby land after, but this was not observed. Potentially, birds migrating over LUD in autumn originate from a much wider area than the Dutch coast. For example, arrivals in autumn may originate from southern Scandinavia. Alternatively, fluxes at lower altitudes at rotor height (up to 300 m) may not reflect the general migration patterns. It is known that flight height positively correlates with migration intensity (Welcker 2019). This could be caused by birds usually departing with good tail-wind conditions (Bradarić *et al.* 2020), and then quickly climb to higher altitudes to optimally profit from the wind lift (Kemp *et al.* 2013). Due to the distance of our study site from departure locations at the coast, the massive bird migration after sunset observed in offshore areas likely occurs at altitudes above 300 m (cf. Krijgsveld *et al.* 2011; Fijn *et al.* 2012).

The large effect sizes of the observational-level random effects and the weak correspondence between observed and predicted fluxes show the poor fit of the model. In particular, the large effect sizes of the observational-level random effects indicate that there are substantial unexplained variances in the model, *e.g.,* there are important drivers of bird flux that are currently not included in the model. This is no surprise, as the drivers of bird migration are myriad and complex (Newton 2010), and this model is obviously a great simplification of reality. For example, intense migration across the northern parts of the Netherlands in autumn not only requires good departure conditions in southern Scandinavia, but also the build-up of large numbers of migrants in the days before, due to adverse weather conditions (Shamoun-Baranes & van Gasteren 2011). High fluxes were particularly poorly predicted by the model. Obviously, these are relatively rare events while

the focus of the model is on the mean flux. Moreover, high fluxes might be caused by local weather circumstances deviating from the situation at meteorological stations at the coast. For instance, local adverse weather conditions, such as sudden strong head winds, low visibility due to precipitation or sea fog, can lead to a decrease in flight altitude of migrating birds, causing them to fly lower, causing high flux rates at lower altitudes (Hüppop *et al.* 2006). Beside including better predictors of high intensity migration as discussed above, potential solutions to this in the future is to not use flux as a response variable directly, but to use the occurrence of high intensity migration above a certain threshold as a binomial response variable.

Moreover, note that flux data were missing for about half of the hourly records in the study periods. Missing values were not randomly or evenly distributed across time; periods with high proportions of missing values clustered within, *e.g.*, spring and autumn 2020. It is difficult to gauge the effect of this missing data on the outcomes without data from more years to estimate the usual fluxes during extended periods of missing data.

6 Flight height

6.1 Methods

6.1.1 Radar altitude profiles

Based on the vertical radar data of tracks intersecting with the flux lines as used in the flux calculations (see §4.1), we composed altitude profiles of all tracks in height bands of 5 meters. Also, the daily MTRs as reported in §4.2 were split into fluxes below-, at- and above the rotor-swept zone (25-137 meters).

6.1.2 Observed species composition per height class

The analysis of the observed species composition during visual observations was performed based on three different data types, namely (i) the height of tagged tracks as recorded by the radar, (ii) observer estimated heights of visual observations and (iii) LRF measurements. Therefore, this analysis deviates from the one used to calculate monthly species compositions in general (§3.2) as more data sources were used. As visual observations were carried out by observers who estimated the height of the bird, these visual estimations of flight height will always come with some inaccuracy. Therefore, for visual field observation seven height classes were used to estimate the flight height, namely 0-3 m, 3-10 m, 10-25 m, 25-50 m, 50-100 m, 100-200 m, >200 m above sea level. The height of tagged tracks measured by the radar and the height of tracks measured with the LRF were successively also classified into these height classes to able to combine all data sources. Subsequently, a species composition was determined for each height class.

6.1.3 Species-specific flight height distributions

The above-described data on species-specific flight heights during visual observations were not collected with an equal effort in each height class. Therefore, these data could not directly be used to calculate species-specific flight height distributions. Hence, we first applied the species compositions in each height class per month (based on the measurements described in §6.1.2) to the absolute monthly daylight fluxes of tracks in each height class (for methods of these flux calculations see §4.1). This provided for each species per month an absolute flux within each height class, which we summed to get a yearly total and subsequently converted to flux per meter by correcting for the number of meters in each height class. We only defined species-specific flight height distributions for species with at least 30 observations. The number of observations in the two height classes above 100 meters were too limited to calculate a representative species composition. Therefore, we combined all data between 50 and 200 meters, as representative for fluxes at rotor height. Furthermore, we excluded the lowest three meters from the presented flight height distributions, as radar measurements in these altitudes are likely overestimated due to wave clutter (also see §6.2.1).

6.2 Results

6.2.1 Radar altitude profiles

Based on the altitudes of the bird targets measured by the vertical radar, we determined general altitude profiles. The highest number of bird tracks was measured at altitudes below 5 meters, while another peak is visible at the altitude range of 30-40 meters and a smaller one around 120 m (figure 6.2.1). The remarkably high numbers of bird tracks below 5 meters are likely to be an overestimation due to the presence of wave clutter at these altitudes. Above altitudes of 120 meters, the number of detected tracks steadily decreased with altitude. Altitudes above 300 meters are not depicted on figure 6.2.1, but the numbers further decreased also at these altitudes.

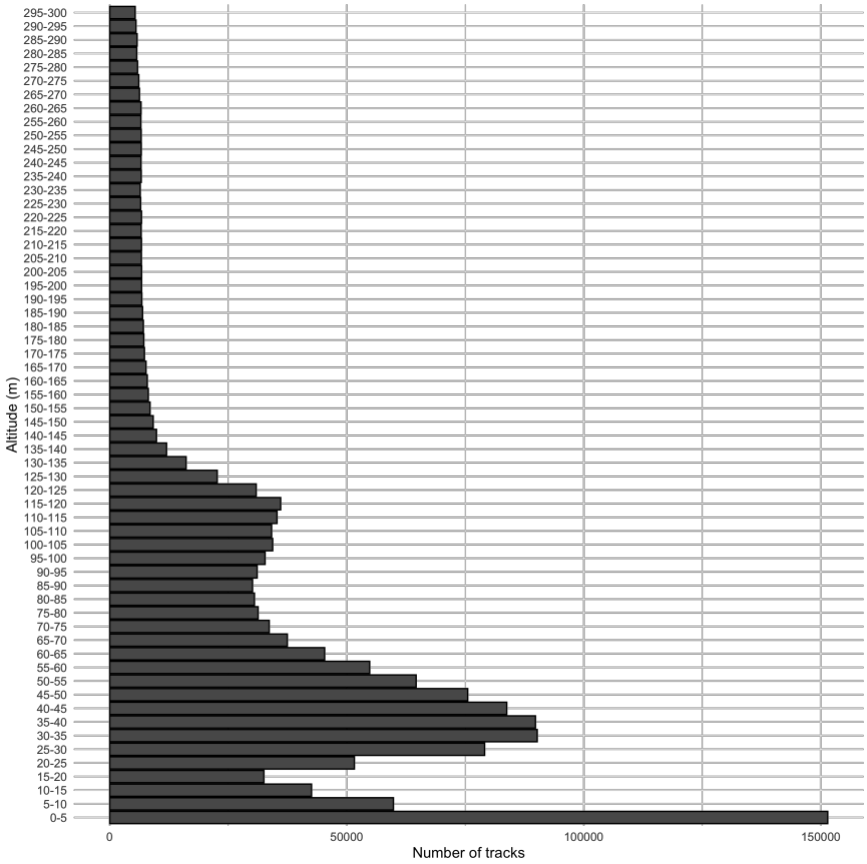

Figure 6.2.1 Altitude profile up to 300 m per 5 m altitude classes in Luchterduinen.

By grouping the altitudes relative to the rotor height at Luchterduinen (considering a hub height of 81 m and a rotor radius of 56 m), on average 48% of the total flux measured by the radar occurred at the height of the rotor-swept zone of 25 – 137 m. Furthermore, the proportion of tracks above the rotor-swept zone indicated that in the migration periods in spring and autumn a relatively higher proportion of birds pass by at higher altitudes than in the summer and winter (figure 6.2.2). In autumn 2021, a remarkably high proportion of tracks was recorded below rotor-swept zone.

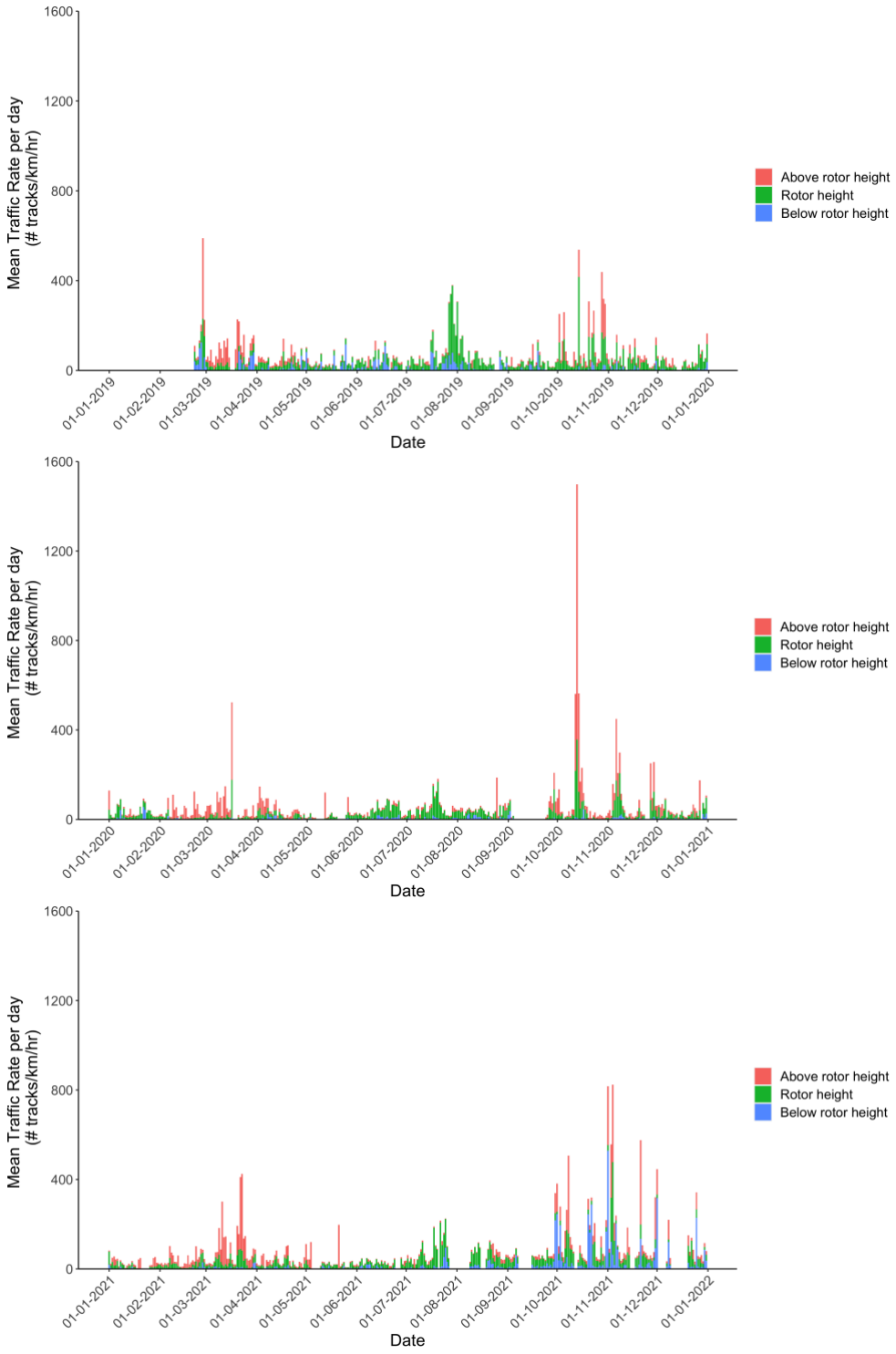

Figure 6.2.2 *Daily variation in mean traffic rate (MTR) in Luchterduinen separated for different altitude segments relative to rotor height: above rotor height (red bars), at rotor height (green bars), and below rotor height (blue bars), for 2019 (top figure), 2020 (middle figure) and 2021 (bottom figure). Each bar indicates the average MTR during each day.*

6.2.2 Observed species composition per height class

The combined dataset of the tagged radar tracks, visual observations and LRF measurements resulted in a total of 3,512 observations, of which lesser black-backed gull was by far the most numerous species in the dataset (n = 1,190), followed by great cormorant (n = 544) and black-legged kittiwake (n = 490).

The majority of the bird flight heights were from visual observations (2,495), followed by LRF (994) and only a few vertical radar tracks were used (23). Most LRF observations were carried out between 25 and 200 metres. However, visual observations accounted for the highest number of records in every height class. Finally, radar observations were only present above 10 metres.

Most birds were recorded between altitudes of 25 and 50 meters (figure 6.2.3). A total of 1,077 birds flew in this height class, which corresponds to 31% of the observations. Between 10 and 25 meters 1,050 birds were seen (30%), followed by 1,005 (18%) birds between 3 and 10 meters, 815 (14%) birds between 25 and 100 meters, and 239 (7%) birds between 0 and 3 meters. Respectively only 16 and 5 birds were recorded between 100-200 meters and above 200 meters.

The lesser black-backed gull was the most numerous species in all height classes above 10 metres. It was especially dominant in height classes 25-50, 50-100 and 100-200 metres with more than 40 percent of the observations in those height classes being a lesser black-backed gull. Below 10 metres, the great cormorant had the most observations of all species.

Above flight height values refer to point observations or to means of a flight track. However, birds do not necessarily fly at a constant altitude during their flight. Using the LRF, 33 birds could be followed for a longer period, resulting in at least two altitude measurements per track and hence providing the possibility to calculate variation in height during their flight. For 27 of the 33 birds, the range between the maximum and minimum heights was less than 10 metres. The highest measured range was 26 metres, where the minimum height of a lesser black-backed gull was 41 metres, and the maximum height was 67 metres. Although the measured flight heights are still a good representation of the flight height distribution, it is important to keep in mind that birds will always show some variation during their flights.

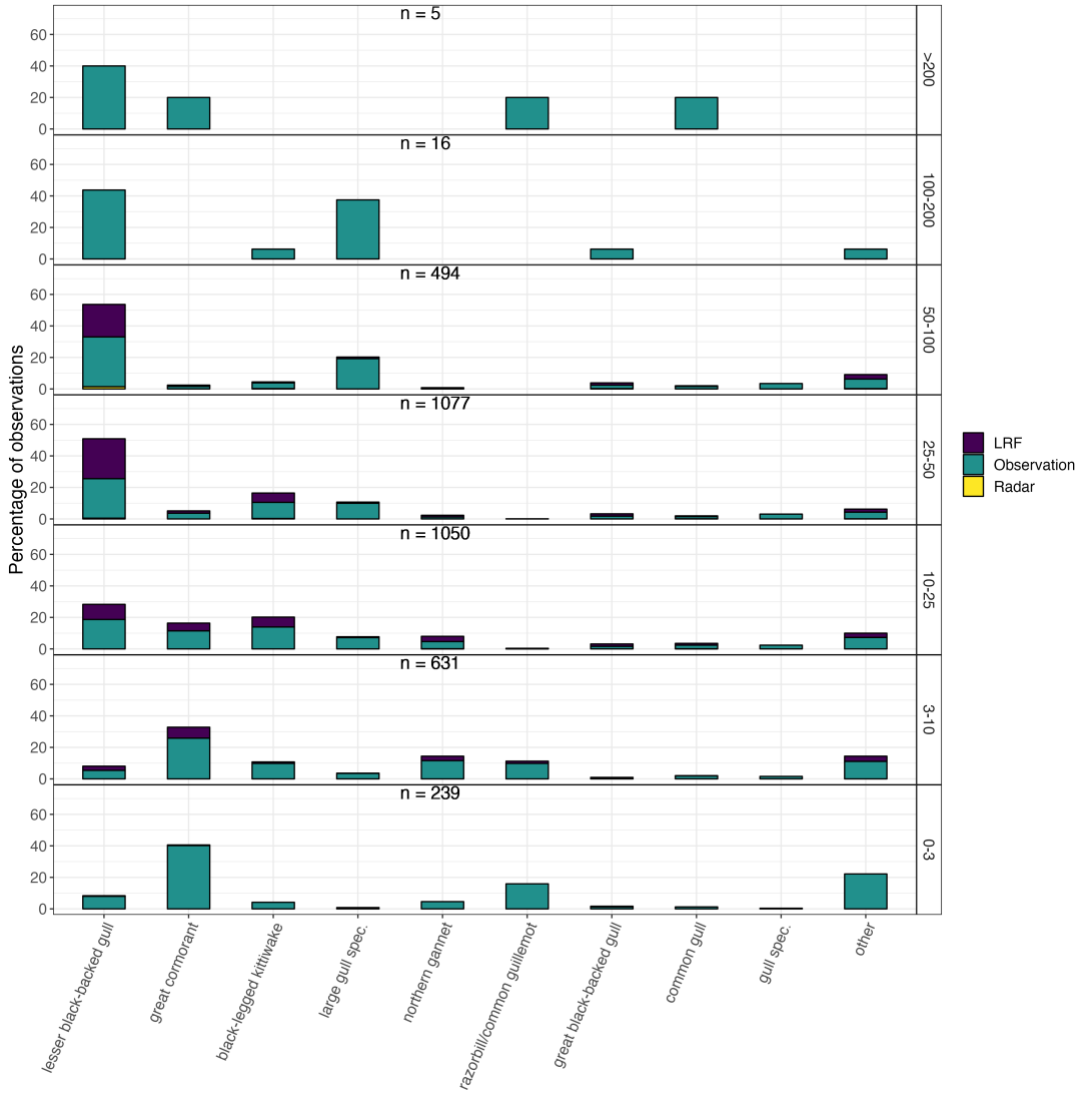

Figure 6.2.3 *Percentages of the observations that were done per species per height band based on tagged radar data, LRF measurements and visual observations. The number behind the species name shows the sample size.*

6.2.3 Species-specific flight height distributions

Combining the radar flux measurements per height class (§6.2.1) and the visual observations (§6.2.2) yielded 12 species (groups) with more than 30 observations. Five species (black-headed gull, common guillemot, great cormorant, northern gannet and razorbill) mostly flew at altitudes between 3-10 meters (figure 6.2.4). Of these, common guillemot and razorbill flew almost exclusively at this altitude category. However, note that the lowest three meters were excluded from this analysis, while some of these species may actually prefer to fly at these altitudes. Sandwich terns mostly flew between 10-25 meters. Lastly, the flux of black-legged kittiwake, common gull, great black-backed gull, herring gull, lesser black-backed gull and songbirds was highest within an altitude of 25-50 meters.

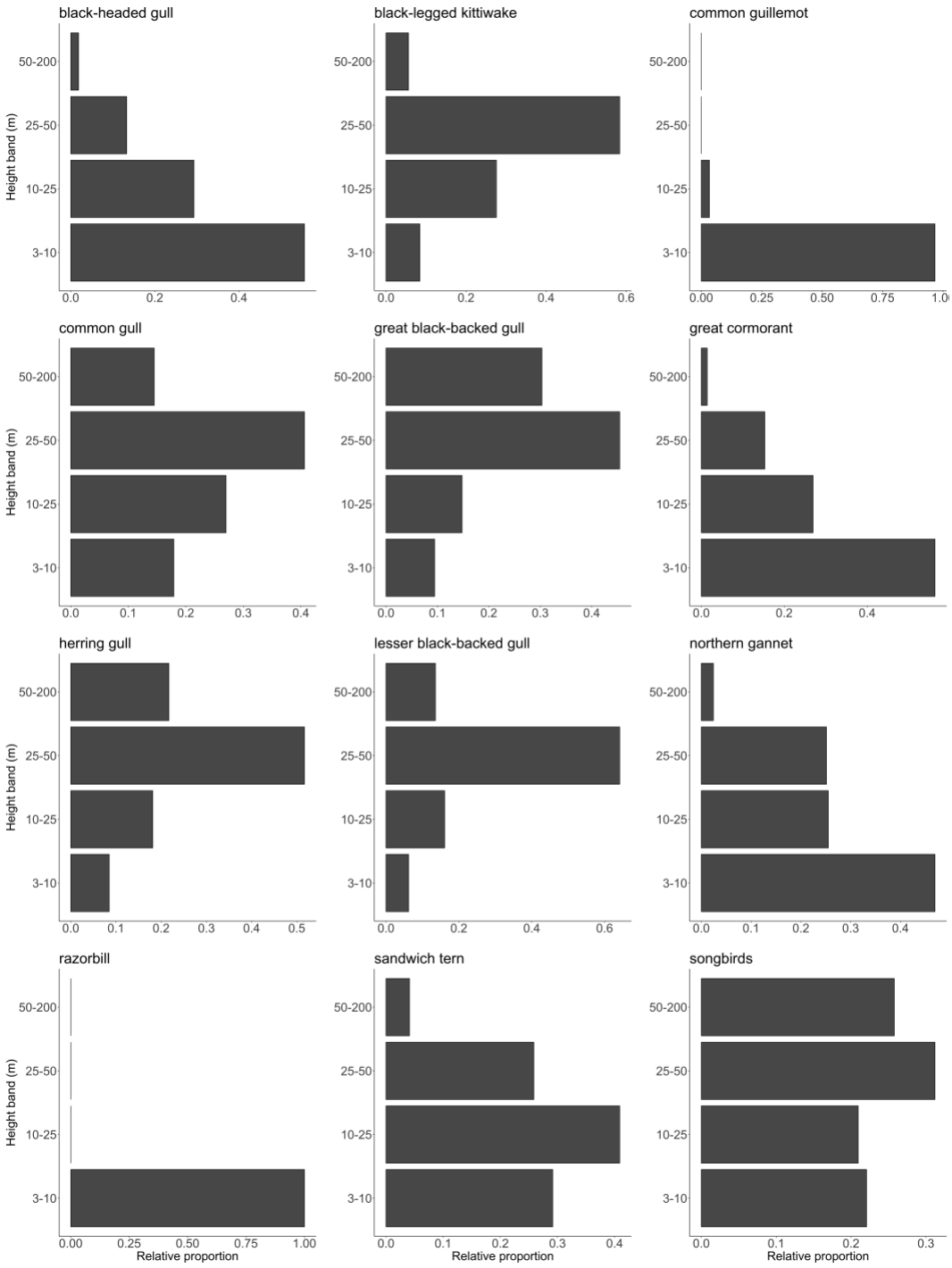

Figure 6.2.4 *Species-specific flight height distribution of species with more than 30 observations, calculated by applying species compositions to the fluxes measured by the radar in each height band. Bars show for each height band the proportion of flux relative to the width of the height band.*

6.3 Discussion

In this chapter, we present the altitude profile of the vertical radar in Luchterduinen. We found that most radar tracks were detected at altitudes below 5 meters, which might be explained by the fact that several species of seabirds tend to fly mostly just above the sea surface. However, it is very likely that wave clutter also significantly contributed to this pattern. Furthermore, we found that above 120 meters the number of detected tracks steadily decreased with altitude. We found no evidence of an increase in the number of tracks during the night at high altitudes as might be expected during nocturnal migration, especially in periods with favourable tailwinds. This could indicate an issue of detection loss towards higher altitudes, or alternatively that massive nocturnal migration might even occur at higher altitudes than 1.5 km, the indicated scanning range of the vertical radar.

We determined species-specific flight height distributions based on a combination of visual observations and radar measurements. We followed an indirect method to define flight height distributions, in order to avoid any biases due to unequal effort among different height bands, and also because birds at higher altitudes tend to be increasingly overlooked by visual observers (Thaxter *et al.* 2015; Borkenhagen *et al.* 2018). Consequently, the relative proportion of birds at higher altitudes could have been underestimated if flight height distributions were determined based exclusively on visual observations. Furthermore, birds flying at very low altitudes above the water surface or at very high altitudes are also challenging to be measured by a laser range finder (Borkenhagen *et al.* 2018). To avoid these biases, we separately calculated species compositions for each height band, instead of making a specific height distribution per species. Therefore, we had to assume that in each height band all species have an equal chance of being detected by an observer. While this assumption is arguable, we believe that this method still provides the best applicable species-specific flight height distributions considering biases of visual observations. Furthermore, the results are subject to the same uncertainties in the calculated monthly fluxes and species compositions as discussed before in §4.3 and §3.3.

We assumed that at altitudes higher than 200 m visual observers cannot provide reliable species compositions, hence the presented species-specific flight height distributions concentrated exclusively on altitudes below 200 m. Although a limitation, these altitudes are the most relevant in the context of wind energy and wildlife impacts (Piggott *et al.* 2021), which is also the case for Luchterduinen wind farm with a rotor swept zone at 26 – 136 m altitude. Furthermore, the number of observations for each species was not sufficient to calculate flight height distributions in height bands of 1 meter. This decreases the usability of the presented flight height distributions in the extended Band collision risk model that requires flight height distributions with height bands of 1 meter up to an altitude of 300 meter (Band 2012). Nevertheless, our results can be useful in for example the basic Band model that uses absolute fluxes at rotor height (Band 2000). For future studies it is important to define the observational height categories in agreement with the local lower and upper tips of the rotors, in order to be able to calculate species-specific percentages of birds at rotor height precisely.

Almost no tagged radar tracks were used in the calculation of species compositions per height band, as only vertical radar tracks allow for height analyses. Most tagged tracks from

the vertical radar were also detected by the horizontal radar, leading to a combined track. Heights of combined tracks were not always reliable, which is why they were left out of each height analysis. However, this led to only 23 tagged vertical radar tracks that could be used.

Finally, we determined species-specific fluxes per altitude band. For these calculations, we applied the species compositions per altitude band to the number of tracks measured by the vertical radar in that altitude band. While according to the visual observations only 4% of the birds were seen in the altitude class 0 – 3 m, the radar had the highest number of measurements at an altitude 0 – 5 m. Although the measurements of very low-flying birds by visual observers can be challenging (Borkenhagen *et al.* 2018), the mismatch between the visual- and radar observations is striking and points towards the contamination of the lowest altitude range of the radar measurements by wave clutter. Therefore, in the reported species-specific fluxes, this altitude band (0 – 3 m) was discarded. Nevertheless, due to our method to calculate fluxes per altitude band independently from each other, these high fluxes at very low altitudes do not influence the species-specific fluxes calculated for the rotor-swept zone (see §6.2.4).

Based on our results, common guillemot and razorbill flew almost exclusively at the lowest altitude category up to 10 m, corresponding with the general knowledge of flight altitude of these species (Cook *et al.* 2012; Johnston *et al.* 2014). Also the relatively low flight Sandwich terns at the altitude band of 10-25 meters matched expectations (van Bemmelen *et al.* 2022). The preferred altitude band of 25-50 meters for black-legged kittiwake, common gull, great black-backed gull, herring gull, lesser black-backed gull and songbirds is higher than could be expected based on for example the work of Johnston *et al.* (2014), summarizing a large number of observations on offshore flight heights. Note, however, that those measurements mainly relied on visual observations, with all their limitations pinpointed above. GPS measurements showed that 65% of the herring gull flights occurred below 25 m (Gyimesi *et al.* 2017), versus 76% estimated by Johnston *et al.* (2014). For lesser black-backed gulls the GPS measurements showed 63% of flights below 25 m, versus 79% estimated by Johnston *et al.* (2014). Such underestimations of flight heights by visual observers have already been reported earlier (Harwood *et al.* 2018). In contrast, Borkenhagen *et al.* (2018) already reported that large gulls and cormorants have a preferred flight height that corresponds with the rotor-swept area.

7 Flight speed

7.1 Methods

As mentioned before, the horizontal radar can collect data of various parameters, of which one is the airspeed of the detected bird. Airspeed is the speed of an object corrected for the wind speed and direction, as measured by the weather station of the radar. However, that weather station is positioned next to the radar on the turbine and hence measured wind speeds and wind directions are likely influenced by the wind turbine and the radar itself. Moreover, the guidance issued alongside the Band (2012) model, and consequently the sCRM (Marine Scotland 2018), clearly states that in collision risk models ground speeds, which is the speed of an object relative to the ground, should be considered. Therefore, in this chapter we present flight speed as ground speed, calculated as the travelled distance of a track divided by the duration of it for each radar track that was tagged during visual observations. In this analysis, only species with at least 5 tagged horizontal radar tracks were used (also see §3.2.2).

7.2 Results

The average flight speed was calculated for the eleven most frequently tagged bird species(groups), which consisted of eight gull species(groups) and three other species, namely northern gannet, Sandwich tern and great cormorant. The horizontal radar dataset consisted mainly of lesser black-backed gulls (n = 543), followed by great cormorants (n = 159) and black-legged kittiwakes (n = 56).

Interestingly, the eight gull species(groups) all had lower average flight speeds than the other three species considered in this analysis (figure 7.2.1 and table 7.2.1). The fastest flying species was the great cormorant with an average of 16.49 m/s, followed by the northern gannet (14.90 m/s) and the Sandwich tern (13.90 m/s). On average, the slowest species was the common gull, with an average flight speed 11.43 m/s. The most abundant species, the lesser black-backed gull, had an average flight speed of 12.25 m/s.

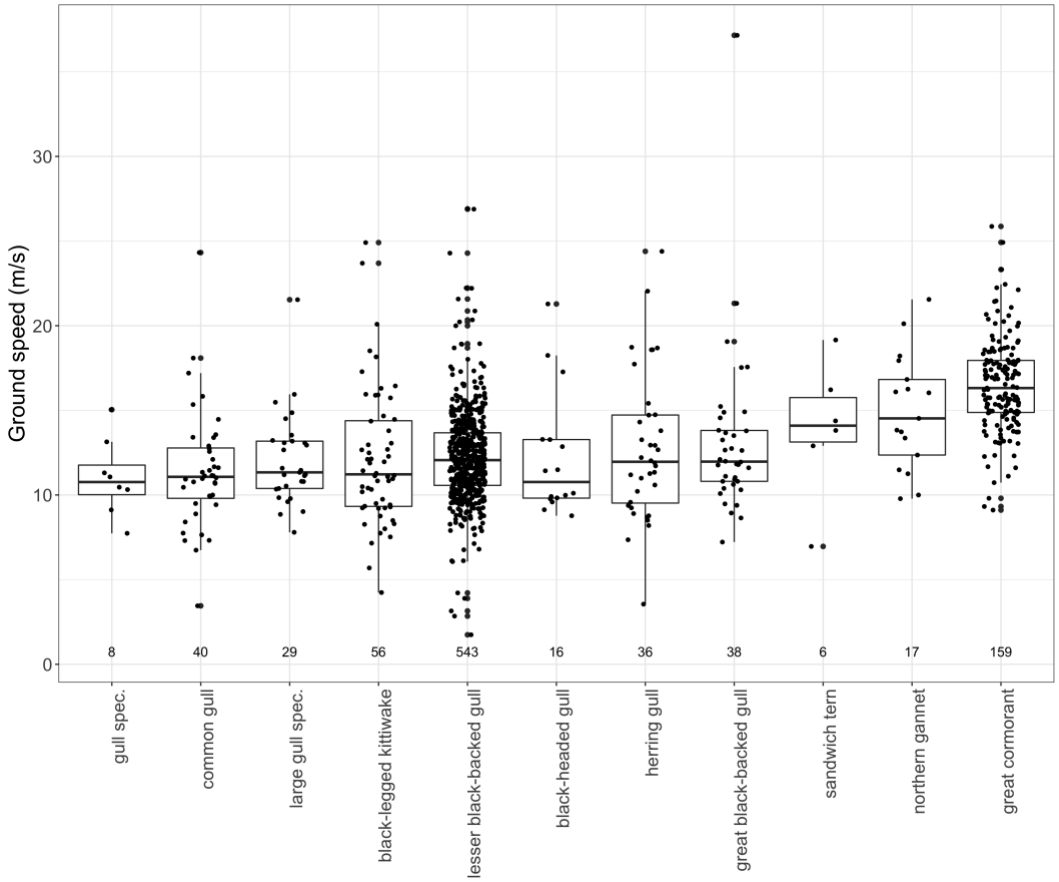

Figure 7.2.1 *Boxplots of the species(group)-specific groundspeeds, as measured by the horizontal radar. Only species with at least 5 measurements are shown, with dots giving the individual measurements. Boxes represent the 25th and 75th percentiles, with the lines within giving the median. Error bars above and below the boxes are 1.5 times the size of the box. Numbers below boxplots show the sample sizes of that species(group).*

7.3 Discussion

In this chapter, the average flight (ground) speed of the most abundant species was calculated based on tagged radar tracks. Results showed higher flight speeds for cormorants, Sandwich terns and northern gannets, compared to gull species. Interestingly, all gull species showed very similar flight speeds. Variation within species could be the result of varying wind direction and wind speed but also different kind of flights, *e.g.* commuting versus foraging flights (Cleasby *et al.* 2015; Fijn & Gyimesi 2018; Masden *et al.* 2021). Nevertheless, all measured flight speeds fall within the range of previously published values, which were also used in CRM calculations (table 7.2.1).

When compared with other published ground speed data gathered with GPS-loggers, which are available for Sandwich terns (Fijn & Gyimesi 2018), lesser black-backed gull and herring gull (Gyimesi *et al.* 2017), the radar measurements seem to give relatively high flight speeds (table 7.2.1). Data from GPS-loggers resulted in a mean flight speed of 10.3 m/s for Sandwich terns, which is 3.6 m/s lower than what the tagged radar measurements

indicated. Also, lesser black-backed gulls had a large difference in speed when compared between radar and GPS. Finally, the herring gull showed a smaller difference, but still had a 1.6 m/s higher flight speed based on radar data than what was measured by GPS-loggers. Interestingly, the largest deviations with previously published flight speed data occurred when compared with GPS logger data: comparisons with airspeed data from Alerstam *et al.* (2007) resulted in smaller differences. This could either point towards GPS loggers affecting the speed of birds, or more likely that birds adjust their flight speed once entering or flying around a wind farm. This may also be reasonable if birds are found in specific kind of flights in and around the wind farm, leading to higher flight speeds. For example, Fijn & Gyimesi (2018) found that Sandwich terns had a higher flight speed when commuting than when foraging. The average flight speed of commuting flights in that study was 12.3 m/s, still lower than the 13.9 m/s that was measured by the radar, but the difference is considerably smaller than when compared with the overall mean of 10.3 m/s reported by Fijn & Gyimesi (2018). If this also holds for other species, it could give an indication that more commuting birds were recorded by the radar suggesting a suppressed foraging behaviour of birds in the wind farm. However, air turbulence caused by the wind turbines could might eventually affect birds' flight height (Thaxter *et al.* 2018). Moreover, it is important to note that the difference in the types of measurements between GPS-loggers and radar could also result from different measurement errors. Moreover, the sample size of the radar measurements is rather low compared with the GPS-loggers, and hence conclusions about the average flight speed should be made with caution.

Table 7.2.1 *Overview of the mean ground speeds and their standard deviations (SD) as measured by the radar, compared to flight speeds used in CRM calculations for the KEC (Leopold et al. 2015; Potiek et al. 2022).*

Species	sample size	ground speed (m/s) (radar)	SD	flight speed in CRMs
black-headed gull	16	12.3	3.7	11.9[1]
black-legged kittiwake	56	12.1	4.1	13.1[1]
great black-backed gull	38	13.2	4.9	13.7[1]
great cormorant	159	16.5	2.8	15.2[1]
herring gull	36	12.8	4.4	11.3[2]
lesser black-backed gull	543	12.3	2.8	9.4[2]
common gull	40	11.4	3.5	13.4[1]
northern gannet	17	14.9	3.4	14.9[3]
Sandwich tern	6	13.9	4.1	10.3[4]

Data come from (1) airspeeds in Alerstam *et al.* (2007); (2) ground speeds measured by GPS-loggers in Gyimesi *et al.* (2017); (3) airspeed in Pennycuick (1990); (4) ground speeds measured by GPS-loggers in Fijn & Gyimesi (2018).

Data that are known for the other species, such as great cormorant, come from Alerstam *et al.* (2007) and Pennycuick (1990). It is important to note here that these flight speeds are measured based on airspeed. As mentioned, airspeed is the ground speed corrected for the wind speed and direction and can therefore deviate somewhat from the ground speed. However, the flight speeds measured in the two mentioned studies are relatively similar to the ground speeds measured in this study. For instance, measured flight speeds of the northern gannet are precisely the same in our study as reported by Pennycuick

(1990). The largest difference in flight speed between this study and that of Alerstam *et al.* (2007) is for the common gull, which is 2.0 m/s, still smaller than the differences with GPS-logger measurements. As both Alerstam *et al.* (2007) and Pennycuick (1990) intended to carry out measurements on “steadily” flying birds, which should be best represented by commuting or transit flights, and even excluded foraging or searching flights, our above points on behavioural differences in flight behaviour leading to the flight speed differences could also hold for these species.

8 Nocturnal activity

8.1 Methods

Monthly nocturnal activity was calculated using vertical radar data of tracks intersecting with flux lines as used in the flux calculations (§4.1). For each month, the absolute number of tracks was divided between tracks during day and tracks during night based on the local sunrise and sunset times retrieved from the R package 'suncalc' (Thieurmel & Elmarhraoui 2019). Also, we determined for each month the number of daylight and night-time hours that were present in the filtered dataset. We then calculated the relative percentage of tracks per day and night by correcting for the number of daylight and night-time hours in each month.

8.2 Results

The relative percentage of tracks during day and night shows a clear pattern with an increasing proportion of night-time tracks during spring and autumn migration in their respective peak months March and October (figure 8.2.1). Outside the migration periods, in January, June, July, August and December, more than 63-73% of the tracks were detected during daytime. If without any further information on species composition during the night we assume that migratory birds were absent during these months (which could only partly be the case), these results could suggest that local birds together show a maximum nocturnal activity between 27-37%. If we further assume that the nocturnal activity of local birds remains constant during the year (which may differ due to varying species composition), then these results could imply that nocturnal bird migration causes about 39-49% of all tracks during March and 33-43% of all tracks during October. Following this reasoning, this would mean that on average roughly 52,000-65,500 birds migrate per km through Luchterduinen in March during the night, while in October this would be 57,500-75,000 birds.

For the daily patterns in MTRs during day and night throughout the study period see §4.2.

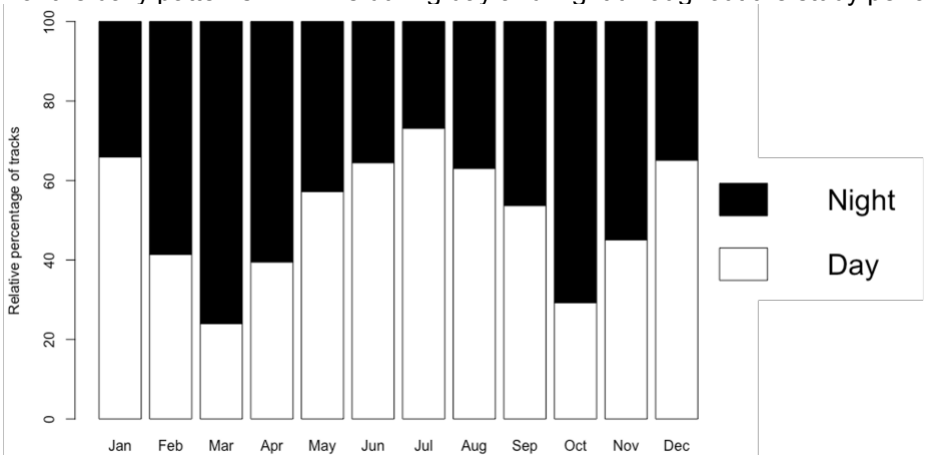

Figure 8.2.1 *Percentage of tracks during night (black) and day (white) in each month corrected for the monthly numbers of daylight and night-time hours.*

8.3 Discussion

Our results show a clear pattern in the monthly nocturnal activity in Luchterduinen. In this study we could not determine species compositions at night, due to the practical limitations to do visual observations at night. Therefore, we could not determine species-specific nocturnal activities. However, based on the rough assumption that no migration occurs in the months January, June, July, August and December, we calculated that local birds together might show a nocturnal activity between 27-37%. Previous assumptions on nocturnal activity of the most numerous birds in the area lay between 0% and 50% (Potiek *et al.* 2022). Therefore, the overall (mean) nocturnal activity likely lies between these percentages, and is thus comparable to our results. The presented results could therefore be in line with what could be expected.

Using several rough assumptions, we estimated that approximately 52,000-65,500 birds migrate per km at altitudes within range of the vertical radar through Luchterduinen in March during the night, while in October this would be 57,500-75,000 birds. As discussed before (§4.3), the actual numbers will likely be underestimated, as respectively 28% and 41% of all hours are filtered out in March and October. Correcting for this would mean that in March and October respectively roughly 72,200-91,000 and 97,500-127,000 birds per km migrate through Luchterduinen at night. This might partly be compensated, however, as fluxes may quickly be overestimated if rain showers or wave clutter were still present in the filtered dataset. Excluding the lowest three meters from this calculation results in a flux at night in March and October of respectively roughly 71,500-89,500 and 94,000-120,000 birds per km. This implies that these numbers come with great uncertainty. However, the numbers seem within the same order of magnitude as reported by Krijgsveld *et al.* (2011) in offshore wind farm OWEZ. Krijgsveld *et al.* (2011) reported for spring and autumn a total flux (day and night together) of respectively 167,980 and 329,524 tracks per km. If we apply the percentages of nocturnally migrating birds presented in this study to these total numbers in OWEZ, we could estimate that roughly 65,000-82,000 nocturnally migrating birds in spring and 109,000-142,000 in autumn pass by in OWEZ. These results suggest that the spring flux of nocturnal birds in Luchterduinen is slightly higher, and the autumn flux is slightly lower than in OWEZ. However, considering the large uncertainties around these measurements and the two different radar set ups including different tracking algorithms, we could conclude that the results in fact are largely comparable.

9 Macro-avoidance

9.1 Methods

9.1.1 Visual observations

During field days, the observers made observations within and outside the wind farm (§2.2.3). Therefore, these visual observations (corrected for observation effort) provided a dataset with the numbers of each species inside and outside the wind farm, with which we calculated species-specific macro-avoidance rates. Data gathered during observations from WTG 33 and 39 were not considered in this analysis, as from these turbines only observations within the wind farm were done, leaving only data collected from WTG 41. We consider the areas included in the observations inside and outside the wind farm to be of the same size as both sides were observed according to a standard protocol (§2.2.3).

For a selection of species, we statistically tested whether the numbers of birds within the wind farm were significantly different from the numbers outside the wind farm. We considered all species with at least 50 observations and added two seabird species with less observations, resulting in the species list of lesser black-backed gull (n = 945), black-legged kittiwake (n = 421), great cormorant (n = 369), northern gannet (n = 219), razorbill/guillemot (n = 139), great black-backed gull (n = 119), common gull (n = 91), common guillemot (n = 66), herring gull (n = 60), sandwich tern (n = 42) and razorbill (n = 34). The statistical comparison was carried out using generalized linear mixed models (GLMM). A separate model was made per species to assess the effect within species. When dealing with count data, the most appropriate distribution in GLMM is a Poisson distribution. However, using Poisson distributions can lead to two difficulties. The first issue is zero-inflation, caused by a large number of zero observations (*i.e.* no bird of a specific species seen during a count). In this analysis, we dealt with zero-inflation by removing all days where a particular species was not observed either within- or outside the wind farm. The other issue can be a violation of the assumption that the mean of the response variable is equal to its variance. For some species, this was not the case, meaning there was a higher- or lower variance than the mean. This is called over- or underdispersion, respectively. The way to deal with over- and underdispersion is to switch to another distribution, namely the negative binomial distribution. Therefore, for cormorant, great black-backed gull, common gull, Sandwich tern and razorbill a negative binomial distribution was used. All analyses were done using the 'glmmTMB' package in R (Brooks *et al.* 2017).

9.1.2 Radar measurements

Another analysis to quantify macro-avoidance was based on the filtered data of bird tracks crossing the beam of the vertical radar. For the number of tracks inside the wind farm, a detection line was drawn starting at WTG 42 (*i.e.* the location of the radar) running toward WTG 41 (figure 9.1.1). The length of this line within the wind farm was 1,100 m. A line of

the same length running from WTG 42 in the opposite direction (towards NW) was used to calculate the number of tracks outside the wind farm. A difference in the number of tracks that crossed outside the wind farm relative to the number of tracks inside the wind farm was considered as an indication of macro-avoidance. To investigate the effect of distance to the wind farm (*i.e.* the turbine on which the radar was installed), the flux line was divided into segments with a length of 100 m each and the fluxes along these segments pairwise compared inside and outside the wind farm.

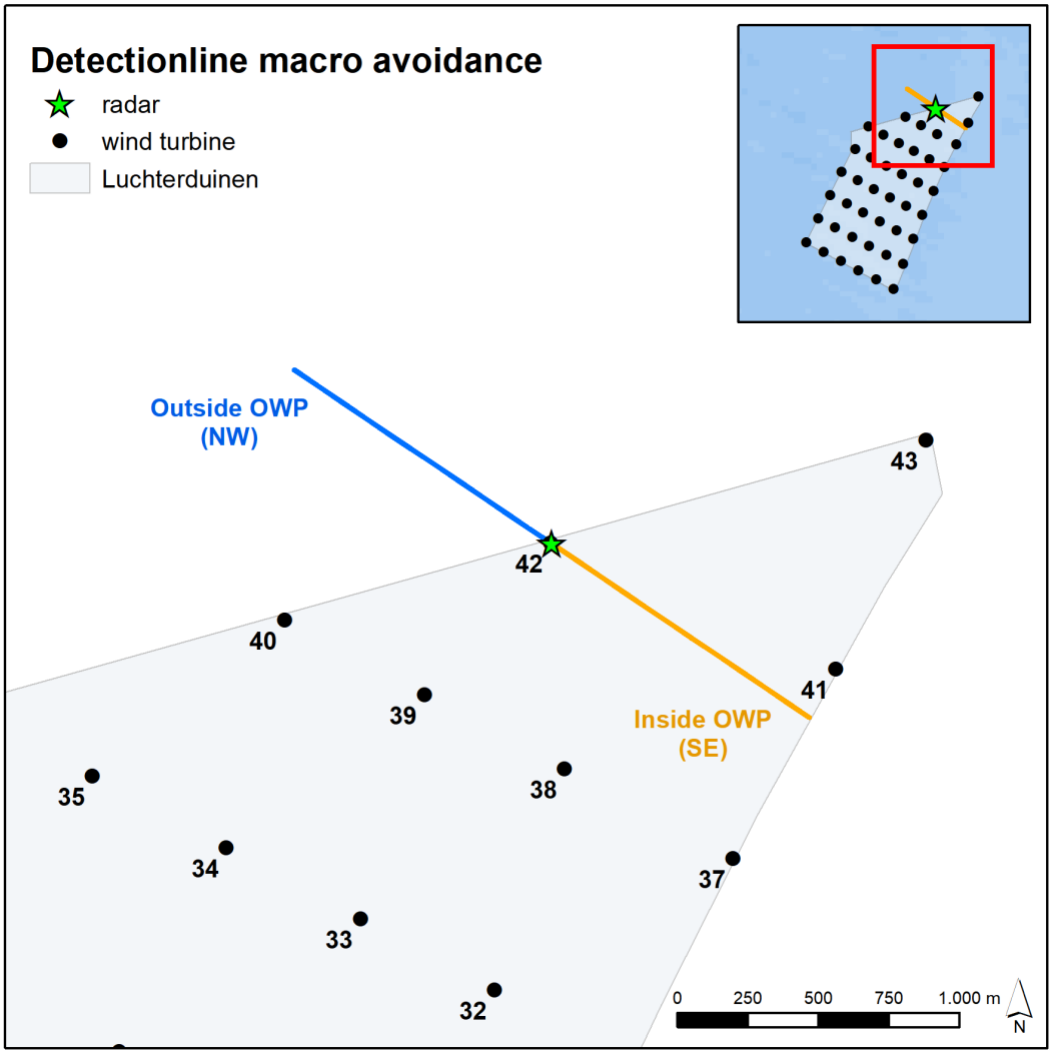

Figure 9.1.1 *Detection line used for the macro-avoidance calculations based on radar measurements. Blue line indicates the detection line for the number of tracks outside the wind farm, while the yellow line was used for the number of tracks inside the wind farm.*

We also considered other factors that might affect the number of tracks that crossed the detections line, being average height of the track and season. Average height (m) was determined for each track by averaging the height over all track points (*i.e.* single radar measurements during each turn of the radar, compiling to a track). Only tracks with an average height of more than 0 m were included. Season was defined as spring (March,

April and May), summer (June, July and August), autumn (September, October, November) and winter (December, January, and February).

To estimate the difference in bird flux between the area inside and outside the OWF, the bird flux was modelled using a Generalized Linear Model (GLM) in the package `R-INLA`. As data exploration showed that the direction of the effect of the OWF differs between seasons, with lower flux inside compared to outside the OWF in spring and summer and the other way around autumn and winter, a single model was fitted with the number of intersecting bird tracks per day as the response variable, and an OWF-effect, season, and the interaction between OWF and season as fixed effects. Random intercepts were included for 100 m segments and for date. Note that in this way, date is not directional or sequential. Finally, the log of the number of hours with data on each day was included as an offset, effectively modelling the number of passes per segment per hour. The response, the number of tracks per segment per day, was assumed to follow a negative binomial distribution. The joint posterior distributions of fluxes inside and outside the OWFs were used to estimate the proportion attraction (higher flux inside the OWF than outside) or avoidance (higher flux outside the OWF than inside) for each season. The posterior distribution of the ratio between these two (1 - $FLUX_{inside}$ / $FLUX_{outside}$) are then compared with 0. If 0 is within the 95% highest density interval (HDI), the absence of an effect of OWF on flux cannot be excluded, whereas an effect of the OWF is supported if 0 is outside the 95% HDI.

9.2 Results

9.2.1 Visual observations

Visual observations of the eleven species that we considered showed that for most species generally more observations were recorded outside the wind farm than inside (table 9.2.1). The exceptions to this rule were great cormorant (48% more observations inside the wind farm), herring gull (40%) and common gull (33%). Moreover, only one more observation of the great black-backed gull was noted outside the wind farm (n = 60) than inside (n = 59). The most numerous species in the study area, the lesser black-backed gull, was 10% less present inside the wind farm than outside. The species that seemed to avoid the wind farm the most was the Sandwich tern, with 60% less observations within the wind farm than outside.

Model estimates of the GLMM testing for differences in the number of birds inside and outside the wind farm per hour for the eleven most observed species are depicted in figure 9.2.1. Interestingly, all gull species considered in this analysis, showed no significant difference in their presence within and outside the wind farm, which means that based on our visual observations there was no evidence for macro-avoidance. On the other hand, the great cormorant was significantly more abundant within the wind farm than outside it. In contrast, several species were significantly more often present outside the wind farm than inside, which was the case for northern gannet, guillemot, Sandwich tern and the combined group of razorbill/guillemot. Finally, for razorbills, just as for gulls, no difference

in number of observations was found, but this species had the lowest number of observations.

Table 9.2.1 *Summary of the raw data of visual observations inside and outside the wind farm. The percentage shows the abundance (number of birds observed per hour) inside the wind farm relative to outside the wind farm. The p-value shows the outcome of the GLMM. Significant differences in the number of observations between inside and outside the wind farm are indicated with an asterisk (*). The days are the number of days taken into account in these models.*

Species	**Inside observations**	**Outside observations**	**Total observations**	**Difference**	**P-value**	**Days**
lesser bl.-b. gull	447	498	945	-10.24%	0.82	28
bl.-leg. kittiwake	195	226	421	-13.72%	0.72	19
great cormorant	220	149	369	47.65%	<0.0001*	39
northern gannet	85	134	219	-36.57%	0.02*	32
razorbill/guillemot	47	92	139	-48.91%	0.02*	20
great bl.-b.gull	59	60	119	-1.67%	0.78	22
common gull	52	39	91	33.33%	0.34	24
common guillemot	24	42	66	-42.86%	0.01*	17
herring gull	35	25	60	40%	0.20	23
Sandwich tern	12	30	42	-60%	<0.0001*	11
razorbill	15	19	34	-21.05%	0.87	8

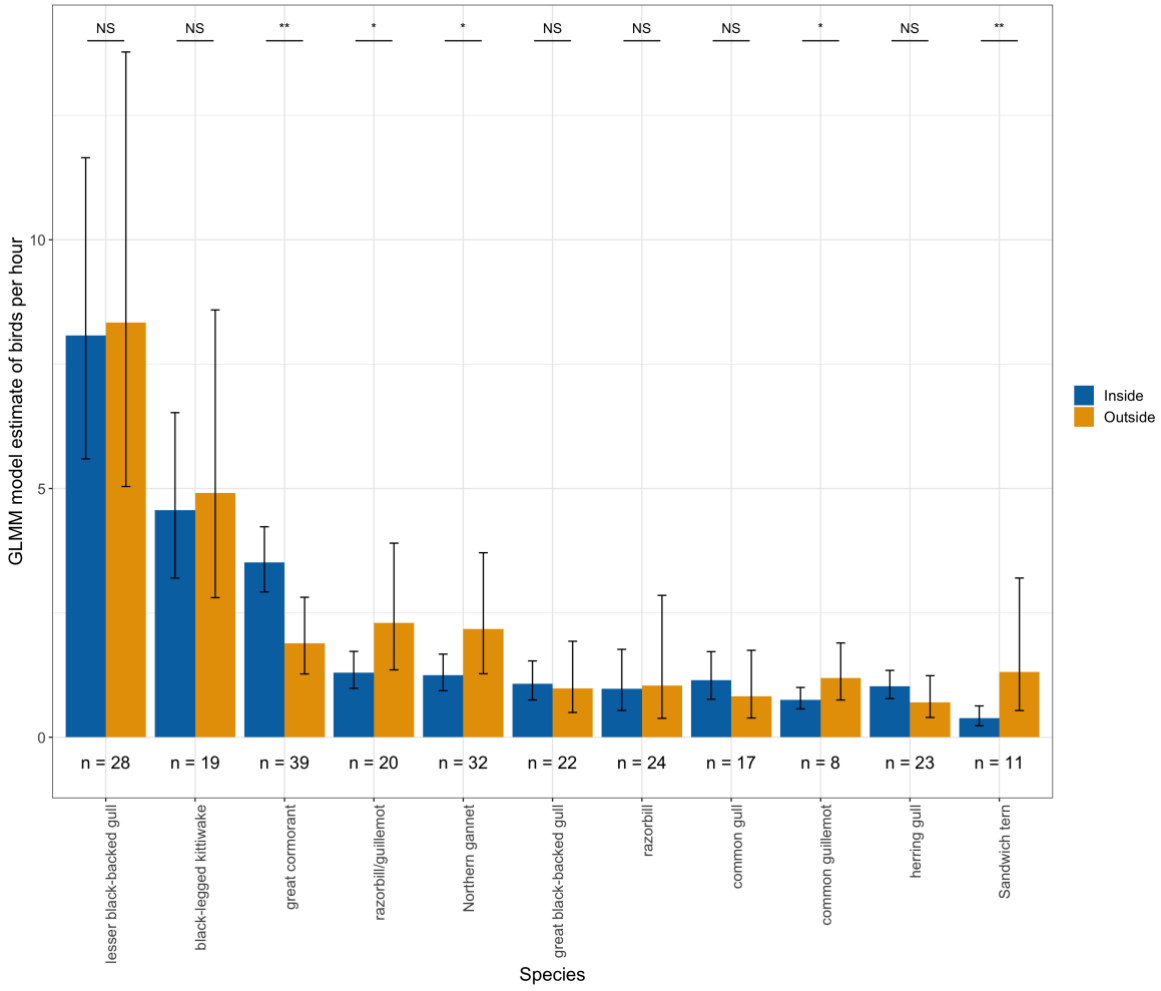

Figure 9.2.1 *Bar plot of the model estimates of the GLMMs when testing for differences between the number of observations outside the wind farm and inside the wind farm. The model estimates were calculated on the log scale, the figure depicts exp(model estimate) converted values. The error bars show ± standard errors. Annotations above the bars stand for non-significant (NS), p-value < 0.05 (*) or p-value < 0.01 (**). The numbers below the bars show for each species the number of observation days that were included in the model.*

Behaviour inside and outside the wind farm

The different kind of behaviours inside and outside the wind farm for species with at least 100 visual observations are shown in table 9.2.2. The most frequent kind of behaviour was 'flying'. This was the case for every species. Landing and sitting on the water were seen for almost all species inside and outside the wind farm. Interestingly, cormorants landed in 8.5% of the observations, while this was only the case for 2.7% of the observations outside the wind farm. Although this landing could be either on the water or on a turbine, given the location of the wind farm which is more than 20 km out of the Dutch coast, this indicates that cormorants occupy the wind farm as expansion of their foraging areas. This is supported by the fact that many of the cormorants were seen sitting on a turbine, which is known to be a popular resting place during foraging trips. Finally, the species that sat the

most on the water were razorbill/guillemots in the wind farm as well as outside of the wind farm.

	great cormorant		great bl.-b. gull		bl.-l. kittiwake		lesser bl.-b. gull		northern gannet		razorb./ guillemot	
Behaviour	*In*	*Out*	*In*	*Out*	*In*	*Out*	*In*	*Out*	*In*	*Out*	*In*	*Out*
Other	-	-	-	-	-	1 (0.4%)	-	-	-	-	-	-
Diving	-	-	-	-	1 (0.5%)	1 (0.4%)	-	-	3 (3.5%)	3 (2.2%)	-	-
Dynamic soaring	-	-	-	1 (1.7%)	1 (0.5%)	1 (0.4%)	2 (0.4%)	-	-	-	-	-
Landing	18 (8.5%)	4 (2.7%)	4 (6.8%)	2 (3.3%)	2 (1.0%)	-	6 (1.3%)	8 (1.6%)	1 (1.2%)	1 (0.7%)	-	2 (2.4%)
On turbine	16 (7.5%)	-	-	-	-	-	3 (0.7%)	-	-	-	-	-
On water	1 (0.5%)	-	1 (1.7%)	1 (1.7%)	1 (0.5%)	3 (1.3%)	13 (2.9%)	15 (3.0%)	1 (1.2%)	2 (1.5%)	9 (19.6%)	13 (15.5%)
Flying up	2 (0.9%)	2 (1.4%)	-	-	-	-	1 (0.2%)	-	-	-	-	-
Flying	175 (82.5%)	142 (95.9%)	54 (91.5%)	56 (93.3%)	187 (97.4%)	217 (97.3%)	421 (94.4%)	474 (95.4%)	80 (94.1%)	128 (95.5%)	37 (80.4%)	69 (82.1%)

Table 9.2.2 Overview of the different kind of behaviours that were observed inside and outside the wind farm. The six species with at least 100 observations are displayed here.

9.2.2 Radar measurements

After carrying out the filtering steps, 16,209 hours out of a total of 25,056 hours remained in the dataset for analysis.

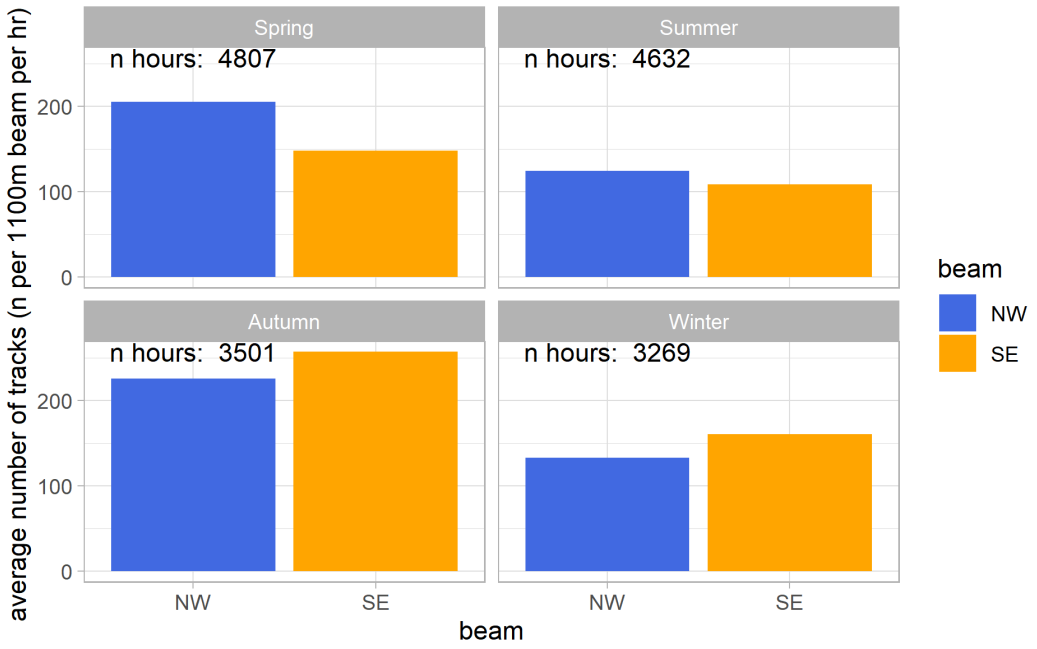

Figure 9.2.2 *Average flux per hour for the different seasons on NW and SE side of the radar.*

We did not find a consistent difference between the number of tracks outside or inside the wind farm (*i.e.* respectively NW vs SE from the radar) (figure 9.2.2), with a higher number of tracks outside the wind farm in spring and summer, and a higher number of tracks inside the wind farm in autumn and winter.

To further specify these results and investigate the effect of distance to the wind farm, the flux line was divided into segments with a length of 100 m each. Subsequently fluxes were further broken down into average fluxes per hour per month (figure 9.2.3). Note that detection loss of the radar may generally affect the actual number of tracks per segment. Therefore, this analysis did not intend to compare average fluxes between segments on the same side of the radar. For instance, within the distances used for this analysis, the flux increases with the distance to the radar on both sides of the radar. In general, this analysis revealed similar patterns between segment pairs to the average fluxes along the entire flux line.

Statistical analysis of the flux per day per segment revealed that flux was higher outside the OWF during spring and summer, but this difference was reversed in autumn and winter (figure 9.2.4, table 9.2.2). A strong difference between inside and outside the OWF was found for winter, spring and autumn, but not for summer. Remarkably, in both autumn and winter, 36% more birds were detected within the OWF compared to outside the OWF, suggesting attraction to the OWF (figure 9.2.4). The statistical analysis showed that 0 falls clearly outside the posterior distributions of the difference between inside and outside the OWF (table 9.2.2), indicating that this difference was significant. In spring, ca. 29% less birds were detected within compared to outside the OWF (figure 9.2.4). Again, with 0 falling clearly outside the posterior distribution, this difference could also be considered as significant (table 9.2.2). In summer, the difference between inside and outside the OWF

was small, and the results are inconclusive as to whether there was an effect of the OWF on flux (figure 9.2.4, table 9.2.2).

Table 9.2.2 *Macro-avoidance rates. Values above 0 indicate avoidance, with higher flux outside compared to inside the OWF, values below 0 indicate attraction, with lower flux outside compared to inside the OWF.*

Season	Macro-avoidance rate	Lower 95% HDI	Upper 95% HDI
Winter	-0,36	-0,67	-0,09
Spring	0,29	0,13	0,43
Summer	0,07	-0,15	0,27
Autumn	-0,36	-0,64	-0,12

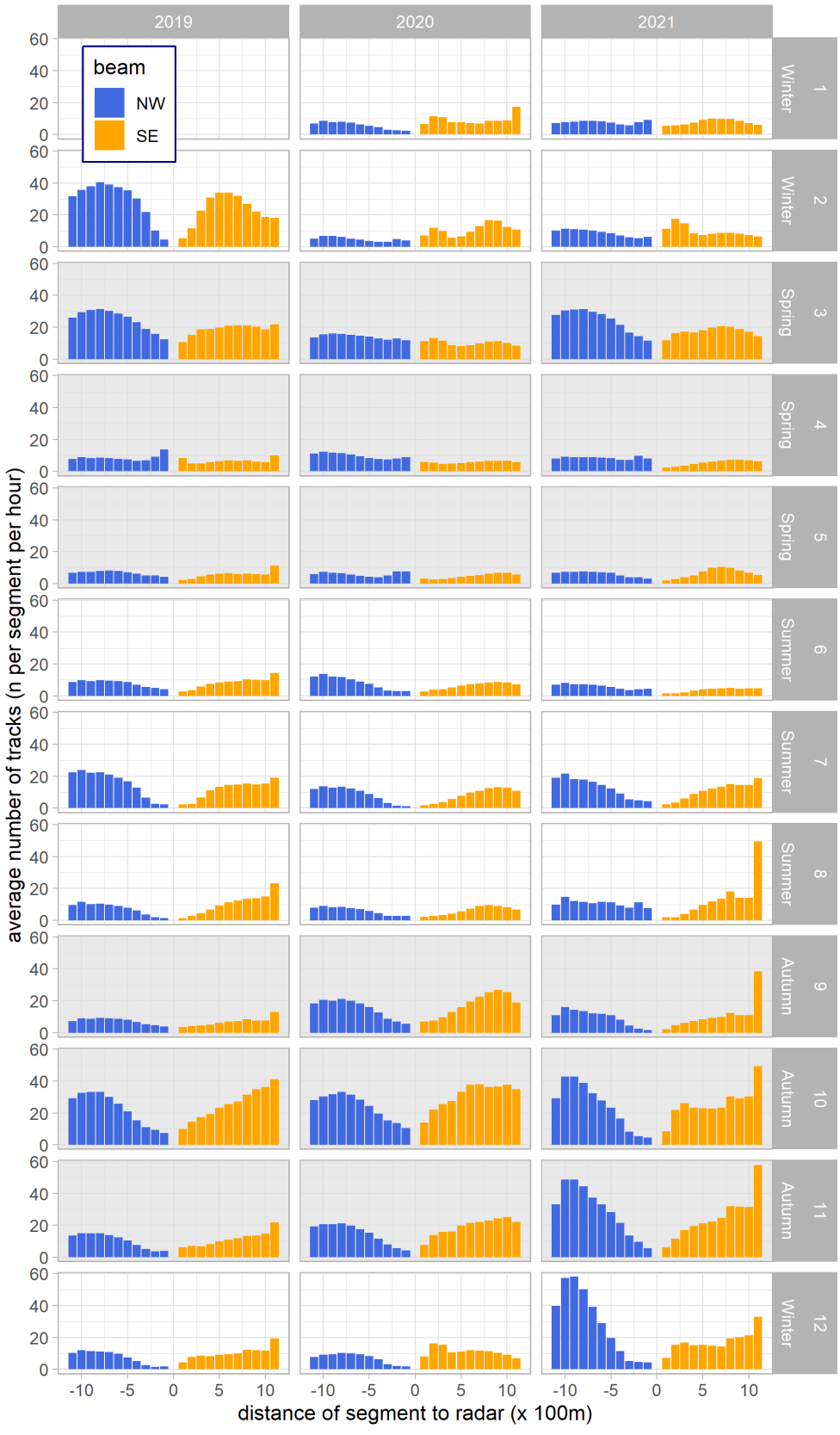
2019
2020
2021
beam
NW
SE
Winter 1
Winter 2
Spring 3
Spring 4
Spring 5
Summer 6
Summer 7
Summer 8
Autumn 9
Autumn 10
Autumn 11
Winter 12
average number of tracks (n per segment per hour)
0
20
40
60
-10
-5
0
5
10
distance of segment to radar (x 100m)

Figure 9.2.3 *Average flux per beam per hour for each month and separated for different distances to the radar in segments of 100 m.*

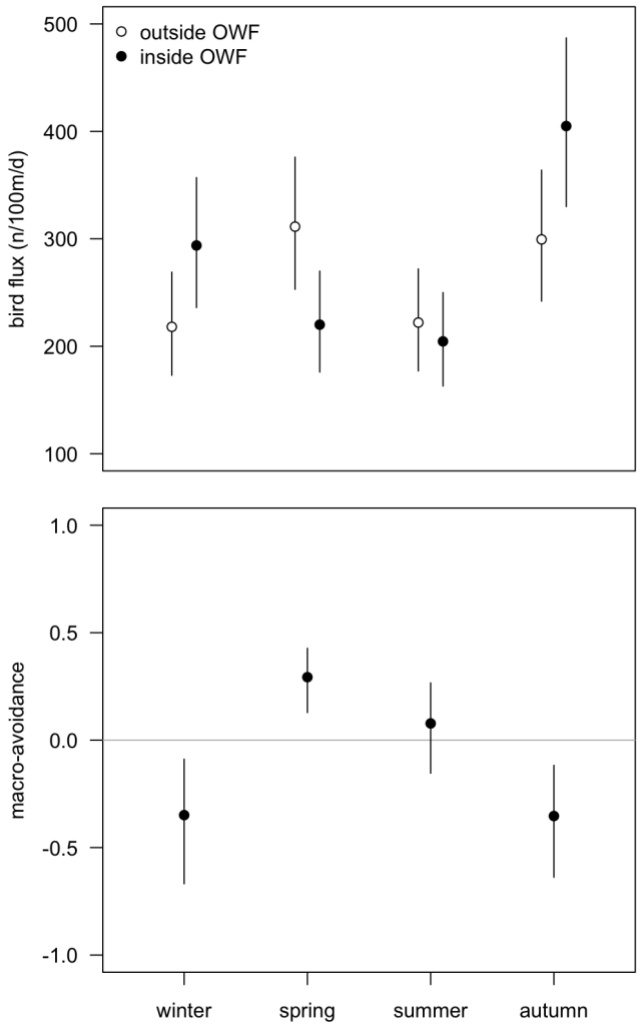

Figure 9.2.4 *Posterior distributions of the model parameters of the flux per day for four seasons outside (white) and inside (black) the OWF (upper figure). In the lower figure, joint posterior distributions of the avoidance rate between inside versus outside the OWF. Negative values indicate higher fluxes inside compared to outside the OWF, suggesting attraction; positive values suggest avoidance. The horizontal line indicates 0, i.e., no effect. If 0 falls within the posterior distribution, the absence of an effect of the OWF on bird flux cannot be excluded, conversely, an effect is indicated when 0 falls clearly outside the posterior distribution.*

9.3 Discussion

9.3.1 Visual observations

Based on the visual observations, we statistically tested if there was evidence for differences in numbers of individuals between inside and outside the wind farm for eleven of the most observed species. Interestingly, there were species with higher numbers inside the wind farm than outside, but also species for which we found the opposite pattern. One species that was significantly attracted to the wind farm is the great cormorant. Species that significantly avoided the wind farm were northern gannet, common guillemot (and the species group razorbill/guillemot) and Sandwich tern.

That cormorants were attracted to the wind farm concurs with literature (Dierschke *et al.* 2016). Dierschke *et al.* (2016) reported that in four wind farms more cormorants were observed within the wind farm than outside, namely the Robin Rigg, North Hoyle (both UK), Prinses Amalia and Egmond aan Zee (both the Netherlands) windfarms. There could be a few explanations for these increases in cormorants around wind turbines. First, there might be increased prey availability around wind farms. Second, the wind turbine structures allow cormorants to extend their foraging grounds further from the coast, offering resting places to dry their wings (Krijgsveld *et al.* 2011; Krijgsveld 2014). Petersen *et al.* (2006) also found that cormorants used the turbine structures as resting places but found no overall effect of attraction in the Horns Rev wind farm. In this wind farm, however, migrating cormorants showed a different, more panicking, response towards the wind farm than foraging cormorants.

Also, avoidance of wind farms by northern gannets, common guillemots and Sandwich terns is supported by literature (Dierschke *et al.* 2016). Presence of northern gannets of a colony in Helgoland was reduced up to 37% within the wind farm relative to areas outside the wind farm in a study using GPS tags in the southern North Sea (Peschko *et al.* 2021). This percentage exactly matches the reduction in numbers within the wind farm we found in our study. Peschko *et al.* (2021) could, however, determine that 87% of the gannet individuals predominantly showed avoidance behaviour around the wind farm, and hence only 13% of the individuals were bold enough to remain using the wind farm area. However, Skov *et al.* (2018) found that northern gannets avoid wind farms at a higher rate (*i.e.* 79,7%) than according to our results, suggesting that avoidance behaviour may be location specific, depending likely on wind farm configuration (Leopold *et al.* 2013), distance of the wind farm to the coast and colonies (Goodale & Milman 2020; Pollock *et al.* 2021), but also on age composition and sex ratios of the local population (Lane *et al.* 2020; Pollock *et al.* 2021; Hamer *et al.* in prep.), and the season the measurements were carried out (Lane *et al.* 2020).

In another study with GPS tags, common guillemots showed 63% reduction in numbers inside the wind farm compared with outside the wind farm in spring and 45% in the breeding season (Peschko *et al.* 2020a). Avoidance even increased when turbines were operative. Moreover, guillemots mainly entered the wind farms when resting on the water or when diving, meaning that during commuting flights, avoidance was the highest. The percentage

of avoidance in spring is higher than the 43% we found in our study, but matches the results for the breeding season (Peschko *et al.* 2020a), which on its turn also corresponds well with 50% found in the Dutch OWEZ and PAWP wind farms close to Luchterduinen (Leopold *et al.* 2011). Hence, besides seasonal differences, these results again suggest locally diverging effects of wind farms.

Finally, breeding Sandwich terns were found to show macro-avoidance of wind farms between 5-22% based on GPS tracks (van Bemmelen *et al.* 2022). This exercise was based on individually tagged terns, while our much higher avoidance percentage (*i.e*. 60%), is a numerical decrease considering all individuals of the species in the surroundings. Again, this could point towards individual-level differences in how birds cope with the presence of wind farms (cf. Peschko *et al.* 2021 for northern gannets).

Finally, gulls tended to show indifferent responses towards the wind farm in our study. For instance, lesser black-backed gulls only showed a 10 percent reduction in numbers inside the wind farm compared with outside, and this reduction was not significant. Skov *et al.* (2018) defined macro-avoidance rates for all large gull species and black-legged kittiwakes, but a review of existing literature indicated that gull species show no consistent response towards the presence of an offshore wind farm (Cook *et al.* 2018). This was also supported by visual observations in the Dutch wind farm OWEZ (Krijgsveld *et al.* 2011). Also, GPS telemetry studies with lesser black-backed gulls showed no avoidance of wind farms and used the wind farm areas regularly. For instance, targeted analyses conducted by Vanermen *et al.* (2022). on the distribution of lesser black-backed gulls inside and near the wind farms could not detect meso- nor macro-avoidance responses. Also Thaxter *et al.* (2018) showed that the species did not avoid wind farms as a whole. However, in the same study, individual gulls seemed to avoid the rotor swept zones of wind turbines indicating meso-avoidance behaviour, although this was based on GPS data of only two individuals. Also, Krijgsveld *et al.* (2011) mentioned observations of gulls not avoiding the wind farm but reporting that the birds were well aware of the turbines, indicating micro- or meso-avoidance.

Besides the large gull species, we found no significant effect of the wind farm on the smaller gull species either. Regarding the effects of offshore wind farms, black-legged kittiwakes have been the subject of a number of studies. In their review, Dierschke *et al.* (2016) also concluded that kittiwakes belong to the species group that are hardly affected by offshore wind farms. Although Peschko *et al.* (2020b) found that the relative density of kittiwakes decreased by 45% in offshore wind farms in the breeding season, but in spring (*i.e*. outside the breeding season) only not significantly by 10%. This latter figure matches our results (*i.e*. a not significant reduction by ±14%), also resulting mainly from observations outside the non-breeding season, as most of our observations on this species occurred in the period October-March (see table 4.2.1).

9.3.2 Radar measurements

Based on a comparison of the number of vertical radar tracks outside and inside the wind farm, we did not find a clear indication of macro-avoidance across seasons. We

investigated macro-avoidance up till 1,100 m from the radar, which was positioned at the edge of the wind farm. However, macro-avoidance may be initiated already at a larger distance from the wind farm, considering wind farms should be well visible for seabirds – under good weather conditions – at distances of 10 km or more. Skov *et al.* (2018) used 3 km outside the wind farm as a distance within which macro-avoidance could occur. Therefore, at least part of the birds that intend to avoid the wind farm, could do that already at distances that were not investigated here. On the other hand, our measurements on macro-avoidance from the wind farm inherently encompass also meso-avoidance behaviour, as birds may also display avoidance behaviour of the turbine where the radar was installed.

Also, effects of detection capabilities of the radar were not taken into account in our analysis. Detection rate within the radar beam is dependent on the width of the beam and the distance from the radar, but these relationships are not linear. Further from the radar, detection loss can occur due to a weakened radar signal. Nevertheless, such effects should occur on both sides of the vertical radar. Thus, in our comparison of the number of tracks inside and outside the wind farm, such effects should cancel out each other. However, one artefact in the radar measurements could be side-dependent and should be further investigated in the future. In figure 9.2.3, a large number of tracks are depicted in the second half of 2019 and 2021 in the furthest segment on the southeast side of the radar, where one would expect a decreasing number of tracks due to detection loss, rather than such an apparent increase. These measurements were conducted within the wind farm, with the furthest segment reaching WTG 41 (see figure 9.1.1). As in another study, we found indications in wind farm Borssele that wind turbines may induce tracks that enter the database as birds (Leemans *et al.* 2022), it should be explored whether these tracks are not caused by wind turbines instead of by actual birds.

In summary, there might be various reasons for the lack of consistent macro-avoidance in the radar measurements. First of all, the radar is now located at the edge of the wind farm, so the radar measurements 'inside' the wind farm are actually at the periphery of the wind farm (see figure 9.1.1). We have observed on numerous occasions that birds avoided passing through the widest part of the wind farm and crossed in between the wind turbines in this edge of the wind farm instead of flying around the most northerly wind turbine (*i.e.* WTG 43), *i.e.*, the part that is covered by the radar. While these birds could also be recorded by the vertical radar, our visual observations were oriented towards the centre of the wind farm and are probably less influenced by this side effect. In the future, it would be interesting to compare the flux outside the wind farm to a flux further inside the wind farm, such as the setup in Borssele wind farm will allow.

Furthermore, most birds around Luchterduinen did not show avoidance behaviour. Assuming most of the unidentified gulls belonged to one of the large gull species, approximately half of all birds showed neither attraction, nor avoidance (see § 3.2). Adding the small gull species that did not show a significant difference in numbers inside and outside the wind farm leads to two third of all birds showing no clear avoidance behaviour. In fact, only northern gannet, common guillemot (and the species group razorbill/guillemot) and Sandwich tern showed a significant avoidance response to the wind farm, equalling

12,5% of all birds around Luchterduinen. Against this proportion of birds, the great cormorants, with more than 15% of the observations and showing a very strong attraction, already compensate for the number of birds clearly avoiding the wind farm.

10 Meso-avoidance

10.1 Methods

10.1.1 Horizontal meso-avoidance

For the analysis of meso-avoidance, we calculated the number of tracks detected by the horizontal radar that intersected with a detection line along the turbines WTG 37 – WTG 40 over the period 22-02-2019 till 31-12-2021 (25,056 hours). The horizontal track data were filtered per hour for rainy periods and clutter (see §2.1.2), after which 9,826 hours remained in the dataset.

Along the detection line, we distinguished three types of segments (figure 10.1.1):
1) along the width of the rotor-swept zone (RSZ) plus 10 m buffer (2 x 65 m and 2 x 130 m; further referred to as 'turbine' segment);
2) segments in between the turbines but close to the RSZ (6 x 135 m; referred to as 'inter' segment);
3) and segments halfway in between two turbines (3 x 150 – 250 m; referred to as 'further' segment).

Seasons most likely affect the number of crossings, since the number of crossings is expected to be higher during migration in spring and autumn. Therefore, season was defined as in §9.1. For all seasons, fluxes were determined per line segment and corrected for length of the segment.

For statistical analysis, the data was aggregated per day. In addition, the two distance categories away from the turbine were joined, so that a single parameter for meso-avoidance could be estimated, based on the difference in flux between the turbine zone and the two zones away from the turbine. Despite these aggregations, a substantial proportion of the response variable consisted of zeros (27%, n = 4,803). Such a high proportion can be problematic in modelling, because distributions are not always able to capture such a large proportion of zeros. Therefore, four Generalized Linear Mixed Models (GLMMs) were fitted: a Poisson GLMM, negative binomial GLMM, zero-inflated Poisson GLMM and a zero-inflated negative binomial GLMM. The zero-inflated models had no covariates in their binomial part (the part modelling zeros versus positive values). The fit of the resulting models was compared using the Widely Applicable Information Criterion (WAIC), and the model with the lowest WAIC was selected. Models included the category for proximity to the turbine (two levels) and season (four levels), plus their interaction, as response variables. In addition, random intercepts were included for year and date, as well as for segment. Finally, the log of the length of the segment (in km) divided by the number of hours with data was included as an offset, thereby effectively modelling the number of tracks per km per hour. Subsequently, the joint posterior distributions of the estimates per season were compared between close the turbine and away from the turbines to show the

strength of the effect and whether an absence of an effect could be excluded: when the 95% high density interval (HDI) did not include 0.

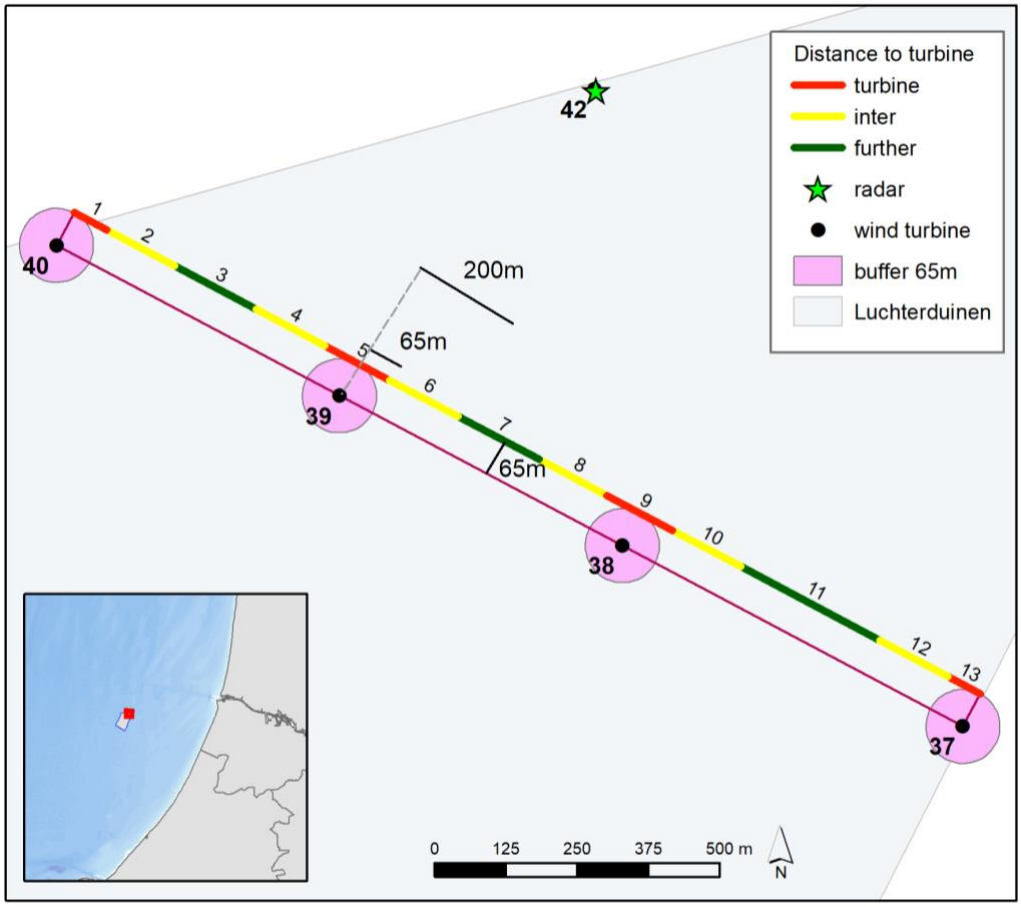

Figure 10.1.1 *The detection line used to investigate meso-avoidance is classified in segments based on the distance to the buffer zone (rotor-swept zone + 10 m) of the nearest turbine. Segments are numbered individually. For reference, also the location of the radar on turbine 42 of wind farm Luchterduinen is provided.*

10.1.2 Vertical meso-avoidance

To analyse the effect that the wind farm has on meso-avoidance in the vertical plane, we looked at all data from the vertical radar between April 2019 and April 2021, covering every season exactly two times. Within the northwest-southeast orientation of the beam of the vertical radar, one turbine (WTG 41) is positioned at 1,100 m to the southeast. We considered vertical meso-avoidance to be a vertical change of the flight path in the proximity of the turbine, compared to other locations within the vertical beam, either being in the wind farm or at the same distance from the radar but outside the wind farm. To exclude tracks that might be generated by the turbine and falsely detected by the radar as birds, or conversely have to deal with missing tracks due to the shadowing effect of the turbine, we did not use the number of tracks at or below rotor height for the comparisons. Therefore, we chose another approach and compared the number of birds in the same altitude band just above the rotor height. Here we made the assumption that more birds

flying in the zone just above rotor height around the turbine, compared to numbers at the same distance from the radar but outside the wind farm or elsewhere within the wind farm along the vertical radar beam, might indicate that birds elevate their flight altitude when nearing a turbine. In order to investigate a direct reaction on the presence of the wind turbine, we only considered an altitude bin just above the tip height, namely the tip height plus one rotor swept area (112 meters), resulting in an altitude bin of 137 to 249 meters above sea level. Birds flying higher were assumed to be able to pass the wind farm area without any change in their flight behaviour.

This analysis focused on the number of tracks that were present in each 100-meter segment measured from the radar. To exclude altitude measurements in the vicinity of the radar that might be compromised by reflections of the turbine the radar is situated at, we only considered segments >500 meters from the radar. Turbine 41 to the southeast of the radar has a rotor swept area of 110 m, and hence we assumed that vertical meso-avoidance could occur in segments from 1000 to 1200 meters (segments 11 and 12 in this analysis).

10.2 Results

10.2.1 Horizontal meso-avoidance

Table 10.2.1 shows the total length of the three segment types along the detection line, the number of tracks that crossed these segments and the number of tracks corrected for the segment lengths (*i.e.* density of tracks). The density of tracks increased with the distance to the turbines, indicating the occurrence of meso-avoidance. The average flux density along the detection line was 0.03301 tracks per meter per hour (total number of tracks (583,845) / total detection length (1,800m) / total number of hours (9,826)).

When comparing the density of tracks passing through the segments belonging to the turbine zone (0.02303 tracks/m/h) with the average flux along the whole line (*i.e.* including also the segments inter and further), we found that 43.4% less birds flew along the footprint area of the turbine plus rotor-swept zone with a 10 m buffer, than one could expect in case of a uniform distribution of the total flux along the line.

Table 10.2.1 The total length of the three segment types along the detection line (turbine = segment along the rotor-swept zone (RSZ) + 10 m buffer; inter = outside the RSZ close to the turbine; further = halfway the detection line; see also figure 10.1.1), the number of tracks that crossed these segments and the number of tracks corrected for the segment lengths and the total number of observation hours (9,826), resulting in density of tracks.

Segment relative to the nearest turbine	length (m)	n tracks	density (n tracks per m per hour)
Turbine segment	390	88,252	0.02303
Inter segment	810	272,561	0.03425

Further segment	600	223,032	0.03783

The average seasonal flux per hour shows an interesting pattern, with the average flux along the category ‘turbine’ segment is in all seasons lower than along the surrounding segments (figure 10.2.1). Also, the category ‘further’ has in general a higher flux than the surrounding ‘inter’ segments. Furthermore, we found that the west side of the flux line seems to have a higher flux than the east side (figure 10.2.2). The average flux is relatively high in summer and autumn, compared to winter and spring.

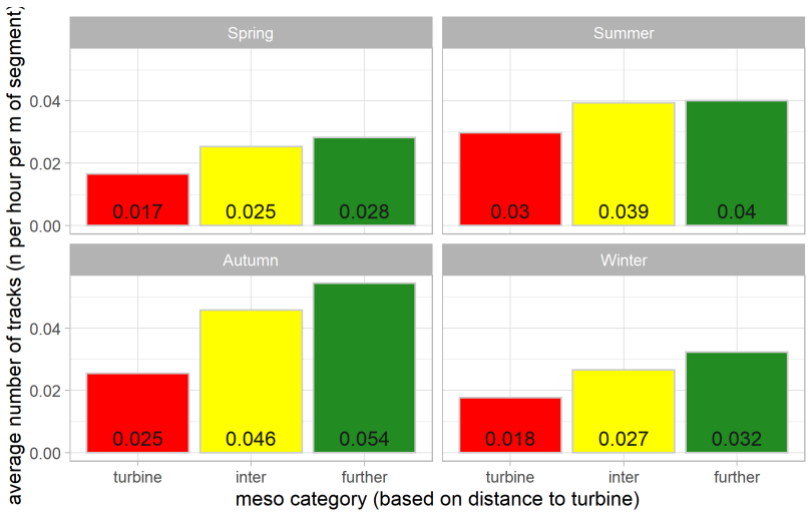

Figure 10.2.1 *Average flux per segment relative to the nearest turbine (see figure 10.1.1) for all seasons. Note that these fluxes include birds that flew below and above rotor height.*

The model with a negative binomial distribution had a much better fit than the other models, with the next-best model being the zero-inflated negative binomial model (ΔWAIC = 3486). Flux was consistently higher away from the turbines compared to segments close to the turbines, in all seasons. This translated in ratios between the two distance categories, indicating meso-avoidance (figure 10.2.3, table 10.2.2). In all seasons, flux was *ca.* 60% lower close to the turbine than further away, and all 95% HDI of these estimates were clearly above zero (figure 10.2.3, table 10.2.2).

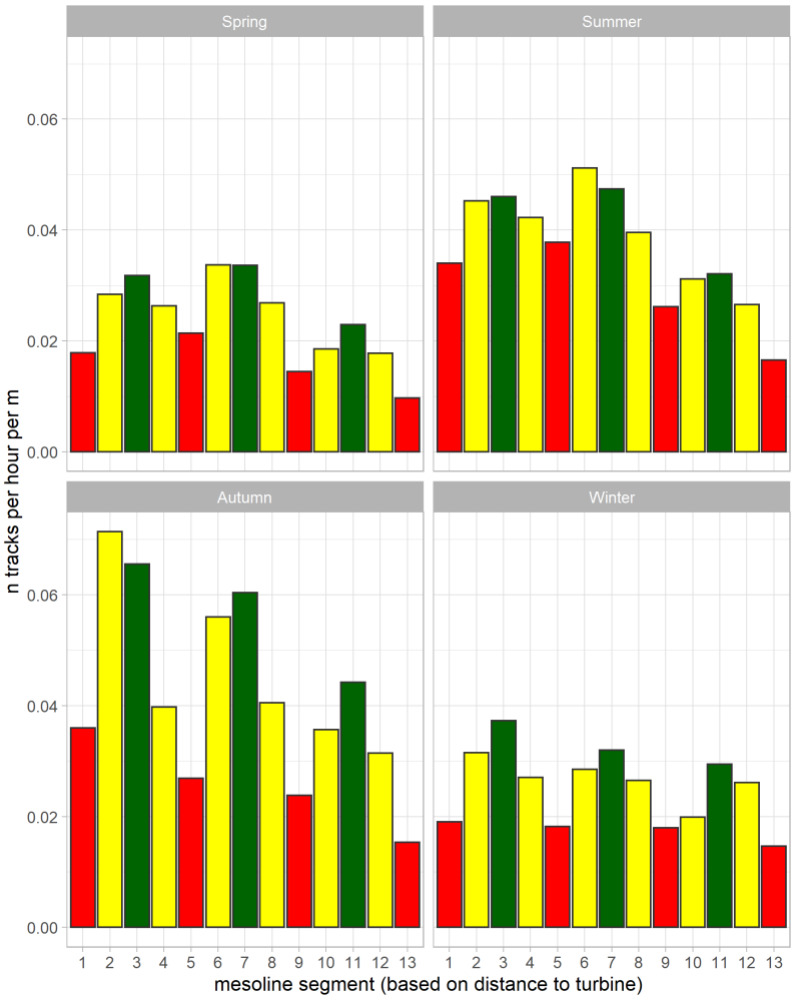

Figure 10.2.2 *Average number of tracks that crossed the detection line per season and per segment. The segment id's and colours correspond to the segments of figure 10.1.1, where id=1 is located on the far west of the detection line and id=13 on the far east. Similarly, red indicates 'turbine', yellow indicates 'inter', and the green 'further'.*

Table 10.2.2 *Meso-avoidance rates. Values above 0 indicate avoidance, with higher flux outside compared to inside the turbine zone.*

Season	Meso-avoidance rate	Lower 95% HDI	Upper 95% HDI
Autumn	0.61	0.44	0.75
Winter	0.58	0.41	0.73
Spring	0.59	0.43	0.71
Summer	0.67	0.41	0.87

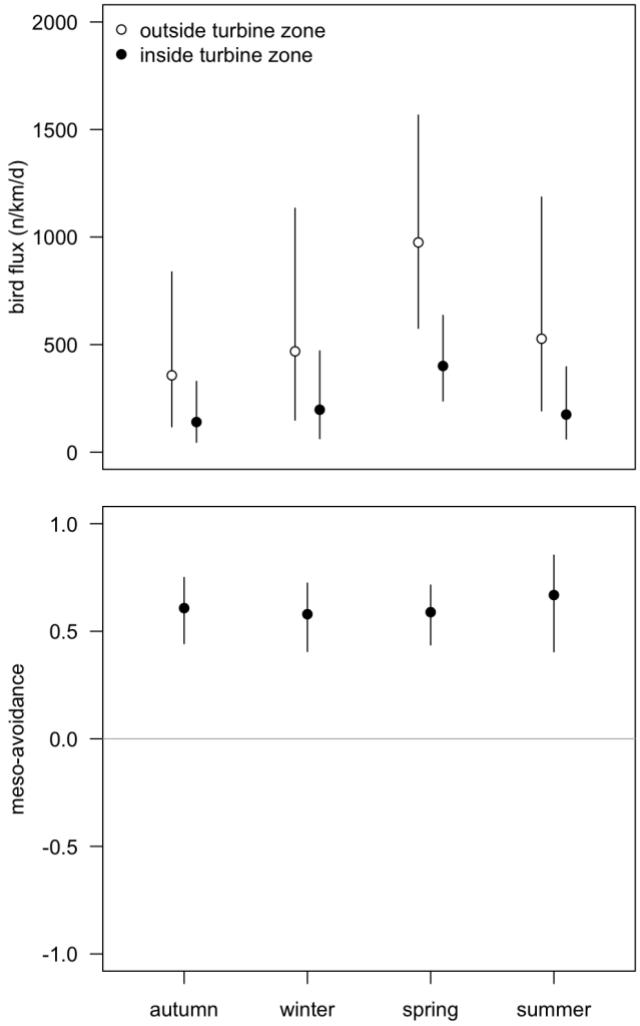

Figure 10.2.3 *Posterior distributions of the model parameters of the flux per day for four seasons outside (white) and inside (black) the turbine zone. In the lower panel, joint posterior distributions of the difference between inside vs. the turbine zone are shown. Negative values indicate higher fluxes inside compared to outside the turbine zone. The horizontal line indicates 0, i.e., no effect. 0 falls clearly outside the posterior distributions indicating a strong effect.*

10.2.2 Vertical meso-avoidance

Our analysis provided some indications of vertical avoidance, although the results were not utterly convincing. First of all, in all seasons more birds flew just above rotor height inside the wind farm than outside the wind farm (table 10.2.3). Interestingly, both sides of the radar showed very similar patterns, with an increase in the number of tracks just above rotor height with distance from the radar peaking at 1,100 meters where turbine in the radar beam is situated (figure 10.2.4). However, within the wind farm this peak at segment 11 was visible in almost each season (table 10.2.4), while this differed per season outside the

wind farm between 1,000-1,100 and 900-1,000 meters from the radar. The largest absolute difference in numbers above rotor height inside the wind farm occurred in autumn (table 10.2.4).

Table 10.2.3 Number of bird tracks per hour just above rotor height in both beams per season.

Season	NW	SE
Spring	1.21	1.38
Summer	1.43	2.17
Autumn	6.15	8.17
Winter	3.51	4.13

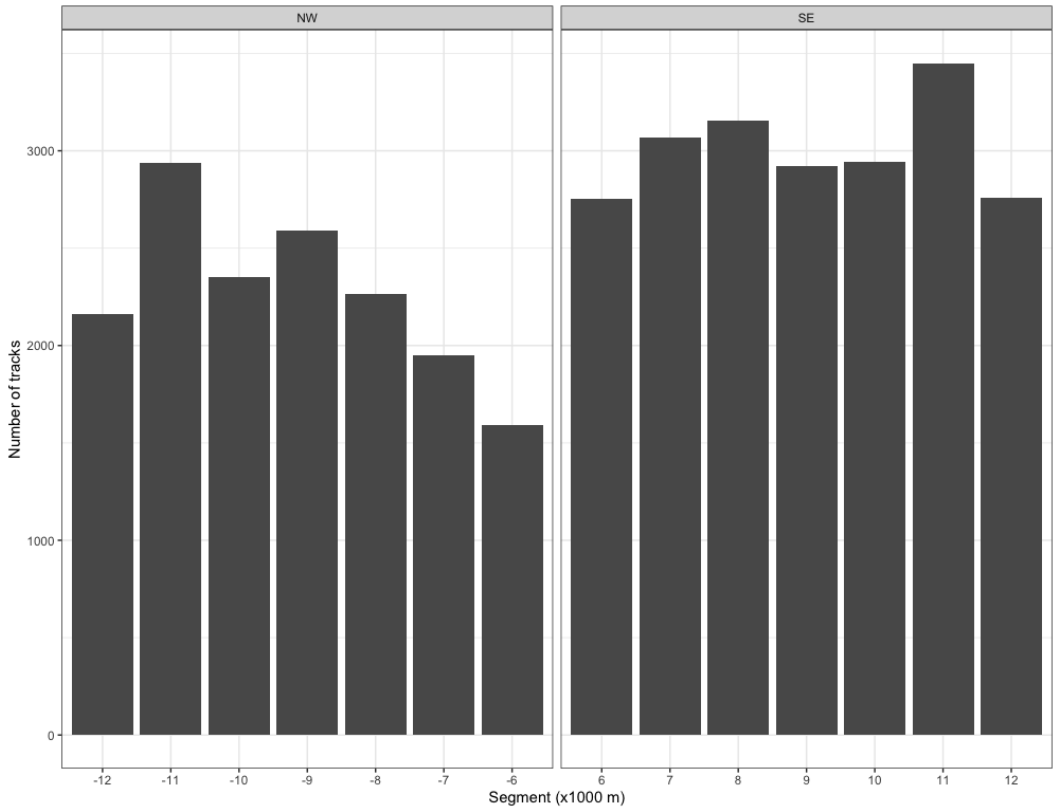

Figure 10.2.4 Number of tracks with an average altitude just above rotor height (137 – 249 meter) per segment at both sides of the radar. The turbine to the southeast is at 1100 meters from the radar, which means that the rotors span the segment 10-12.

Table 10.2.4 Number of bird tracks to the southeast of the radar per hour per segment per season just above rotor height. Note that the wind turbine is situated at around 1,100 meter.

Season	800-900m	900-1,000m	1,000-1,100m	1,100-1,200m
Spring	0.20	0.23	0.27	0.18
Summer	0.29	0.32	0.39	0.24
Autumn	1.13	1.14	1.34	1.07
Winter	0.59	0.49	0.54	0.44

10.3 Discussion

10.3.1 Horizontal meso-avoidance

Based on an analysis of the number of radar tracks crossing a virtual line along a row of turbines within the wind farm, birds seem to show strong meso-avoidance and try to pass by as far as possible in between single wind turbines. This is in contrast with the radar measurements to investigate macro-avoidance, which did not show consistent patterns of avoidance of the wind farm as a whole. In §9.3.2 we discussed that macro-avoidance behaviour is likely very species-specific (cf. Marques *et al.* 2021) and our measurements were relatively close to the wind farm. The level of meso-avoidance is of course also species-specific (Cook *et al*. 2018), but while macro-avoidance considers the boldness of the different species, entering the wind farm not necessarily means that birds would directly become a victim of a collision. In contrast avoiding a wind turbine at the meso-scale is essential in terms of survival, and thus also the population-level effects are expected to be larger (Cook *et al.* 2018, Skov *et al.* 2018).

Despite the statistically significant results, the calculated meso-avoidance rate of ca. 60% is lower than the values reported in previous studies for large seabirds like gulls and gannets, all having an assumed meso-avoidance rate >80% (Cook *et al.* 2018, Skov *et al.* 2018). However, our estimates are higher compared to earlier radar measurements in the Dutch OWEZ wind farm, reporting a meso-avoidance rate of 34%, based on bird densities within 50 m from a wind turbine compared with densities elsewhere in the wind farm (Krijgsveld *et al.* 2011). As radar measurements are not species-specific, the difference between avoidance rates based on visual observations and radar observations may point towards certain species, for instance nocturnal migrants, showing a smaller level of meso-avoidance.

Nevertheless, our seasonal specification of the results showed that the difference between the number of tracks along turbines compared with the space in between was the largest in autumn and summer, in the period with the most intense nocturnal migration (see figures 10.2.1 and 10.2.2), when at least one third of all recorded bird tracks are expected to originate from migrants during the night (see §8.2). The finding that in the migration period the level of meso-avoidance was larger than in winter and spring,suggests that nocturnal migrants also seem to be well capable of avoiding wind turbines, probably showing an even higher level of avoidance than local birds.

This latter may well be the case, if we consider that our analysis does not distinguish between birds simply passing by the wind farm or using the area as part of their habitat. For instance, Vanermen *et al.* (2019) have shown that lesser black-backed gulls extensively use wind turbines for perching, which corresponds with observations of Thaxter *et al.* (2018). This behaviour likely holds for all large gull species, given most of the individuals present in the wind farm area during daytime. Hence, many local birds have the potential to cross the ‘turbine’ segment used in our analysis without effectively risking a collision. This was also shown in a recent study in Aberdeen wind farm, where all gull species were recorded moving linearly through the wind farm array with limited interactions

with turbines and rotors as well as recorded feeding in between and close to turbines (Tjørnløv *et al.* 2021). By drawing our detection line along the first line of turbines relative to the position of the radar, our analysis focused on assuring that the shading of turbines, or on the contrary the generation of clutter by turbines, can be avoided. In other words, we do not consider radar measurements applicable to draw conclusions on the fate of radar tracks crossing this line and entering the rotor-swept zone. Tracks may end in this zone either because birds land on the turbine platform, or because the radar tracking software can not follow the bird in the clutter of the turbine anymore, or because the individual eventually did collide with the wind turbine.

In addition to the above point, it also needs to be stressed that using the horizontal radar measurements limits our conclusions on the so-called horizontal meso-avoidance. Namely, the horizontal radar data does not contain altitude information of the tracks. Although the horizontal radar beam along our detection line does include relevant altitudes of the rotor-swept zone (*i.e.* maximum altitudes along the detection line range from ±250 m at the point closest to the radar to ±500 m at the farthest point), even birds crossing our detection line along the turbine segments may have passed below or above the rotor-swept zone.

10.3.2 Vertical meso-avoidance

Based on the number of vertical radar tracks with an average altitude of 137 to 249 meters, the presence of vertical meso-avoidance was not clearly distinguishable. Although in spring, summer and autumn, there was a peak in number of tracks per hour within the wind farm just above the turbine, the difference in numbers was rather small. No clear effects of vertical avoidance have recently also been shown in a study in Aberdeen windfarm. Video data on vertical meso avoidance behaviour showed that in 96.8% of the recordings the target species avoided the rotor-swept zone by flying in between the turbines with very few avoiding by changing their flight altitude in order to fly either below or above the rotors (Tjørnløv *et al.* 2021).

In addition, this pattern was also visible outside the wind farm, especially in winter. This means that an effect of radar detection patterns cannot be ruled out, such as the still slightly expanding beam of the vertical radar with distance. The latter might lead to a slight increase in detection chance of a bird flying further away from the radar. In contrast, this might be balanced out by detection loss that increases with distance from the radar. However, the comparison with the same segment in the other beam of the radar is essential in analysing these spatial effects.

Unfortunately, due to unreliable measurements by the radar just around a turbine (tracks generated by the rotors or shadowing by the wind turbine), it was not possible to analyse the percentage of tracks directly above rotor height compared to the number of tracks at- or below rotor height or to the number of tracks generated by per segment. Therefore, we were not able to test whether the distribution in number of bird tracks above and on rotor height changed around the turbine. In such a comparison, a shift towards number of tracks above rotor height would give a more direct indication that birds fly higher around the wind turbine.

As discussed in 10.3.1, meso-avoidance is likely to be in the horizontal plane as well as in the vertical plane. However, these two types of avoidance might affect each other, meaning that meso-avoidance horizontally, might lead to a lack of meso-avoidance vertically and vice versa. Despite these difficulties in quantifying vertical meso-avoidance, our results provide interesting insights in certain patterns, such as the largest difference in number above rotor height with the surrounding segments occurring in autumn, in the period when the majority of the radar measurements originate from nocturnal migrants. Analogous with the other results of horizontal meso-avoidance, this could indicate that nocturnal migrants are well capable of avoiding offshore wind turbines.

11 Influence of fishing vessels

An important determinant of the collision rate of birds with wind turbines is the intensity of bird movements, the 'flux.' Temporally high bird fluxes at offshore wind farms (OWFs) can be related to migration events but may also occur when birds are attracted to foraging opportunities either inside or close to the OWF. Conceivably, attraction of seabirds to active fishing vessels, where seabirds (particularly large *Larus* gulls (great and lesser black-backed gull and herring gull)) can forage on discarded offal and bycatch, can bring large numbers of seabirds close to or within OWFs, but this has not yet been studied.

In this chapter, horizontal radar data is used to first classify potentially actively fishing vessels and subsequently test whether bird fluxes within the OWF are higher when active fishing vessels are nearby.

11.1 Methods

Horizontal radar data were collected between 22 February 2019 and 31 December 2021. For steps undertaken to filter the data see §2.1.2.

Ship tracks

To classify potential active fishing vessels, all radar tracks classified as ships were exported from the database. For each ship, the following data were collected: average speed (in m/s), tortuosity of the ships' track (straight line path between start- and endpoint divided by the total path length) and maximum reflected surface. Classification certainty (*i.e.* as a ship) by the radar software was included as a 'score' ranging from 0 to 1. In addition, whether a track intersected with the OWF polygon was also assessed. Finally, the number of tracks of birds, classified as medium-sized or large-sized birds (*i.e*. bird sizes expected to follow fishing vessels), within 500 meters from the ship during the time the ship was detected, as well as the number of bird tracks that intersected with the ships' track were calculated per ship track. The number of bird tracks was divided by the number of minutes that the ship was detected to arrive at a standardized index of bird presence close to the ship.

Characteristics of radar tracks classified as ships were first visually explored (figure 11.2.1), before filtering those tracks that satisfied the following criteria: 1) ground speed between 2.314998 and 3.85833 m/s, which corresponds to towing speeds for fishing vessels (Poos *et al.* 2013), 2) radar 'score' above -0.95, 3) duration between 1 and 167 min, 4) total distance travelled above 500 m, 5) straightness index above 0.5 (*i.e*. assuming that towing fishing vessels are largely move in a straight line), 6) minimum distance to the radar below 3 km giving a reasonable detection of both ships and birds and 7) no intersection with the OWF as no fishing is allowed in the wind farm.

An unsupervised cluster analysis was performed on the characteristics of this subset of 'ships', using the kmeans-method. The optimal number of clusters was estimated by plotting the sum of squares for models with 2 to 10 clusters. Where the relation between the number of clusters and the sum of squares levels off is regarded as the best number

of clusters. Using that number of clusters, ships that were part of the cluster with most associated birds were considered to most likely refer to actively fishing vessels, and these were used for further analyses to represent the potential presence of active fishing vessels.

Bird data

In order to investigate an elevated activity within the wind farm in periods of a fishing vessel in the vicinity, the number of radar tracks classified as medium-sized or large-sized birds that crossed the line between turbines 39 and 43 were summed per 5 min interval.

Statistical analysis

The number of 'birds' per 5 min interval followed a strongly left-skewed distribution, with 28% zeros. A Poisson Generalized Linear Model (GLM) of the bird count as a function of the presence or absence of 'ships' was overdispersed. Therefore, a negative binomial GLM was used. In addition, Poisson GLMs were fit to model 1) the number of medium/large-sized bird tracks within 500 m from each 'ship' track as a function of the maximum number of medium/large-sized birds detected within the OWF, and 2) the number of medium/large-sized bird tracks intersecting each 'ship' track as a function of the maximum number of medium/large-sized birds detected within the OWF.

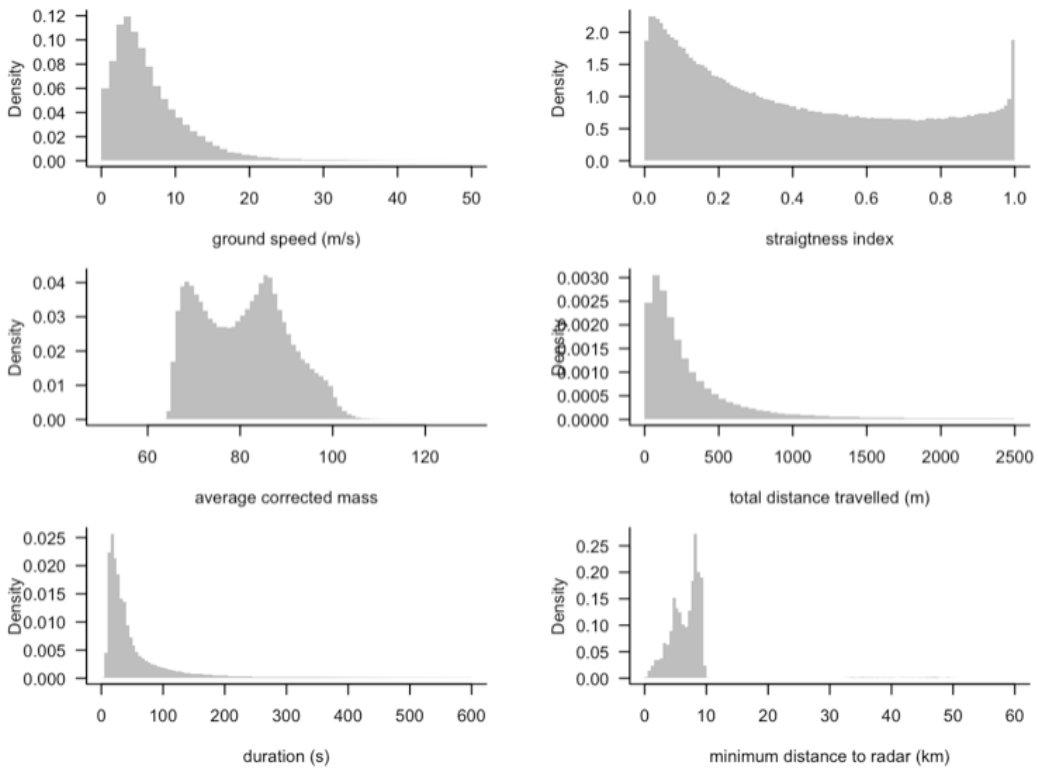

Figure 11.2.1 *Exploration of tracks that have been automatically classified as ships: a) ground speed, excluding values of 50 m/s up to 235 m/s, b) straightness, c) corrected mass, d) total length of the track, excluding values 2.5 km up to 150 km, e) duration of the track, excluding extreme values of 10 min up to 22 hrs, and f) minimum distance to the radar.*

11.2 Results

Exploration of tracks classified as ships

The raw data of tracks that have automatically been classified as ships shows huge ranges in almost all characteristics (figure 11.2.1). Ground speeds were mostly limited to around 5 m/s, with a maximum of 235 m/s. Straightness values were distributed across the entire range from 0 and 1, with most records closer to 0 than to 1.

Potential fishing vessels

No clear clustering could be observed in the ship track data. Using kmeans-clustering with several values for the number of clusters k showed the largest decrease in the sum of squares up to about 4 clusters (figure 11.2.2). However, these four clusters showed extensive overlap in their characteristics (figure 11.2.3).

Relation between bird flux inside OWF and presence of potential fishing vessels

There was no relation between the number of birds inside the wind farm and the presence or absence of ships classified as potential active fishing vessels (β = 0.4657, 95% CI = 0.2717 – 0.6708). The number of 'bird tracks' within 500 m from the 'ship' track did very weakly correlate with the number of birds in the OWF (β = -0.0016, 95% CI = -0.0021 – -0.0011). The same was true for the number of 'bird tracks' intersecting with the 'ship' track (β = -0.0025, 95% CI = -0.0052 – 2e-04, figure 11.2.4).

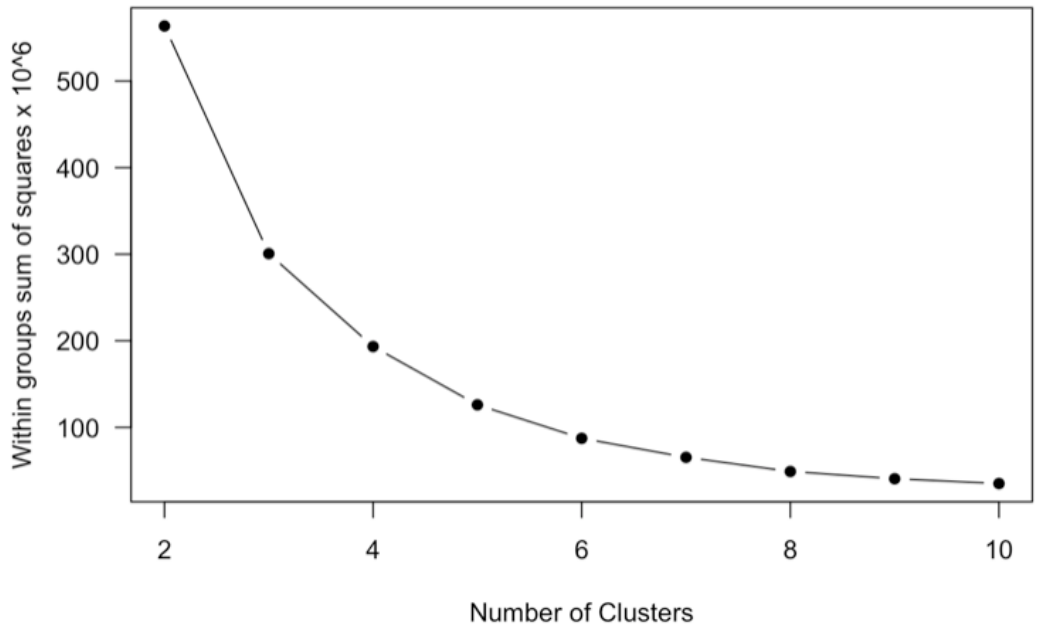

Figure 11.2.2 Relation between sum of squares and number of clusters in kmeans, for filtered radar data classified as ships.

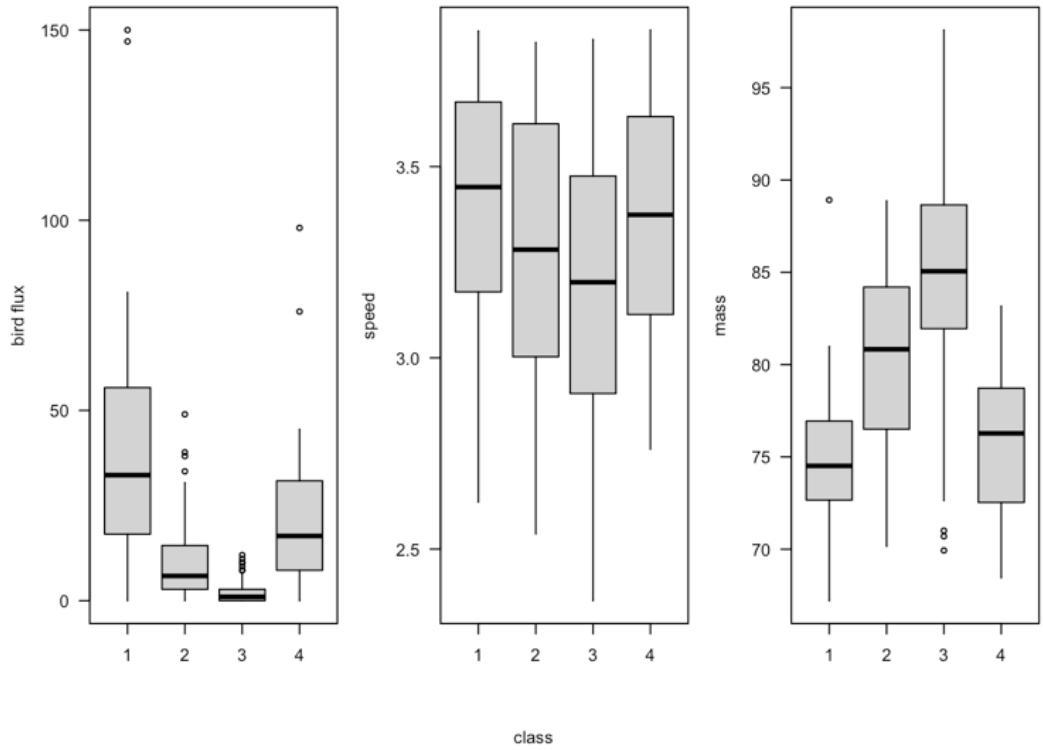

Figure 11.2.3 Cluster characteristics based on kmeans, for filtered radar data classified as ships.

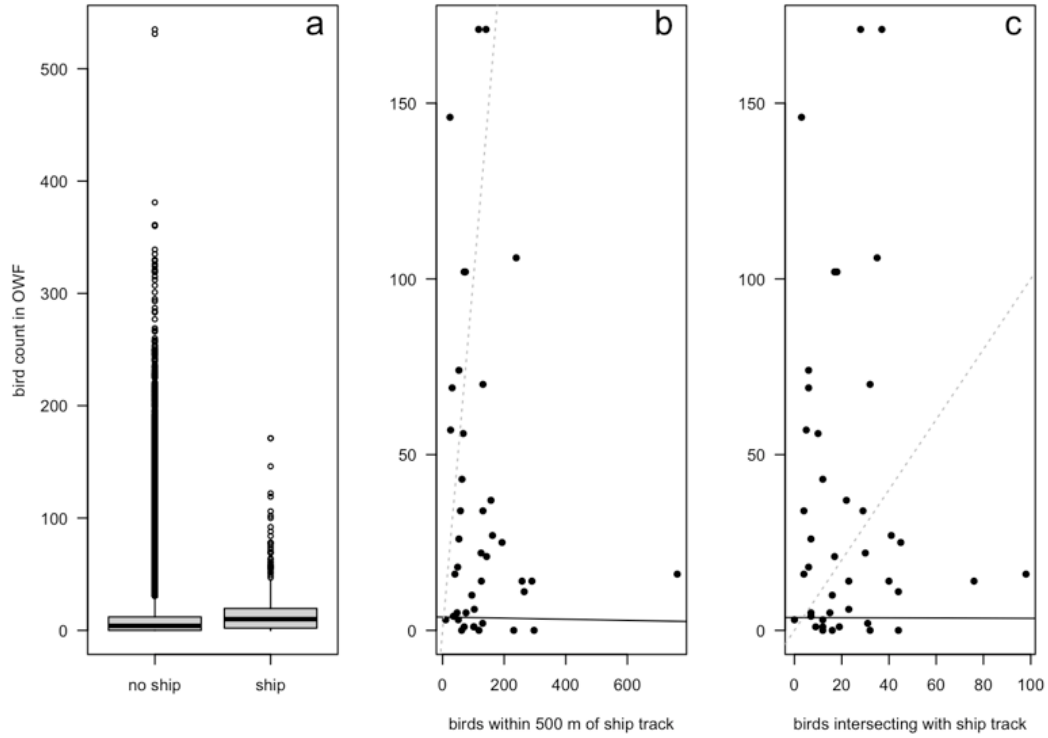

Figure 11.2.4 Relation between the number of medium/large birds in the OWF a) in the absence and presence of radar tracks classified as potential active fishing vessels, b) with the number of medium/large birds within 500m of a potential fishing vessel and c) with the number of medium/large birds intersecting the track of a potential fishing vessel. Dotted lines in b and c show x=y and solid lines the model estimates.

11.3 Discussion

We did not detect an increase in bird flux when potential fishing vessels were near the offshore wind farm. Although the slopes between the number of birds in the wind farm and within 500 m or intersecting the 'ship' tracks differed slightly from zero, they were extremely small: even if a 'ship' would be accompanied by 800 birds, that would increase the number of birds within the wind farm by only 32 individuals in relation to a 'ship' with 0 birds.

Our analysis intended to investigate whether bird fluxes within the wind farm increase in the presence of an active fishing vessel in the vicinity. Our results could of course also mean that this is not the case, and that birds around fishing vessels either have already accompanied the vessel earlier, or elevated numbers around fishing vessels occur in periods when the bird numbers in the surrounding area are higher anyhow. However, the results from this analysis should be regarded as extremely uncertain and no policies should be based on it. In particular, the classification of ships in general and of actively fishing vessels in particular, is associated with tremendous uncertainty. Radar tracks classified as ships included data with characteristics that are very hard to reconcile with any type of ship. For example, ground speeds ranged up to 235 m/s, or 847 km/h, which is obviously not realistic. It should be noted that the steps taken to filter out tracks that did not respond to ships are highly arbitrary; in the raw data, no clear clusters could be detected. Even in the filtered data, characteristics of clusters identified by kmeans-clustering showed large overlap, indicating that there are no well-defined clusters in this data set.

So far, the classification of ships by the radar has not received much attention. Collecting more visual observations might be valuable in this respect but building a decent sample size likely takes much effort.

Another difficulty not tackled in this study is that the radar detection probability will decrease with distance much less strongly for large objects (such as vessels) than for birds. This likely results in underestimating the number of birds associated with distant ships. Here, we filtered data within a range of 3 km from the radar to overcome this problem, but it would be good to study the potential relation between ship and bird detection in more detail, in order to take this into account in future analyses. This is important as the number of birds surrounding a vessel is both indicating that the vessel is actively fishing and will also be important for the number of birds potentially ending up within the OWF perimeter.

This analysis should ideally be repeated using fishing vessel (VMS) data, which can provide a much higher certainty regarding fishing vessel presence and behaviour. However, it should be noted that this has only a 2h temporal resolution, which is relatively low compared to the studied area and the usual speed of actively fishing vessels.

12 Synthesis

This study aimed to measure variables that are needed to improve collision risk model (CRM) estimates, and also to understand which factors determine the number, species composition and spatial distribution of birds in and around an offshore wind farm, in our case the Dutch Luchterduinen wind farm. Hence, the results presented in this report include data on (species-specific) bird fluxes, flight height, flight speed, nocturnal activity, as well as on macro- and meso-avoidance. Furthermore, we present the species composition throughout the year and the temporal and seasonal variability in bird fluxes, as well as the effect of wind on these fluxes and on possible influence of fishing vessels on bird fluxes. Some of the presented results may directly be applied in CRMs, while other results come with uncertainty and should thus be interpreted with care.

Due to our relatively intensive field work effort, we could present a reliable image of the bird **species composition** in and around the wind farm throughout the year. On a yearly basis, lesser black-backed gull was the most numerous species (±30% of all observations) in and around the windfarm, followed by great cormorant (15% of all observations) and black-legged kittiwake (15% of all observations). Other species have provided less than 10% of all observations. However, it has to be stressed that our results are only representative for situations under favourable weather circumstances and during daylight. Due to logistical challenges, our field work effort of four observation days each month can be considered as high for offshore situations, yet such a sample size remains limited to present monthly species compositions come with a significant certainty. Hence, also the presented species-specific fluxes should be interpreted with care, as these fluxes are additionally prone to uncertainties in the monthly fluxes detected by the radar. The species-specific fluxes presented in this study should thus mainly be seen as an indication of the order of magnitude of the fluxes for each species in each month. The susceptibility of the radar to register clutter as birds and the strong filtering under unfavourable circumstances poses a significant challenge to calculate absolute fluxes based on the radar data. However, the presented temporal and seasonal variability in the mean traffic rates, as well as the effect of wind on these fluxes are generally in line with what one would expect ecologically.

Moreover, our results also clearly identify future study directions to further elaborate on automatic measurements of offshore bird movements by dedicated radars. For instance, bird radars are developed to measure **fluxes of birds**, in contrast with other forms of offshore bird surveys that provide a snapshot of bird numbers at a certain moment. For instance, we could determine a year-round mean traffic rate of 65 birds/km/hour, but also identify that peak fluxes above 500 birds/km/hour during periods of seasonal migration (especially in the autumn during October and November, but also in spring during February and March) occurred in 1.4% of all measurement hours, mainly at the start of the night. These measurements are valuable as one of the current challenges of CRMs is to convert bird densities based upon offshore bird surveys to fluxes of birds flying through the rotor-swept zone. It was beyond this study to carry out in-depth calculations on this matter, but radar measurements could provide a tool to better understand the relationship between local snapshot counts and fluxes of birds in the area. However, before we reach that stage,

we also need a better comprehension of what the radar measurements comprise of. For instance, we currently could not exclude that 1) rain showers still enter the database as birds (see §4.3); 2) elevated fluxes at high wind speeds are not caused by high waves detected by the radar as birds (see §5.3); 3) rotating turbines in certain periods are not recorded by the vertical radar as birds (see §9.3.2). We believe that there are possibilities to make progress in the quality of the radar measurements in the future, which would make offshore radar studies more reliable. However, as radar measurements are not species-specific, it also remains a challenge to couple radar tracks to species information, either based on visual observations or camera recordings.

The method used in our study to calculate species-specific **flight-height distributions** is based on several assumptions and the collected data naturally comprises measurement uncertainties. However, with the available data we believe that this method still provides the most accurate species-specific flight height distributions based on the available data. For instance, our observations revealing flight heights of auks exclusively close to the water surface match previous studies and hence strengthen available impact assessments of wind farms on these species. Moreover, also the recorded flight heights of gulls that largely overlap with the rotor-swept zone, which holds to a lesser extent also for terns and gannets, are also very valuable for evaluating the effects of offshore wind farms on these seabird species. However, our presented flight-height distributions were restricted to a number of height bands at altitudes below 200 m. Therefore, these flight height distributions are not appropriate for the extended Band model (Band 2012) that requires flight height distributions with height bands of 1 meter up to an altitude of 300 meter. Nevertheless, our measurements can be used as input in the more general basic Band model (Band 2000), that uses proportion of bird movements at rotor height. Therefore, also future studies should focus on collecting species-specific measurements of birds by taking the lower and upper tips of the rotors into account.

The species-specific **flight speeds** presented in this study provide an accurate measure of the ground speed of birds in and around offshore wind farms, and hence they can be used reliably for collision risk modelling. For some species, the flight speeds recently used by Potiek *et al.* (2022) originate from (relatively) old literature and thus the flight speeds presented in this study may improve the accuracy of future collision risk modelling. However, also our results, and the relative mismatches with previously reported flight speeds, emphasize that it is essential to take the flight behaviour displayed in offshore wind farms into account, as flight speeds during, for instance, commuting and foraging can largely vary.

As we were not able to perform measurements on the species-specific activity of birds at night, we cannot provide data on species-specific **nocturnal activity**, which is needed as input for collision risk modelling. However, general patterns in the ratio between fluxes during day and night throughout the year provided interesting indications of the number of nocturnally migrating birds in each month, as well as the average nocturnal activity of birds in the area. Using several rough assumptions, we estimated that in March and October respectively roughly 72,200-91,000 and 95,000-124,000 birds per km migrate along

Luchterduinen wind farm at night. Furthermore, we could indicate that all local birds considered together might show a nocturnal activity between 27-37%.

Avoidance used in collision risk modelling, such as the Band model, is commonly calculated by combining rates for macro-, meso- and micro-avoidance (Band 2012, Cook *et al.* 2014, Skov *et al.* 2018). In our report we presented species-specific **macro-avoidance** rates for eight seabird species, of which three species (northern gannet, Sandwich tern and common guillemot) and one species group (razorbill/guillemot) showed significant avoidance of the wind farm, while the great cormorant showed significant attraction behaviour. For all other species no significant effect of the wind farm could be determined. Our result of a general **meso-avoidance** level of 43% of wind turbines within the wind farm relied on radar measurements, and hence is not species-specific. Moreover, macro- and meso-avoidance levels cannot be used as a stand-alone parameter in collision risk models, and thus should be combined with species-specific micro-avoidance rates. This last step in defining avoidance behaviour of Luchterduinen wind farm, including species-specific measurements on meso- and micro-avoidance are part of the parallel running MEP-LUD research in Luchterduinen conducted by DHI, under the license obligation of Eneco. The results of the integration of the two studies are expected to be published later in 2022 and will be added to this report.

Literature

Alerstam, T., M. Rosén, J. Bäckman, P.G.P. Ericson & O. Hellgren, 2007. Flight Speeds among Bird Species: Allometric and Phylogenetic Effects. PLoS Biology 5(8): e197. doi: 10.1371/journal.pbio.0050197.

Aschwanden, J., H. Stark, D. Peter, T. Steuri, B. Schmid & F. Liechti, 2018. Bird collisions at wind turbines in a mountainous area related to bird movement intensities measured by radar. Biological Conservation 220: 228-236.

Band, W., 2000. Windfarms and birds: calculating a theoretical collision risk assuming no avoiding action. Guidance Note. Scottish Natural Heritage

Band, W., 2012. Using a collision risk model to assess bird collision risks for offshore windfarms. SOSS, The Crown Estate, London, Uk.

van Bemmelen, R.S.A., W. Courtens, M.P. Collier & R.C. Fijn, 2022. Sandwich Terns in the Netherlands in 2019-2021. Distribution, behaviour, survival and diet in light of (future) offshore wind farms, Rapport 21-310. Bureau Waardenburg, Culemborg.

Borkenhagen, K., A.-M. Corman & S. Garthe, 2018. Estimating flight heights of seabirds using optical rangefinders and GPS data loggers: a methodological comparison. Marine Biology 165(1): 17.

Brabant, R. & N. Vanermen, 2020. Collision Risk For Six Seabird Species In The First Belgian Offshore Wind Farm Zone. In: S. Degraer, R. Brabant, B. Rumes & L. Vigin (Eds.), *Environmental Impacts of Offshore Wind Farms in the Belgian Part of the North Sea: Empirical Evidence Inspiring Priority Monitoring, Research and Management*. Royal Belgian Institute of Natural Sciences, OD Natural Environment, Marine Ecology and Management, Brussels.

Bradarić, M., 2022. "Seasonal drivers of nocturnal bird migration flight altitudes offshore and implications for wind energy." in Conference on Wind energy and Wildlife Impacts, Egmond aan Zee.

Bradarić, M., W. Bouten, R.C. Fijn, K.L. Krijgsveld & J. Shamoun-Baranes, 2020. Winds at departure shape seasonal patterns of nocturnal bird migration over the North Sea. Journal of Avian Biology 51(10): doi: 10.1111/jav.02562.

Brooks, M.E., K. Kristensen, K.J. Van Benthem, A. Magnusson, C.W. Berg, A. Nielsen, H.J. Skaug, M. Machler & B.M. Bolker, 2017. glmmTMB balances speed and flexibility among packages for zero-inflated generalized linear mixed modeling. The R journal 9(2): 378-400.

Cleasby, I.R., E.D. Wakefield, S. Bearhop, T.W. Bodey, S.C. Votier & K.C. Hamer, 2015. Three-dimensional tracking of a wide-ranging marine predator: flight heights and vulnerability to offshore wind farms. Journal of Applied Ecology 52(6): 1474-1482.

Cook, A.S.C.P., A. Johnston, L.J. Wright & N.H.K. Burton, 2012. A review of flight heights and avoidance rates of birds in relation to offshore wind farms. BTO Research Report Number 618. British Trust for Ornithology, Thetford.

Cook, A.S.C.P., E.M. Humphreys, F. Bennet, E.A. Masden & N.H.K. Burton, 2018. Quantifying avian avoidance of offshore wind turbines: Current evidence and key knowledge gaps. Marine Environmental Research in press.

Desholm, M. & J. Kahlert, 2005. Avian collision risk at an offshore wind farm. Biology Letters 1(3): 296-8.

Dierschke, V., R.W. Furness & S. Garthe, 2016. Seabirds and offshore wind farms in European waters: Avoidance and attraction. Biological Conservation 202: 59-68.

Dokter, A.M., A. Farnsworth, D. Fink, V. Ruiz-Gutierrez, W.M. Hochachka, F.A. La Sorte, O.J. Robinson, K.V. Rosenberg & S. Kelling, 2018. Seasonal abundance and survival of North America's migratory avifauna determined by weather radar. Nature ecology & evolution 2(10): 1603-1609.

van Erp, J.A., E.E. Loon, K.J. Camphuysen & J. Shamoun-Baranes, 2021. Temporal Patterns in Offshore Bird Abundance During the Breeding Season at the Dutch North Sea Coast. Marine Biology 168: 150.

Fijn, R.C. & A. Gyimesi, 2018. Behaviour related flight speeds of Sandwich Terns and their implications for wind farm collision rate modelling and impact assessment. Environmental Impact Assessment Review 71: 12-16.

Fijn, R.C., K.L. Krijgsveld, M.J.M. Poot & S. Dirksen, 2015. Bird movements at rotor heights measured continuously with vertical radar at a Dutch offshore wind farm. Ibis 157(3): 558-566.

Fijn, R.C., A. Gyimesi, M.P. Collier, D. Beuker, S. Dirksen & K.L. Krijgsveld, 2012. Flight patterns of birds at offshore gas platform K14. Flight intensity, flight altitudes and species composition in comparison to OWEZ, Rapport 11-112. Bureau Waardenburg, Culemborg.

Furness, R.W., H.M. Wade & E.A. Masden, 2013. Assessing vulnerability of marine bird populations to offshore wind farms. Journal of Environmental Management 119: 56-66.

Goodale, M.W. & A. Milman, 2020. Assessing Cumulative Exposure of Northern Gannets to Offshore Wind Farms. Wildlife Society Bulletin 44(2): 252-259.

Gyimesi, A., 2020. Variation in species composition between observations from different turbine locations of Luchterduinen. Notitie 18-0178/20.02362/AbeGy. Bureau Waardenburg, Culemborg.

Gyimesi, A., J.W. de Jong & R.C. Fijn, 2017. Validation of biological variables for use in the SOSS Band model for Lesser Black-backed Gull *Larus fuscus* and Herring Gull *Larus argentatus*. report nr. 16-042. Bureau Waardenburg, Culemborg.

Gyimesi, A., J.J. Leemans, R.P. Middelveld, M.P. Collier & R.S.A.v. Bemmelen, 2020. First results on bird fluxes and macro- and meso-avoidance in Luchterduinen. Interim report. Report nr. 20-025, Rapport. Bureau Waardenburg, Culemborg.

Hamer, K.C., W.J. Grecian & J. Lane, in prep. Fine-scale foraging behaviour of adult and immature northern gannets: distributions, movements and potential interactions with offshore wind-farms.

Harwood, A.J.P., M.R. Perrow & R.J. Berridge, 2018. Use of an optical rangefinder to assess the reliability of seabird flight heights from boat-based surveyors: implications for collision risk at offshore wind farms. Journal of Field Ornithology. 1-12.

Heinänen, S. & H. Skov, 2018. Offshore Wind Farm Eneco Luchterduinen Ecological Monitoring of Seabirds T3 (Final) Report

Hüppop, O., K. Hüppop, J. Dierschke & R. Hill, 2016. Bird collisions at an offshore platform in the North Sea. Bird Study 63(1): 73-82.

Hüppop, O., J. Dierschke, K.-M. Exo, E. Fredrich & R. Hill, 2006. Bird migration studies and potential collision risk with offshore wind turbines. Ibis 148: 90-109.

Johnston, A., A.S.C.P. Cook, L.J. Wright, E.M. Humphreys & N.H.K. Burton, 2014. Modelling flight heights of marine birds to more accurately assess collision risk with offshore wind turbines. Journal of Applied Ecology 51: 31-41.

Kemp, M.U., J. Shamoun-Baranes, A.M. Dokter, E. Loon & W. Bouten, 2013. The influence of weather on the flight altitude of nocturnal migrants in mid-latitudes. Ibis 155(4): 734-749.

Kleyheeg-Hartman, J.C. & A. Potiek, 2020. Analyse nachtelijke vogeltrek met behulp van 3D-vogelradar: Showcase Eemshaven. Resultaten najaar 2018 en voorjaar 2019, Rapport 19-176. Bureau Waardenburg, Culemborg.

Krijgsveld, K., R.C. Fijn & R. Lensink, 2015. Occurrence of peaks in songbird migration at rotor heights of offshore wind farms in the southern North Sea. Report nr 15-119. Bureau Waardenburg, Culemborg.

Krijgsveld, K.L., 2014. Avoidance behaviour of birds around offshore wind farms. Overview of knowledge including effects of configuration. Bureau Waardenburg, Culemborg.

Krijgsveld, K.L., R.C. Fijn, M. Japink, P.W. van Horssen, C. Heunks, M.P. Collier, M.J.M. Poot, D. Beuker & S. Dirksen, 2011. Effect Studies Offshore Wind Farm Egmond aan Zee. Final report on fluxes, flight altitudes and behaviour of flying birds, Rapport 10-219. Bureau Waardenburg, Culemborg.

Lane, J.V., R. Jeavons, Z. Deakin, R.B. Sherley, C.J. Pollock, R.J. Wanless & K.C. Hamer, 2020. Vulnerability of northern gannets to offshore wind farms; seasonal and sex-specific collision risk and demographic consequences. Marine Environmental Research 162: 105196.

Leopold, M.F., R.S.A. van Bemmelen & A.F. Zuur, 2013. Responses of Local Birds to the Offshore Wind Farms PAWP and OWEZ off the Dutch mainland coast. Report number C151/12. Imares, Wageningen.

Leopold, M.F., E.M. Dijkman, L. Teal & t.O. team, 2011. Local birds in and around the Offshore Wind Farm Egmond aan Zee (OWEZ) (T-0 & T-1, 2002-2010). Imares, Texel, Netherlands.

Leopold, M.F., M. Booman, M.P. Collier, N. Davaasuren, R.C. Fijn, A. Gyimesi, J. de Jong, R.H. Jongbloed, B. Jonge Poerink, J.C. Kleyheeg-Hartman, K.L. Krijgsveld, S. Lagerveld, R. Lensink, M.J.M. Poot, v.d.W. J.T. & M. Scholl, 2015. Building blocks for dealing with cumulative effects on birds and bats of offshore wind farms and other human activities in the Southern North Sea. IMARES Report C166/14 IMARES, Wageningen.

Lindgren, F. & H. Rue, 2015. Bayesian spatial modelling with R-INLA. Journal of statistical software 63: 1-25.

Marine Scotland, 2018. Stochastic Band CRM – GUI User manual. Available at https://www2.gov.scot/Topics/marine/marineenergy/mre/current/StochasticCRM

Marques, A.T., H. Batalha & J. Bernardino, 2021. Bird Displacement by Wind Turbines: Assessing Current Knowledge and Recommendations for Future Studies. Birds 2(4): 460-475.

Marques, A.T., H. Batalha, S. Rodrigues, H. Costa, M.J.R. Pereira, C. Fonseca, M. Mascarenhas & J. Bernardino, 2014. Understanding bird collisions at wind farms: An updated review on the causes and possible mitigation strategies. Biological Conservation 179: 40-52.

Masden, E., 2015. Developing an avian collision risk model to incorporate variability and uncertainty. Marine Scotland Science

Masden, E.A. & A.S.C.P. Cook, 2016. Avian collision risk models for wind energy impact assessments. Environmental Impact Assessment Review 56: 43-49.

Masden, E.A., D.T. Haydon, A.D. Fox & R.W. Furness, 2010. Barriers to movement: Modelling energetic costs of avoiding marine wind farms amongst breeding seabirds. Marine Pollution Bulletin 60(7): 1085-1091.

Masden, E.A., A.S.C.P. Cook, A. McCluskie, W. Bouten, N.H.K. Burton & C.B. Thaxter, 2021. When speed matters: The importance of flight speed in an avian collision risk model. Environmental Impact Assessment Review 90: 106622.

Mateos-Rodriquez, M., 2009. Radar technology applied to the study of seabird migration across the strait of Gibraltar. PhD thesis University of Cadiz, Cadiz, Spain.

Newton, I., 2010. Bird Migration. Harper Collins Publishers, London, UK.

Odinga, J., D. Barbé, A. van Mastrigt, J. van den Berg & S. Mulder, 2021. Wozep midterm evaluation. Royal HaskoningDHV, Amersfoort.

Patrick, S.C., S. Bearhop, D. Grémillet, A. Lescroël, W.J. Grecian, T.W. Bodey, K.C. Hamer, E. Wakefield, M. Le Nuz & S.C. Votier, 2014. Individual differences in searching behaviour and spatial foraging consistency in a central place marine predator. Oikos 123(1): 33-40.

Pennycuick, C.J., 1990. Predicting wingbeat frequency and wavelength of birds. Journal of Experimental Biology 150: 171-185.

Peschko, V., M. Mercker & S. Garthe, 2020a. Telemetry reveals strong effects of offshore wind farms on behaviour and habitat use of common guillemots (*Uria aalge*) during the breeding season. Marine Biology 167: 118.

Peschko, V., B. Mendel, M. Mercker, J. Dierschke & S. Garthe, 2021. Northern gannets (*Morus bassanus*) are strongly affected by operating offshore wind farms during the breeding season. Journal of Environmental Management 279: 111509.

Peschko, V., B. Mendel, S. Müller, N. Markones, M. Mercker & S. Garthe, 2020b. Effects of offshore windfarms on seabird abundance: Strong effects in spring and in the breeding season. Marine Environmental Research 162: 105157.

Petersen, I.K., T.K. Kjær, J. Kahlert, M. Desholm & A.D. Fox, 2006. Final results of bird studies at the offshore wind farms at Nysted and Horns Rev, Denmark. Århus, Denmark, National Encironmental Research Institute, Department of Wildlife Ecology and Biodiversity.

Piggott, A., A. Vulcano & D. Mitchell, 2021. Impact of offshore wind development on seabirds in the North Sea and Baltic Sea: Identification of data sources and at-risk species. Summary Report. Stichting Birldlife Europe, Birdlife International, Brussels, Belgium.

Pollock, C.J., J.V. Lane, L. Buckingham, S. Garthe, R. Jeavons, R.W. Furness & K.C. Hamer, 2021. Risks to different populations and age classes of gannets from impacts of offshore wind farms in the southern North Sea. Marine Environmental Research 171: 105457.

Poos, J.J., M.N.J. Turenhout, H.A.E. van Oostenbrugge & A.D. Rijnsdorp, 2013. Adaptive response of beam trawl fishers to rising fuel cost. ICES Journal of Marine Science 70(3): 675-684.

Potiek, A., J.J. Leemans, R.P. Middelveld & A. Gyimesi, 2022. Cumulative impact assessment of collisions with existing and planned offshore wind turbines in the southern North Sea. Analysis of additional mortality using collision rate modelling and impact assessment based on population modelling for the KEC 4.0, Rapport 21-205. Bureau Waardenburg, Culemborg.

R Core Team, 2020. R: A language and environment for statistical computing. R Foundation for Statistical Computing, Vienna, Austria.

Rijkswaterstaat, 2015. Kader Ecologie en Cumulatie t.b.v. uitrol windenergie op zee Deelrapport B - Bijlage Imares onderzoek Cumulatieve effecten op vogels en vleermuizen. Ministerie van Economische Zaken en Ministerie van Infrastructuur en Milieu, Den Haag.

Rijkswaterstaat, 2019. Kader Ecologie en Cumulatie t.b.v. uitrol windenergie op zee, KEC 3.0. Rijkswaterstaat in opdracht van het Ministerie van Landbouw, Natuur en Voedselkwaliteit, Den Haag.

Shamoun-Baranes, J. & H. van Gasteren, 2011. Atmospheric conditions facilitate mass migration events across the North Sea. Animal Behaviour 81(4): 691-704.

Skov, H., 2019. Bird Radar Luchterduinen: Validation of horizontal and vertical radar. DHI

Skov, H., S. Heinänen, T. Norman, R.M. Ward, S. Méndez-Roldán & I. Ellis, 2018. ORJIP Bird Collision and Avoidance Study. Final report - April 2018. The Carbon Trust, United Kingdom.

Thaxter, C.B., V.H. Ross-Smith & A. Cook, 2015. How high do birds fly? A review of current datasets and an appraisal of current methodologies for collecting flight height data: literature review BTO Research Report No. 666. BTO, Thetford.

Thaxter, C.B., V.H. Ross-Smith, W. Bouten, E.A. Masden, N.A. Clark, G.J. Conway, L. Barber, G.D. Clewley & N.H.K. Burton, 2018. Dodging the blades: new insights into three-dimensional space use of offshore wind farms by Lesser Black-backed Gulls *Larus fuscus*. Marine Ecology Progress Series 587: 247-253.

Thieurmel, B. & A. Elmarhraoui, 2019. suncalc: Compute Sun Position, Sunlight Phases, Moon Position and Lunar Phase. R package version 0.5.0.

Tjørnløv, R.S., H. Skov, M. Armitage, M. Barker, F. Cuttat & K. Thomas, 2021. Resolving Key Uncertainties of Seabird Flight and Avoidance Behaviours at Offshore Wind Farms. Annual report for April 2020 – October 2020. AOWFL, Scotland.

Vanermen, N., W. Courtens, R. Daelemans, L. Lens, W. Müller, M. Van de walle, H. Verstraete, E.W.M. Stienen & S. Votier, 2019. Attracted to the outside: a meso-scale response pattern of lesser black-backed gulls at an offshore wind farm revealed by GPS telemetry. ICES Journal of Marine Science 77(2): 701-710.

Vanermen, N., R.C. Fijn, E.B. Rebolledo, R.J. Buijs, W. Courtens, S. Duijns, S. Lilipaly, H. Verstraete & E.W.M. Stienen, 2022. Tracking lesser black-backed and herring gulls in the Dutch Delta. Distribution, behaviour, breeding success and diet in relation to (future) offshore wind farms, Rapport 21-318. Bureau Waardenburg, Culemborg.

Welcker, J., 2019. Patterns of nocturnal bird migration in the German North and Baltic Seas. Technical report. BioConsult SH, Husum.

NOTE

Rijkswaterstaat Water, Verkeer en Leefomgeving (Lelystad)
R. Hofman
Postbus 2232
3500 GE Utrecht

DATE:	29 September 2022
OUR REFERENCE:	18-0178/22.06209/AbeGy
COMMISSIONER REF:	offerteaanvraag 31140364.0001
AUTHOR:	J.J. Leemans *MSc.* & Dr. A. Gyimesi
PROJECT MANAGER:	Dr. A. Gyimesi
STATUS:	final draft
CONTROL:	M.P. Collier *MSc.*

Avoidance rates of northern gannet in offshore wind farms in the southern North Sea

Background

The intended developments of offshore wind energy in the southern North Sea may lead to cumulative effects on seabird species, in terms of estimated numbers of collision victims. However, direct measurements on collision mortality in the marine environment are challenging, as it is practically impossible to collect corpses or conduct long-term observations on collision events at sea. As more detailed information in collision rates is absent, Collision Rate Models (CRMs) are used to predict the risk posed by offshore wind farms to seabird populations. However, the outcomes of CRMs are known to be highly sensitive to the assumptions made about the behaviour of the species concerned (Masden 2015). Hence, for species with high expected casualty rates in offshore wind farms, it is important to use the best-available assumptions in collision modelling (Thaxter *et al.* 2018), in order to avoid under- or over-estimations of the numbers of casualties. However, empirical data on which assumptions can be based are scarce and could be highly location-specific (Piggott *et al.* 2021). Therefore, more detailed studies in offshore wind farms are required. For this, data collected by specialized bird radars, camera recordings and visual observations are currently the best available methods.

To achieve this goal, RWS has purchased a 3D fixed Robin Radar system, consisting of a horizontal and vertical radar (in short: RWS bird radars). This system was installed in offshore wind farm Luchterduinen in August 2018. Rijkswaterstaat contracted Bureau Waardenburg to carry out analyses of the bird radars and additional field observations to

estimate species-specific fluxes, avoidance- and flight behaviour of birds in and around offshore wind farm Luchterduinen.

Recently, a study in the Framework for Assessing Ecological and Cumulative Effects (in short 'KEC'; cf. the Dutch abbreviation) showed that the cumulative effects of collisions on northern gannets (*Morus bassanus*), one of the seabird species also occurring around Luchterduinen wind farm, may exceed Acceptable Levels of Impact when all existing and realistic wind farms in the southern North Sea up to 2030 are taken into consideration (Potiek *et al.* 2022). Potiek *et al.* (2022) estimated the number of collision victims using the stochastic Collision Risk Model (hereafter 'sCRM'; McGregor *et al.* 2018). This model is based on the SOSS Band model (Band 2012) but allows more detailed input data to be used, specifically in relation to modelling variability around certain parameters (McGregor *et al.* 2018). The accuracy of the input parameters is crucial for the quality of the outcomes of the model.

One of the input parameters with most impact on the outcomes of the sCRM is found to be the avoidance rate (Chamberlain *et al*. 2006, Masden *et al.* 2021). The avoidance rate is defined as the proportion of birds that take effective action to avoid collision with wind turbines. The avoidance rate that is incorporated into sCRMs is a combination of macro-, meso- and micro-avoidance, and calculated as follows (Cook *et al.* 2014, 2018, Skov *et al.* 2018):

Overall avoidance = 1 - ((1 - Macro-avoidance) * (1 - Meso-avoidance) * (1 - Micro-avoidance))

These three types of avoidance refer to the scale on which birds take avoiding action. Birds may avoid the entire windfarm (macro-avoidance), individual wind turbines (meso-avoidance), or take last minute action when flying close to the turbine blades (micro-avoidance). In lack of reliable estimates, meso- and micro-avoidance are sometimes presented as within-wind farm avoidance (Cook *et al.* 2018). In such case, overall avoidance rate is calculated as:

Overall avoidance = 1 - ((1 - Macro-avoidance) * (1 - Within-wind farm avoidance))

Scope of this report

As part of the Dutch governmental Wozep (Offshore Wind Ecological Programme) avian research in and around offshore windfarm Luchterduinen (LUD) concentrating on species-specific fluxes, avoidance- and flight behaviour of birds (Leemans *et al.* 2022a) Bureau Waardenburg was asked to provide a literature review on avoidance estimates for northern gannet. The objective of this review is to specify an avoidance rate for northern gannet based on field measurements conducted in wind farms in the relative vicinity of Luchterduinen (figure 1). The aim of this exercise was to provide a location-specific avoidance rate for cumulative assessments for wind farms in the southern part of the North Sea, relatively far from breeding colonies of northern gannets.

In this review, we will first provide a brief summary of the used methods and the resulting avoidance rates for each of the relevant studies. Based on these studies, we will then provide advice on the avoidance rate for northern gannet in CRM assessments for wind farms approximately at the latitude of the of the Dutch coastline, comprising of Dutch, Belgian and south English wind farms. Numbers of northern gannets in the southern North Sea are generally thought to be highest in autumn, as birds from Iceland, Faeroe Islands, Norway, UK and Germany move into the area. This review will be appended as a note to the main report of the Luchterduinen avian research on species-specific fluxes, avoidance- and flight behaviour of birds (Leemans *et al.* 2022a).

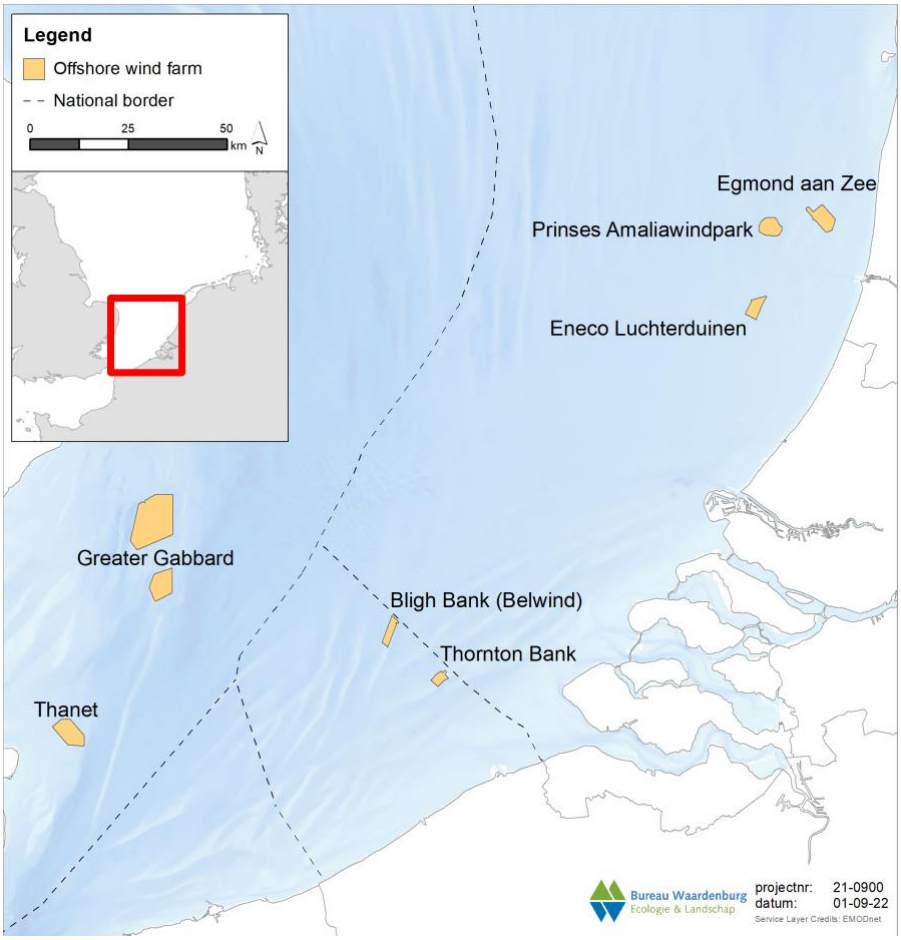

Figure 1. Locations of offshore wind farms at which studies have investigated avoidance rates and are described in this document.

Overview of avoidance studies

This chapter provides an overview of the avoidance rates found for northern gannet in wind farms in the relative vicinity of Luchterduinen (figure 1). In addition, the methods used to determine these avoidance rates are briefly described.

Study: Leemans *et al.* 2022a, b
Country: Netherlands
Wind farm: Luchterduinen
Avoidance rate(s): 0.3657 (macro) / 0.9 (meso)

The macro-avoidance rate of northern gannet found in Luchterduinen is based on visual observations from a wind turbine at the edge of the wind farm. The abundance (number of observations per hour) inside the wind farm is compared with the abundance outside the wind farm. This resulted in a significant macro-avoidance rate of 36.57%. Meso-avoidance was calculated using tagged radar data. The track length density of radar tracks of northern gannet was compared at different distance to wind turbines, resulting in a minimal meso-avoidance rate of 0.9.

Study: Vanermen *et al.* 2016
Country: Belgium
Wind farm: Bligh Bank wind farm (Belwind I)
Avoidance rate(s): 0.82 (macro)

Vanermen *et al.* (2016) provide a Before-After Impact-Control (BACI) analysis to study the displacement of seabirds after the construction of the Bligh Bank wind farm in the Belgium part of the North Sea. Between April 2008 and April 2015, a total of 107 ship-based surveys was performed year-round. The analysis shows that the numbers of gannets decreased with 82% in the impacted area plus 0.5 km buffer. In a buffer zone between 0.5-3 km around the impacted area, the effect on the numbers of gannets was no longer significant.

Study: Vanermen *et al.* 2019
Country: Belgium
Wind farm: Thornton Bank
Avoidance rate(s): 0.98 (macro)

A similar study by Vanermen *et al.* (2019) provide a Before-After Impact-Control (BACI) analysis to study the displacement of seabirds after the construction of the Thornton Bank wind farm in the Belgium part of the North Sea. Between 2005 and 2018, a total of 117 ship-based surveys was performed year-round. The analysis shows that the numbers of gannets decreased with 98% in the impacted area plus 0.5 km buffer. In a buffer zone between 0.5-3 km around the impacted area, the effect on the numbers of gannets was no longer significant.

Study: Krijgsveld *et al.* 2011
Country: Netherlands
Wind farm: Offshore Wind Farm Egmond aan Zee
Avoidance rate(s): 0.64 (macro)

Krijgsveld *et al.* (2011) performed a post-construction study on the effects of the Dutch wind farm Offshore Wind Farm Egmond aan Zee (OWEZ) on flight patterns of birds in the area. Avoidance was based on a total of 405 panoramic scans that were carried out year-round from 2007 to 2009. In total 64% of all gannets did not enter the entire wind farm during their flight. Based on general fluxes at altitudes within the risk-zone of the rotor area, the study reports on a within-wind farm avoidance of 0.976, consisting of a meso- and micro-avoidance rates of respectively 0.66 and 0.93 for all species together (thus not specially for northern gannet).

Study: Leopold *et al.* 2013
Country: Netherlands
Wind farm: Offshore Wind Farm Egmond aan Zee
Avoidance rate(s): 0.74 (macro)

Between 2002 and 2012, Leopold *et al.* (2013) carried out pre- and post-construction ship-based surveys in Offshore Wind Farm Egmond aan Zee. The study found that gannets mostly did not enter the wind farm. While the report does not specifically mention avoidance rates, using the exponential function to calculate an effect size from the model coefficients shows an avoidance rate of approximately 74%.

Study: Leopold *et al.* 2013
Country: Netherlands
Wind farm: Princess Amalia Wind Farm
Avoidance rate(s): 0.93 (macro)

The same study by Leopold *et al.* (2013) also reported on the results of pre- and post-construction ship-based surveys in the Princess Amalia Wind Farm, which is located close to OWEZ. Also here, the study found that gannets mostly did not enter the wind farm. While the report does not specifically mention avoidance rates, using the exponential function to calculate an effect size from the model coefficients shows an avoidance rate of approximately 93%.

Study: Rehfisch *et al.* 2014
Country: United Kingdom
Wind farm: Greater Gabbard
Avoidance rate(s): 0.95 (macro) / 1 (within-wind farm)

In the autumn of 2014, Rehfisch *et al.* (2014) performed four digital aerial surveys to calculate the avoidance rates of northern gannet in the operational Greater Gabbard offshore wind farm, which is located off the coast of East Anglia (United Kingdom) in the southern part of the North Sea. In total, 336 gannets were recorded of which eight birds were recorded within the footprint of the wind farm. This resulted in a change of 95.02% in

the density of gannets inside the footprint compared to the reference area between 4-11 km outside the wind farm. As no birds were recorded within a distance of 359 m from a wind turbine, the data indicated a within-wind farm avoidance of 100%.

Study: Skov *et al.* 2018
Country: United Kingdom
Wind farm: Thanet Wind Farm
Avoidance rate(s): 0.797 (macro) / 0.92 (meso)

The study carried out by Skov *et al.* (2018) was specifically designed to improve avoidance estimates of several seabirds. Data collection took place from 2014 to 2016 in Thanet Wind Farm, which is located off the coast of Kent (United Kingdom) in the southern part of the North Sea. A combination of automated radar measurements and Laser Range Finder data resulted in a total of 1,077 tracks of northern gannet. The track length of these tracks per unit area was 0.797 lower in the wind farm perimeter compared to up to 3 km outside the wind farm. This value was accompanied by a standard deviation of 0.026, or a combined standard deviation of 0.153 when taking into account more sources of uncertainty besides variability in measurements. The study also reported a meso-avoidance rate of 0.9205 (decrease in track length per unit inside rotor-swept zone + 10 m buffer) based on 1,551 tracks recorded by a combination of data from camera and radar (SD: 0.014, combined SD: 0.174). Furthermore, the study reports on a micro-avoidance rate of 0.95 (SD: 0.0128, combined SD: 0.114) for all species together (thus not specially for northern gannet), based on an analysis of video tracks. Combining these avoidance rate results in an overall avoidance of 0.999 (SD: 0.0003, combined SD: 0.003) for northern gannet.

Comparison of avoidance rates

Macro-avoidance

The macro-avoidance rate for northern gannet found in the Luchterduinen study is considerably lower than the macro-avoidance rates found in wind farms in its relative vicinity. As the rate in the Luchterduinen study was based on visual observations, this rate merely reflects the avoidance of gannets close to the wind farm perimeters. This means that individuals that show a macro-avoidance response at greater distances are not included, while the response of northern gannets to offshore wind farms might vary considerably between individuals (Peschko *et al*. 2021). Species such as northern gannet may show a response to wind farms at great distances. Studies on macro-avoidance that examine differences in abundance at greater distances, ideally allowing for other factors influencing abundance or a comparing between pre- and post-construction abundances will provide more accurate input. In collision rate models, macro-avoidance can be seen as a correction of densities measured within a footprint area of a wind farm. Therefore, the studies of Vanermen *et al.* (2016, 2019), Leopold *et al.* (2013) and Rehfisch *et al.* (2014) will be most useful when pre-construction densities are used. The macro-avoidance rates calculated in these studies range from 0.74 to 0.98. On the other hand, the studies of Leemans *et al.* (2022a, b), Krijgsveld *et al.* (2011) and Skov *et al.* (2018) are all based on observations within close distance (<3 km) of the wind farm. Hence, these rates, ranging

from 0.3657 to 0.797, will be most accurate when using post-construction densities in collision rate modelling.

These macro-avoidance ranges indicate considerable variation in the macro-response of northern gannets, depending likely on wind farm configuration (Leopold *et al.* 2013), distance of the wind farm to the coast and colonies (Goodale & Milman 2020; Pollock *et al.* 2021), but also on age composition and sex ratios of the local population (Lane *et al.* 2020; Pollock *et al.* 2021; Hamer *et al.* in prep.), and the season the measurements were carried out (Lane *et al.* 2020), while habituation to existing wind farms cannot be ruled out either (Vanermen *et al.* 2021). In addition, different (analytical) methods to determine the avoidance rates may in itself be a cause of variation. For example, Skov *et al.* (2018) uses radar track-length density as measure of the presence of gannets inside and outside the wind farm. However, the behaviour of individuals is implicitly also incorporated into track-length density, as birds that usually show straight-line flights cause lower track-length densities than birds that, for example, show a circling flight. Thus, if gannets foraged less inside the wind farm, a macro-avoidance rate based on track-length densities is likely to be overestimated.

Meso-avoidance

Meso-avoidance rates for northern gannet were only reported in the studies in Luchterduinen (Leemans *et al.* 2022a, b) and Thanet wind farm (Skov *et al.* 2018). Both rates are nearly identical to each other and imply a strong meso-avoidance response in northern gannets (0.90 and 0.92). Therefore, it is reasonable to assume that such meso-avoidance rate for northern gannet is valid.

Micro-avoidance

No studies report on the micro-avoidance rate for northern gannet. Rehfisch *et al.* (2014) reports a within-wind farm avoidance rate (meso + micro) of 100% for northern gannets, implying a micro-avoidance of 100%. However, the reported rate is based on a limited sample size of four digital aerial surveys. Also, it is clear that collisions of northern gannets in offshore wind farms do occur (Rothery *et al.* 2009, Cook 2021). It is therefore unlikely that a micro-avoidance rate of 100% is completely accurate. Skov *et al.* (2018) report a micro-avoidance rate 0.95 for all species together, while Krijgsveld *et al.* (2011) found a rate of 0.93 for all species together. In Luchterduinen, a micro-avoidance rate of 0.847 was calculated for large gulls (Skov & Tjørnløv 2022). Based on these results, it is reasonable to assume that the micro-avoidance rate of northern gannets will be somewhere between 0.847 and 1.

Recommendations and conclusions

In collision rate modelling for impact assessments of offshore wind farms, it is good practice to consider realistic worst-case scenarios due to the large uncertainties surrounding the models. Therefore, we recommend using the lowest reported macro-, meso- and micro-avoidance rates to calculate overall avoidance of northern gannets. This would imply that if pre-construction densities are used as an input for the CRM, a macro-avoidance rate of 0.74 is appropriate, while a rate of 0.3657 is recommended if post-construction densities in

the immediate vicinity of the wind farm are used (table 1). For meso- and micro-avoidance, rates of respectively 0.9 and 0.847 would be worst-case. Using these rates, overall avoidance rates of 0.996 (pre-construction densities) or 0.990 (post-construction densities) are calculated based on studies in offshore wind farms in the vicinity of Luchterduinen (table 1).

Earlier studies recommended overall avoidance rates for northern gannet of 0.995 (Rehfisch *et al.* 2014, Bowgen & Cook 2018) and 0.989 (Cook *et al.* 2018), while Cook (2021) presents rates ranging from 0.9677 to 0.999 for different levels of macro- and within-wind farm avoidance and different versions of the (stochastic) Band model (either the 'basic' or 'extended' version), including confidence intervals for each rate. For northern gannet, however, these figures are based on estimates from other species-groups. As opposed to these studies, the current review takes into account the most recent species-specific meso-avoidance rates of northern gannet found by Skov *et al.* (2018) and Leemans *et al.* (2022b), being likely to be most relevant figures for use in the North Sea along the Dutch, Belgian and southern English coast.

Table 1. Calculated macro-, meso-, micro- and overall avoidance rates for northern gannet based on studies in offshore wind farms in the vicinity of Luchterduinen, differentiated between using pre- or post-construction densities for collision rate modelling.

Densities	Macro-avoidance	Meso-avoidance	Micro-avoidance	Overall avoidance
Pre-construction	0.74	0.9	0.847	**0.996**
Post-construction	0.3657	0.9	0.847	**0.990**

Considering that avoidance behaviour of northern gannets is likely to be variable depending on several factors (see above), while the outcomes of CRMs are highly sensitive to the avoidance rate, it should be carefully considered in each situation which avoidance rate to use. In that regard, Cook (2021) provide several guidelines to aid the selection of the appropriate avoidance rate, for instance for different types of collision risk models, and types of flight height distributions. Moreover, Cook (2021) also stresses that using site specific values in modelling exercises are preferred above generic values. This considers for example local flight height profiles and flight speeds but should evidently hold also for avoidance rates.

Our report focuses on location-specific avoidance rates for the northern gannet that could eventually be used in cumulative assessments for wind farms in the southern part of the North Sea, relatively far from breeding colonies of northern gannets. As such, we could use the foraging ranges of northern gannets measured from colonies to define wind farm areas where the overall avoidance rates reported in Table 1 could be used, against the more conservative avoidance rate of 0.989 published by Cook *et al.* (2018). The most recent overview of seabird foraging ranges was obtained by Woodward *et al.* (2019). Based on this study, breeding northern gannets have an average foraging range of 120 km and an average maximum foraging range of 315 km. These distances are depicted on Figure 2, with all currently known potential wind farm developments in the southern North Sea in the coming decade (cf. Collier *et al.* 2022). Following the reasoning that breeding northern

gannets are bound to return to the colony, while also being time-restricted in this period, it is reasonable to assume that birds could make different avoidance reactions to offshore wind farms in the relative vicinity to their colonies. The average foraging distance of 120 km could be considered a cautious threshold to define wind farms in the Southern North Sea that lie in the main foraging areas of breeding northern gannets. Namely, this distance is the mean measured in four different colonies, of which in the most southerly colony, i.e. Bempton Cliffs, the average foraging distance was limited to 43 km (Langston *et al.* 2013). At this site, approximately 70% of all foraging trips occurred within 50 km (Langston *et al.* 2013; see Figure 3), and hence using 120 km as a threshold could be considered as a worst-case approach. There is some evidence that the foraging ranges of northern gannets may be density-dependent (Woodward *et al.* 2019), with greater foraging ranges being associated with larger colonies (Davies *et al.* 2013), which in the North Sea are located along the Scottish coast (see Figure 2), far from wind farm developments in the Netherlands, Belgium and South-England.

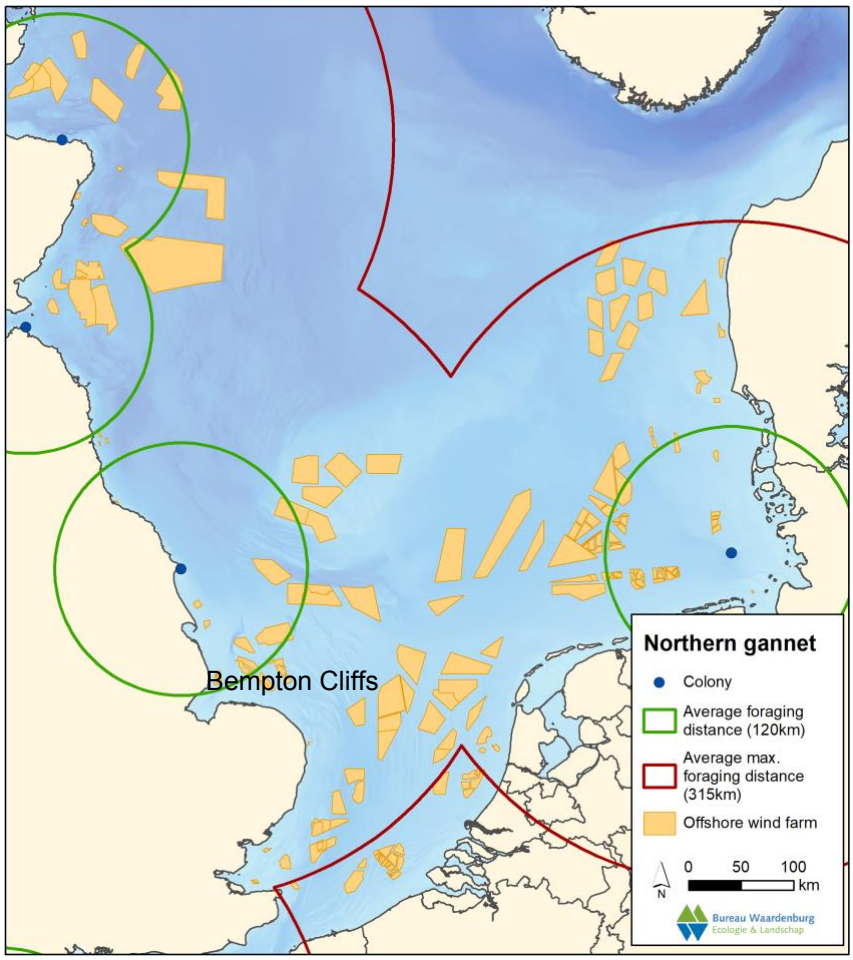

Figure 2. Average and average maximum foraging distances of northern gannets (120 and 315 km) measured from breeding colonies relative to offshore wind farm plans. The most southerly colony, Bempton Cliffs, is the most relevant for wind farms in the Southern North Sea (i.e. along the Dutch, Belgian and South-English coast).

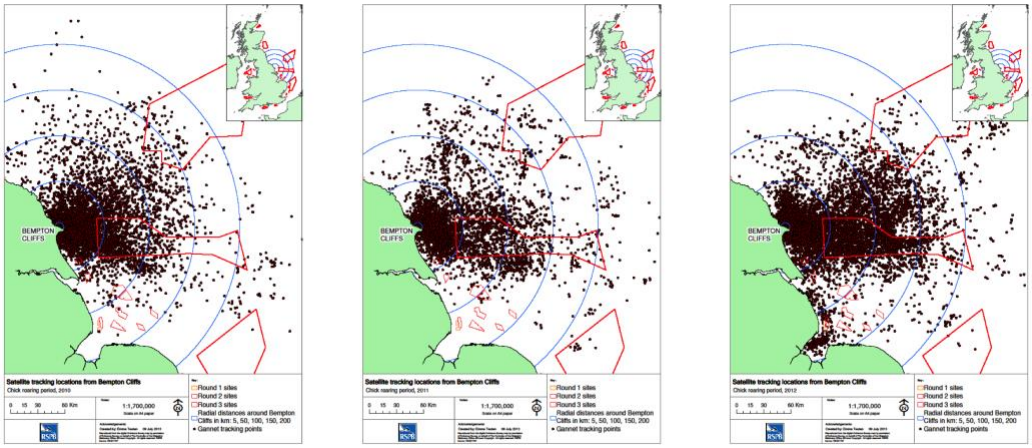

Figure 3. Tracking locations for adult northern gannets from Bempton Cliffs, in 2010 (left panel), in 2011 (middle panel), and in 2012 (right panel) during the chick-rearing period. The concentric blue rings show 50km, 100km, 150km and 200km buffers, to aid interpretation of foraging distances. Inset shows the location of Bempton Cliffs in Great Britain (source: Langston et al. *2013).*

Conclusion

We reason that within the average foraging distance of 120 km from the colonies, northern gannets could show a lower avoidance reaction to wind farms than to ones being farther away, in order to meet energetic requirements of their own and of their offspring in a limited time period. In those wind farms closer to colonies, the more cautious avoidance rate of 98,9% could be used, published by Cook *et al*. (2018). Around wind farms farther away from colonies and outside the breeding period, northern gannets could be expected to show a higher avoidance rate (cf. Rehfisch *et al.* 2014), such as the ones presented in this report (see Table 1).

References

Band, W., 2012. Using a collision risk model to assess bird collision risks for offshore windfarms. SOSS, The Crown Estate, London, UK.

Bowgen, K. & A. Cook, 2018. Bird Collision Avoidance: Empirical evidence and impact assessments. JNCC Report No: 614. JNCC, Peterborough.

Chamberlain, D.E., M.R. Rehfisch, A.D. Fox, M. Desholm & S.J. Anthony, 2006. The effect of avoidance on bird mortality predictions made by wind turbine collision risk models. Ibis 148(1): 198-202.

Collier, M.P., A. Potiek, V. Hin, J.J. Leemans, F.H. Soudijn, R.P. Middelveld & A. Gyimesi, 2022. Northern gannet collision risk with wind turbines at the southern North Sea. Extension of the impact assessment for KEC 4.0, additional analyses of the assessment framework, Rapport 22-052. Bureau Waardenburg, Culemborg.

Cook, A.S.C.P., 2021. Additional analysis to inform SNCB recommendations regarding collision risk modelling. BTO Research Report 739. British Trust for Ornithology, The Nunnery, Thetford, Norfolk.

Cook, A.S.C.P., E.M. Humphreys, E.A. Masden & N. Burton, 2014. The avoidance rates of collision between birds and offshore turbines. BTO Research Report No. 656. British Trust for Ornithology, The Nunnery, Thetford, Norfolk.

Cook, A.S.C.P., E.M. Humphreys, F. Bennet, E.A. Masden & N.H.K. Burton, 2018. Quantifying avian avoidance of offshore wind turbines: Current evidence and key knowledge gaps. Marine Environmental Research 140: 278-288.

Davies, R.D., S. Wanless, S. Lewis & K.C. Hamer, 2013. Density-dependent foraging and colony growth in a pelagic seabird species under varying environmental conditions. Marine Ecology Progress Series 485: 287-294.

Goodale, M.W. & A. Milman, 2020. Assessing Cumulative Exposure of Northern Gannets to Offshore Wind Farms. Wildlife Society Bulletin 44(2): 252-259.

Hamer, K.C., W.J. Grecian & J. Lane, in prep. Fine-scale foraging behaviour of adult and immature northern gannets: distributions, movements and potential interactions with offshore wind-farms.

Krijgsveld, K.L., R.C. Fijn, M. Japink, P.W. van Horssen, C. Heunks, M.P. Collier, M.J.M. Poot, D. Beuker & S. Dirksen, 2011. Effect Studies Offshore Wind Farm Egmond aan Zee. Final report on fluxes, flight altitudes and behaviour of flying birds, Rapport 10-219. Bureau Waardenburg, Culemborg.

Lane, J.V., R. Jeavons, Z. Deakin, R.B. Sherley, C.J. Pollock, R.J. Wanless & K.C. Hamer, 2020. Vulnerability of northern gannets to offshore wind farms; seasonal and sex-specific collision risk and demographic consequences. Marine Environmental Research 162: 105196.

Langston, R.H.W., E. Teuten & A. Butler, 2013. Foraging ranges of northern gannets *Morus bassanus* in relation to proposed offshore wind farms in the UK: 2010-2012. RSPB Report to DECC. The Royal Society for the Protection of Birds, Sandy, Bedfordshire.

Leemans, J.J., R.S.A. van Bemmelen, R.P. Middelveld, J. Kraal, E.L. Bravo Rebolledo, D. Beuker, K. Kuiper & A. Gyimesi 2022a. Bird fluxes, flight- and avoidance behaviour of birds in offshore wind farm Luchterduinen. Bureau Waardenburg Report 22-078. Bureau Waardenburg, Culemborg.

Leemans, J.J., A. Gyimesi, H. Skov & R.S. Tjørnløv, 2022b. Integration of avoidance rates from two bird radar studies in offshore wind farm Luchterduinen. Bureau Waardenburg Report 22-188 Bureau Waardenburg, Culemborg.

Leopold, M.F., R.S.A. van Bemmelen & A.F. Zuur, 2013. Responses of Local Birds to the Offshore Wind Farms PAWP and OWEZ off the Dutch mainland coast. Report number C151/12. Imares, Wageningen.

Masden, E., 2015. Developing an avian collision risk model to incorporate variability and uncertainty. Scottish Marine and Freshwater Science Vol 6 No 14. Scottish Government, Edinburgh.

Masden, E.A., A.S.C.P. Cook, A. McCluskie, W. Bouten, N.H.K. Burton & C.B. Thaxter, 2021. When speed matters: The importance of flight speed in an avian collision risk model. Environmental Impact Assessment Review 90: 106622.

McGregor, R.M., S. King, C.R. Donovan, B. Caneco & A. Webb, 2018. A Stochastic Collision Risk Model for Seabirds in Flight. Marine Scotland.

Piggott, A., A. Vulcano & D. Mitchell, 2021. Impact of offshore wind development on seabirds in the North Sea and Baltic Sea: Identification of data sources and at-risk species. Summary Report. Stichting Birldlife Europe, Birdlife International, Brussels, Belgium.

Pollock, C.J., J.V. Lane, L. Buckingham, S. Garthe, R. Jeavons, R.W. Furness & K.C. Hamer, 2021. Risks to different populations and age classes of gannets from impacts of offshore wind farms in the southern North Sea. Marine Environmental Research 171: 105457.

Potiek, A., J.J. Leemans, R.P. Middelveld & A. Gyimesi, 2022. Cumulative impact assessment of collisions with existing and planned offshore wind turbines in the southern North Sea.

Analysis of additional mortality using collision rate modelling and impact assessment based on population modelling for the KEC 4.0, Rapport 21-205. Bureau Waardenburg, Culemborg.

Rehfisch, M., Z. Barrett, L. Brown, R. Buisson, R. Perez-Dominguez & S. Clough, 2014. Assessing Northern gannet avoidance of offshore windfarms. East Anglia Offshore Wind Ltd, Glasgow.

Rothery, P., I. Newton & B. Little, 2009. Observations of seabirds at offshore wind turbines near Blyth in northeast England. Bird Study 56(1): 1–14.

Skov, H. & R.S. Tjørnløv, 2022. Monitoring bird collisions – meso and micro avoidance at offshore wind farm Eneco Luchterduinen. Final report. DHI.

Skov, H., S. Heinänen, T. Norman, R.M. Ward, S. Méndez-Roldán & I. Ellis, 2018. ORJIP Bird Collision and Avoidance Study. Final report - April 2018. The Carbon Trust, United Kingdom.

Thaxter, C.B., V.H. Ross-Smith, W. Bouten, E.A. Masden, N.A. Clark, G.J. Conway, L. Barber, G.D. Clewley & N.H.K. Burton, 2018. Dodging the blades: new insights into three-dimensional space use of offshore wind farms by Lesser Black-backed Gulls *Larus fuscus*. Marine Ecology Progress Series 587: 247-253.

Vanermen N., W. Courtens, M. Van De Walle, H. Verstraete & E.W.M. Stienen, 2016. Seabird monitoring at offshore wind farms in the Belgian part of the North Sea - Updated results for the Bligh Bank & first results for the Thorntonbank. Rapporten van het Instituut voor Natuur- en Bosonderzoek 2016 (INBO.R.2016.11861538). Instituut voor Natuur- en Bosonderzoek, Brussel.

Vanermen, N., W. Courtens, M. Van De Walle, H. Verstraete & E.W.M. Stienen, 2019. Seabird monitoring at the Thornton Bank offshore wind farm. in (Ed.). *Environmental Impacts of Offshore Wind Farms in the Belgian Part of the North Sea: Marking a Decade of Monitoring, Research and Innovation*. Blz. 85. Royal Belgian Institute of Natural Sciences, OD Natural Environment, Marine Ecology and Management. Brussels.

Vanermen, N., W. Courtens, M. Van De Walle, H. Verstraete & E. Stienen, 2021. Belgian seabird displacement monitoring program. Macro-avoidance of GPS-tagged lesser black-backed gulls & potential habituation of auks and gannets. In: S. Degraer, R. Brabant, B. Rumes & L. Vigin, (Eds.) *Memoirs on the Marine Environment*. Blz. 33. Royal Belgian Institute of Natural Sciences, OD Natural Environment, Marine Ecology and Management, Brussels.

Woodward, I., C.B. Thaxter, E. Owen & A.S.C.P. Cook, 2019. Desk-based revision of seabird foraging ranges used for HRA screening. The British Trust for Ornithology, The Nunnery, Thetford, Norfolk.

For questions regarding this note, please contact Dr. A. Gyimesi.

Signed for publication: Team manager Bureau Waardenburg bv
drs. C. Heunks

Signature:

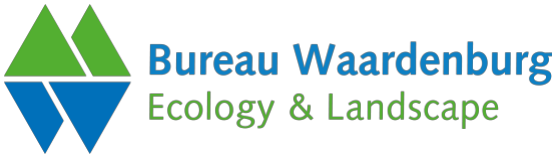

Bureau Waardenburg, Varkensmarkt 9, 4101 CK Culemborg, Netherlands, 0031 (0) 345 512 710, info@buwa.nl, www.buwa.nl

Integration of bird radar studies in offshore wind farm Luchterduinen

J.J. Leemans
R.S. Tjørnløv
H. Skov
A. Gyimesi

WAARDEN BURG

DHI

we consult

Integration of bird radar studies in offshore wind farm Luchterduinen

J.J. Leemans *MSc.*, dr. R.S. Tjørnløv, dr. H. Skov, dr. A. Gyimesi

Status: final report

Report nr:	22-188
Project nr:	18-0178
Date of publication:	28 February 2023
Project manager:	dr. A. Gyimesi
Quality control:	M.P. Collier *MSc.,* R.C. Fijn *MSc.*
Name & address client:	Rijkswaterstaat Water, Verkeer en Leefomgeving Lange Kleiweg 34 2288 GK Rijswijk
Reference client:	RWS-2018/20121 zaaknummer 31140364
Signed for publication:	Team Manager Bureau Waardenburg bv R.C. Fijn *MSc.*

Please cite as: Leemans, J.J., R.S. Tjørnløv, H. Skov & A. Gyimesi, 2022. Integration of bird radar studies in offshore wind farm Luchterduinen. Bureau Waardenburg Report 22-188. Waardenburg Ecology, Culemborg.

Keywords: Robin Radar, wind turbine, avoidance, collision, bird camera, visual observations, North Sea, seabirds

Waardenburg Ecology Varkensmarkt 9, 4101 CK Culemborg, 0345 512710
info@waardenburg.eco, www.waardenburg.eco

Preface

This report includes the results of the integration of two projects carried out using bird radars in offshore wind farm Luchterduinen (LUD). The radar project of Rijkswaterstaat (RWS) is one of the research studies carried out within the Offshore Wind Ecological Programme (Wozep). The other project was initiated by Eneco, the operator of Luchterduinen wind farm, as part of their monitoring and evaluation requirements (MEP-LUD research). The two projects from RWS and ENECO were carried out parallel to each other and the results complement each other. The Danish Hydraulic Institute (DHI) carried out the research for MEP-LUD and is involved as a subcontractor in the RWS research, which was primarily executed by Bureau Waardenburg.

This document reports on the macro-, meso- and micro-avoidance rates found in both projects and determines overall empirical avoidance rates. With these avoidance rates, together with updated values of fluxes and flight speeds, the estimated number of collision victims in wind farm Luchterduinen is calculated for several scenarios and compared to the estimations of the latest version of the Dutch cumulative bird collision assessments of offshore wind farms in the southern North Sea, the so-called Kader Ecologie en Cumulatie (*i.e.* KEC 4.0).

This integration study was commissioned by RWS. This report will be appended to the main report of the Luchterduinen avian research on species-specific fluxes, avoidance- and flight behaviour of birds as part of Wozep (Leemans *et al.* 2022).

Table of contents

1 Introduction

1.1 Background

Recent research in the Ecology and Cumulation Framework (KEC - Rijkswaterstaat 2015, 2019, Potiek *et al.* 2022) and the Environmental Impact Assessments (EIAs) of various offshore wind farms show that substantial numbers of casualties are to be expected among different species of seabirds (especially various gull species and the northern gannet) and migratory birds due to collisions with offshore wind turbines in the southern North Sea. Due to their small natural populations, or because a significant proportion of the flyway population occurs in the southern North Sea, or because a large proportion of the population crosses in concentrated flyways the area during migration between the Netherlands and the UK, some of these bird species are susceptible to additional mortality on top of their natural mortality.

To obtain the best estimates on the numbers of casualties and properly mitigate impacts, it is important to gain knowledge on bird avoidance behaviour, fluxes, flight speeds and flight altitudes in and around offshore wind farms. For collecting such data, specialized bird radars, camera recordings and visual observations are currently the best available methods.

Therefore, RWS has purchased a 3D fixed Robin Radar, consisting of a horizontal Furuno magnetron-based S band radar and a vertical Furuno magnetron-based X band radar (in short: RWS radars). The RWS radars are installed on turbine 42 (*i.e.* WTG 42) of offshore wind farm Luchterduinen (LUD) in August 2018. The aim of the horizontal radar is to detect and track birds within a 6 km scanning range, while the aim of the vertical radar is to detect birds and estimate fluxes within a 1,500 m scanning range. RWS commissioned Bureau Waardenburg to monitor the performance of the radars at LUD, collect supplemental data by visual observations and do analyses on bird behaviour in and around the wind farm, with the main aim to gain knowledge on fluxes, flight behaviour and macro-avoidance.

ENECO, the owner of LUD, has a license obligation to conduct research into bird collisions and fluxes in the wind farm (MEP-LUD research). As part of this obligation, ENECO contracted DHI to do measurements on bird collisions and on meso- and micro-avoidance behaviour. This research used a horizontal radar on the service platform (OHVS) and four cameras on wind turbines. The equipment includes the MUltiSEnsor bird detection system (MUSE) from DHI, developed as a combination of a pan-tilt camera and radar. This camera is activated by digital communication with the radar to turn towards a flying bird, zoom in and focus and continue to track the bird through the wind farm. The installation of this system is carried out in April 2019. The finetuning of the camera settings took longer than expected and the official monitoring period started the 1st of September 2019.

Bureau Waardenburg subcontracted DHI to collaboratively carry out the RWS project, and hence communication between the research teams of the two parallel studies was ensured from the start. Therefore, the two projects could effectively complement and reinforce each

other and thereby provide new knowledge about bird fluxes, number of collisions and (empirical) macro-, meso- and micro-avoidance but also about empirical collision risks. The results aimed to improve estimates of collision casualties but were also intended for developing an early warning system for (future) offshore wind farms to operationalize a stop/start procedure during periods of mass bird migration.

1.2 Research questions

This document reports on the macro-, meso- and micro-avoidance rates found in both projects and combines these rates to determine overall empirical avoidance rates large gulls (such as the lesser black-backed gull and the herring gull) and the northern gannet. These avoidance rates, together with the fluxes and flight speeds measured by the RWS radar were combined with older parameter values to set up a number of scenarios to estimate numbers of collision victims in wind farm Luchterduinen. All these scenarios were compared to the estimations of KEC 4.0 (*cf*. Potiek *et al.* 2022).

2 Methods

2.1 Deployment of the radars

From April 2019 onwards the two radar systems from RWS and ENECO were simultaneously working in the offshore wind farm Luchterduinen. As the two radars are positioned more than three kilometres apart, the main detection areas (approximately 1.5 km; see figure 2.1) supplemented each other:

- The RWS radar was positioned at the edge of the wind farm and had an uninhibited view outside the wind farm and towards the most northern wind turbines.
- The ENECO radar was positioned at the OHVS platform, quite central in the wind farm, providing a good view on bird movements amongst the middle turbine rows.

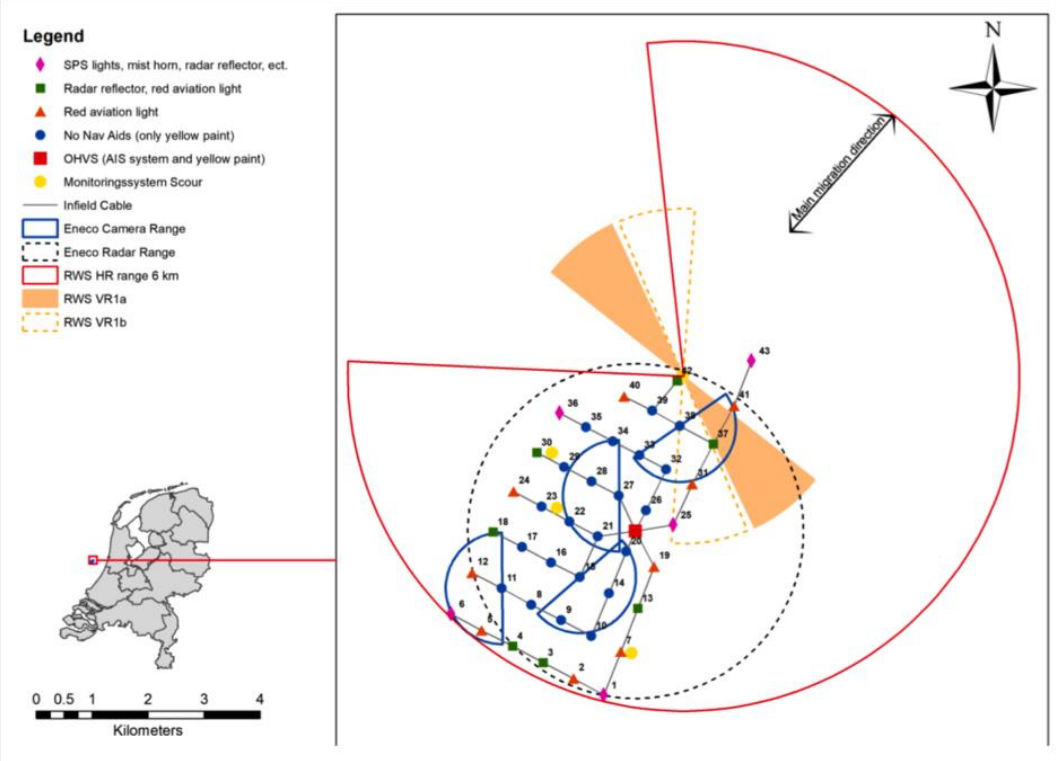

Figure 2.1. Sketch of the positions of the ENECO and RWS radars and the ENECO cameras and their approximate coverage in Luchterduinen.

2.2 Methods

Specifications of both radars and details on the methods for data collection are provided in the main reports (Leemans *et al.* 2022, Skov & Tjørnløv 2022).

2.2.1 Macro-avoidance rates

Species-specific macro-avoidance rates were determined using two different methods. One based on data of tagged radar tracks using the ORJIP methodology (Skov *et al.* 2018)

and the other calculation based on visual observations carried out from wind turbines at the edge of the wind farm.

Radar data (ORJIP methodology)

Macro-avoidance was computed based on a subset of radar tracks that were tagged by observers to provide bird species information (figure 2.2). When consecutive nodes in the same radar track are combined into lines to represent bird flight paths, the total length of these lines can be summarized within a grid of 100x100 m to generate a measure of local species-specific track length densities. Macro-avoidance rates were then calculated by comparing the observed track length density inside the wind farm perimeter with the track density outside the wind farm. Further details on this analysis can be found in Skov *et al.* (2018).

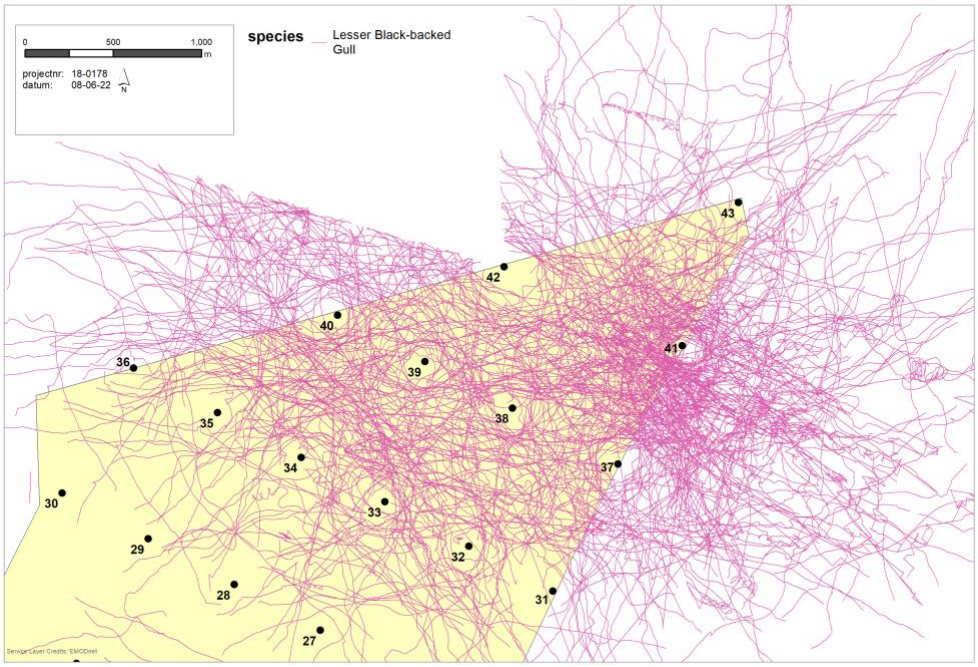

Figure 2.2. Example of tagged radar tracks of lesser black-backed gulls on the RWS radar in and around Luchterduinen wind farm.

Visual observations

Based on visual observations, carried out within and outside the wind farm from WTG 41 and corrected for observation effort, we statistically tested using generalized linear mixed models (GLMM) whether the numbers of birds within the wind farm were significantly different from the numbers outside the wind farm for the 11 most often observed (with at least 50 observations) bird species. We considered the areas included in the observations inside and outside the wind farm to be of the same size as both sides were observed according to the same standard protocol. A separate model was applied per species to assess the effect within species. For further details on this analysis, we refer to §9.1.1 in Leemans *et al.* (2022). The difference between the numbers of birds within and outside the wind farm was used to calculate macro-avoidance rates.

2.2.2 Macro- and meso-avoidance track density profiles

Macro- and meso-avoidance track density profiles were computed based on a subset of radar tracks that had been tagged with species information by a team of bird observers. As described above combining consecutive nodes in the same track into lines to represent bird flight paths, the total length of these lines could be summarized within a grid to generate a measure of local species-specific track length densities. These gridded track length densities were then used to calculate avoidance at different distances from the turbines to determine avoidance profiles.

The analysis of meso- and macro-avoidance profiles was restricted to the area inside and outside the wind farm, respectively, covered by the RWS radar at WTG42. Although macro-avoidance can occur already at several kilometres from an offshore wind farm, we used a sample of species-specific tracks having an initial radar trigger point at least 1,000 m outside the wind farm edge for calculations of macro-avoidance, in order to avoid an apparent distance-bias (i.e. less tracks tagged farther from the wind farm) in the spatial distribution of observations to tag radar tracks. Species-specific meso- and macro-avoidance profiles, computed as a function of distance from the rotor tip of turbines and nearest turbine at wind farm edge, respectively, could then be calculated from the gridded track length densities. By means of model iterations, mean track length densities were computed within a series of distance zones (20 m zone widths for meso-avoidance and 50 m zone widths for macro-avoidance) starting from the outer rotor swept zone (RSZ) +10 m buffer, ending at 330 m for meso-avoidance and 1,000 m for macro-avoidance (zones of interest), respectively.

The relationship between the mean track length density inside a given distance zone and the overall mean track length density (within the zones of interest), was used to calculate species-specific avoidance:

$$\text{Meso/macro-avoidance} = 1 - (N_{in} / N_{ref})$$

where N_{in} is the mean track length density inside the distance zone and N_{ref} is the overall mean track length density within the zones of interest (up to 330 m for meso-avoidance and up to 1,000 m for macro-avoidance, see above).

2.2.3 General meso-avoidance

For the analysis of meso-avoidance, the number of radar tracks/km/hour that intersected a detection line along the width of the rotor-swept zone plus 10 m buffer, was compared with the number of radar tracks/km/hour intersecting segments between wind turbines, using data of the RWS radar. A negative binomial Generalized Linear Mixed Model (GLMM) was fitted, including a category for proximity to the turbine (two levels) and season (four levels), plus their interaction, as response variables. In addition, random intercepts were included for year and date, as well as for segment. Finally, the log of the length of the segment (in km) divided by the number of hours with data was included as an offset, thereby effectively modelling the number of tracks per km per hour. Subsequently, the joint posterior

distributions of the estimates per season were compared between 'close to the turbine' and 'away from the turbines' to show the strength of the effect and whether an absence of an effect could be excluded, *i.e.* when the 95% high density interval (HDI) did not include 0. Further details on this analysis can be found in §10.1.1 of Leemans *et al.* (2022).

2.2.4 Micro-avoidance

Micro-avoidance rates were primarily determined based on videos of birds flying in the rotor-swept zone plus 10 m buffer. It was quantified by calculating the proportion of birds that adjusted their flight path inside this zone. The micro-avoidance rate was thus calculated as (*cf.* Skov & Tjørnløv 2022):

$$\frac{N_{birds\ adjusting\ flight}}{(N_{birds\ adjusting}+N_{birds\ not\ adjusting}+N_{birds\ colliding}}$$

Further details on this analysis can be found in §6.6 of Skov & Tjørnløv (2022).

2.2.5 Overall avoidance rates

The overall avoidance rate is a combination of macro-, meso- and micro-avoidance and defined as the proportion of birds that take effective action to avoid collision with wind turbines. In this report, we calculated the overall avoidance rate in two ways: forwards calculated and backwards calculated.

Forwards calculated

For this calculation, we combined the macro-, meso- and micro-avoidance rates found in the two projects of RWS (*cf.* Leemans *et al.* 2022) and MEP-LUD (*cf.* Skov & Tjørnløv 2022) into overall avoidance rates as follows (*cf.* Cook *et al.* 2018, Skov *et al.* 2018):

Overall avoidance = 1 - ((1 - Macro-avoidance) * (1 - Meso-avoidance) * (1 - Micro-avoidance))

Due to lack of reliable estimates, meso- and micro-avoidance are sometimes presented as within wind farm avoidance (Cook *et al.* 2018). In such case, overall avoidance rate is calculated as:

Overall avoidance = 1 - ((1 - Macro-avoidance) * (1 - Within wind farm avoidance))

Backwards calculated

In the backwards calculations, we determined the overall avoidance based on the number of recorded collisions and number of birds flying through the rotor-swept zone without taking any avoidance action (cf. Skov & Tjørnløv 2022), relative to the average annual within wind farm flux. Although the quality of the collected video data was judged by the video analysts as acceptable during most of the monitoring campaign, the video quality from the cameras seemed to deteriorate during the project. This may have reduced the number of good quality videos during the last part of the monitoring period. Therefore, the

two recorded collisions should be considered as the minimum number and hence also the derived avoidance rates as best-case values. .

The backwards calculations were undertaken using the Band (Basic) model with the turbine and wind farm characteristics of the LUD wind farm, the bird details of lesser black-backed gulls and the annual within wind farm flux per km based on the vertical RWS radar with filtering as Leemans *et al.* (2022), and only including tracks classified as medium or large birds (to represent large gulls), tracks at altitudes between 3-200 m, and tracks during daylight. Furthermore, we corrected this flux for the hours on which the radar was not operational using the mean hourly flux in that month.

2.2.6 Collision Rate Modelling

With the overall avoidance rates as determined in this report and the species-specific estimates of fluxes and flight speeds as presented in Leemans *et al.* (2022), the estimated number of collision victims in Luchterduinen was recalculated and compared to earlier calculations in the KEC 4.0 study (Potiek *et al.* 2022: lesser- and great black-backed gull) or additional calculations as part of the KEC 4.0 study (Soudijn *et al.* 2022: herring gull, Collier *et al.* 2022: northern gannet). Therefore, in line with the KEC 4.0 study, the numbers of collision victims were calculated using the stochastic Collision Risk Model (sCRM), but based on bird fluxes, instead of densities. Specifically, we ran 11 and 7 scenarios respectively for large gulls and northern gannet for each combination of the updated parameter values and parameter values used in the KEC 4.0 study (table 2.1). As bird number input in the calculations, we either used daytime flux at rotor height measured in Luchterduinen wind farm as part of the bird radar research and presented in table 4.2.2 of Leemans *et al.* (2022), or bird densities measured during the Dutch offshore bird monitoring programme (MWTL) presented by Potiek *et al.* (2022) in the KEC 4.0 study. Flight speeds were again taken from these two studies, the one from Luchterduinen presented in table 7.2.1 by Leemans *et al.* (2022). As overall avoidance rates could only be determined for northern gannet, herring gull and great and lesser black-backed gull (see §3.4), the calculations were only done for these four species. Based on the number of birds flying through the rotor-swept zone, we were also able to carry out the backwards calculation of the overall avoidance rate for the three large gull species, and thus we ran scenario 8-11 for these species.

Table 2.1 *Overview of the sources of the updated parameter values in each scenario for modelling the number of collision victims in Luchterduinen. LUD research values are reported by Leemans et al. (2022), while the KEC 4.0 values by Potiek et al. (2022). Avoidance rates presented in this report also rely on measurements in LUD. *) these scenarios were only run for the large gull species.*

Scenario	density/flux	avoidance	flight speed
1	KEC 4.0 density	KEC 4.0	LUD
2	KEC 4.0 density	forwards	KEC 4.0
3	KEC 4.0 density	forwards	LUD
4	LUD flux	KEC 4.0	KEC 4.0
5	LUD flux	KEC 4.0	LUD
6	LUD flux	forwards	KEC 4.0
7	LUD flux	forwards	LUD
8*	KEC 4.0 density	backwards	KEC 4.0
9*	KEC 4.0 density	backwards	LUD
10*	LUD flux	backwards	KEC 4.0
11*	LUD flux	backwards	LUD

3 Results

3.1 Macro-avoidance

3.1.1 Species-specific macro-avoidance rates

Radar data (ORJIP methodology)

Species-specific macro-avoidance rates based on the ORJIP methodology could only be determined for the lesser black-backed gull and the species groups of 'unidentified large gulls' and all 'large gulls' together. The calculations show that within the analysed 1 km zone around Luchterduinen large gulls are attracted to the wind farm, showing macro-avoidance rates of -0.94 to -1.63 (table 3.1).

Table 3.1 Species-specific macro-avoidance rate of large gulls.

Species	macro-avoidance rate
lesser black-backed gull	-1.01
unidentified large gull	-0.94
all large gulls	-1.63

Visual observations

Visual observations of the eleven most often observed bird species showed that for most species generally more birds were recorded outside the wind farm than inside (table 3.2). The exceptions to this rule were great cormorant (48% more observations inside the wind farm), herring gull (40%) and common gull (33%). Moreover, only one more observation of the great black-backed gull was noted outside the wind farm (n = 60) than inside (n = 59). The most numerous species in the study area, the lesser black-backed gull, showed 10% lower numbers inside the wind farm than outside, but this difference was not significant. The species that seemed to avoid the wind farm the most was the Sandwich tern, with 60% less records within the wind farm than outside.

Model estimates of the GLMM showed no significant difference for any of the **gull species** in the presence within and outside the wind farm, which means that based on our visual observations there was no evidence of macro-avoidance. On the other hand, the great cormorant was significantly more abundant within the wind farm than outside. In contrast, several species were significantly more often present outside the wind farm than inside (*i.e.* sings of macro-avoidance), which was the case for **northern gannet**, common guillemot, Sandwich tern and the combined species group of 'razorbill/guillemot'. The difference between inside and outside the wind farm per species expressed in percentages is provided in table 3.2.

Table 3.2 *Summary of the visual observations inside and outside Luchterduinen wind farm. The column 'difference' shows the abundance (number of birds observed per hour) inside the wind farm relative to outside the wind farm. The p-value shows the outcome of the statistical analysis. Significant differences (i.e. p<0.05) are indicated with an asterisk (*). The column 'days' refers to the number of days taken into account in the models. Source: Leemans et al. (2022).*

Species	inside observations	outside observations	total observations	difference	p-value	days
lesser bl.-b. gull	447	498	945	-10.24%	0.82	28
bl.-leg. Kittiwake	195	226	421	-13.72%	0.72	19
great cormorant	220	149	369	47.65%	<0.0001*	39
northern gannet	85	134	219	-36.57%	0.02*	32
razorbill/guillemot	47	92	139	-48.91%	0.02*	20
great bl.-b. gull	59	60	119	-1.67%	0.78	22
common gull	52	39	91	33.33%	0.34	24
common guillemot	24	42	66	-42.86%	0.01*	17
herring gull	35	25	60	40%	0.20	23
sandwich tern	12	30	42	-60%	<0.0001*	11
razorbill	15	19	34	-21.05%	0.87	8

3.1.2 Species-specific macro-avoidance profiles

Based on the measurements of the RWS radar, a macro-avoidance profile was calculated for the **lesser black-backed gull** (figure 3.1). Due to the limited sample size of tagged tracks outside the wind farm for other species, this profile could only be determined for this species. In figure 3.1 positive values indicate that the mean track-length density inside that distance zone is lower than the overall mean, implying an avoidance response, whereas negative values express the opposite (*i.e.* an attraction response). The macro-avoidance/attraction profile suggests that lesser black-backed gulls are attracted to the area <350 m from the edge of the wind farm, while the track-length density is lower than average at distances from approximately 600 m onwards, implying avoidance. However, also these results are potentially biased by unequal effort of tagging radar tracks within the analysed area up to 1 km from the wind farm perimeter.

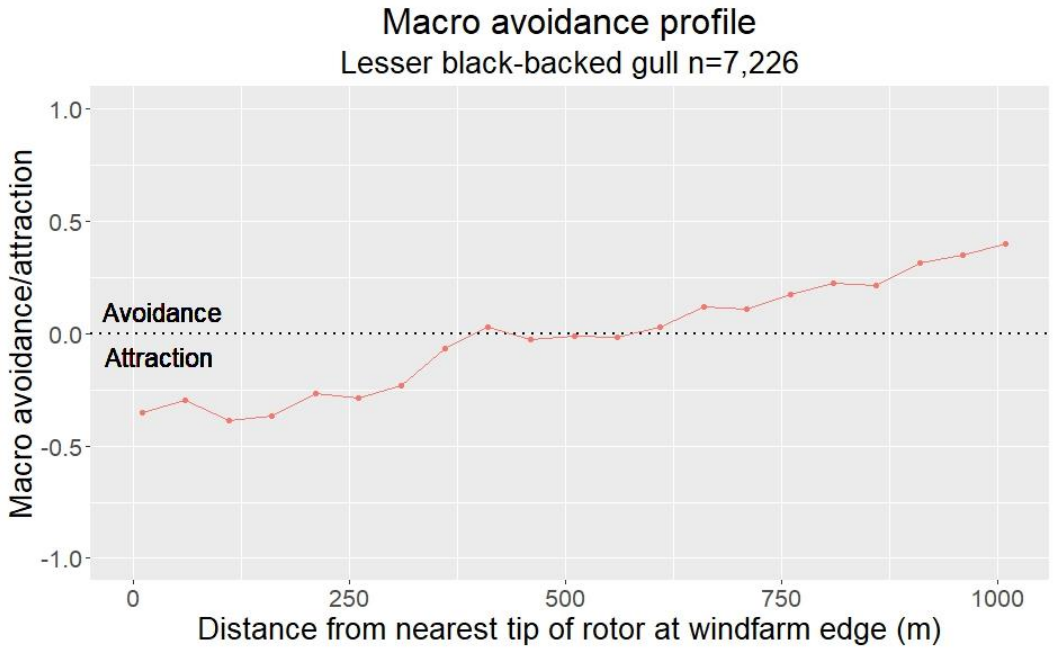

Figure 3.1 *Macro-avoidance/attraction profile of lesser black-backed gull at different distance from the nearest rotor tip of a wind turbine at the wind farm edge. Sample size (n) shows the number of track points.*

3.2 Meso-avoidance

3.2.1 General meso-avoidance rates

Flux was consistently higher away from the turbines compared to segments close to the turbines, in all seasons. This translated into ratios between the two distance categories, indicating meso-avoidance (table 3.3). In all seasons, flux was *ca.* 60% lower close to the turbine than further away, and all 95% HDI of these estimates were clearly above zero (table 3.3).

Table 3.3 *Values above 0 indicate meso-avoidance, with higher flux further away compared to within the turbine zone. Values below 0 indicate attraction, with lower flux further away compared to within the turbine zone. Source: Leemans et al. (2022).*

Season	meso-avoidance rate	lower 95% HDI	upper 95% HDI
Autumn	0.61	0.44	0.75
Winter	0.58	0.41	0.73
Spring	0.59	0.43	0.71
Summer	0.67	0.41	0.87

3.2.2 Species-specific meso-avoidance profiles

Species-specific meso-avoidance/attraction profiles are shown as a function of distance from the turbines for the RWS radar (figures 3.2 and 3.3) and the ENECO radar (figure 3.4). Positive values on the figures indicate that the mean track-length density inside that distance zone is lower than in the zone of interest implying an avoidance response,

whereas negative values express the opposite (*i.e.* an attraction response). The profiles indicate that most of the target species show an increased track-length density in the area between turbine rows at 100-250 m distance from the rotor-swept zone, and express meso-avoidance starting at distances of 50-130 m from the rotor-swept zone.

Based on the RWS radar, **northern gannets** show the strongest meso-avoidance response of all birds with lower track densities of approximately 50%-90% at close distance of the rotor (<50 m). Even more, Skov & Tjørnlov (2022) report that no northern gannets were recorded by the cameras close to the rotor-swept zone, implying a very strong meso-avoidance response of virtually 100%. Therefore, considering the increasing avoidance response at closer distances to the rotor, the meso-avoidance rate of northern gannet is likely to be at least 0.90.

Based on the ENECO radar (figure 3.4), the species groups 'black-backed gulls' and 'unidentified large gulls' show lower tracks densities (at or just above 0.50) at close distance to the turbine, indicating meso-avoidance. Therefore, Skov & Tjørnløv (2022) recommend using a meso-avoidance rate of 0.50 for **large gulls**. Comparably, the meso-avoidance response of large gulls based on the RWS radar lies within a similar range (±0.30-0.70), Based on the RWS radar, herring gulls do not seem to show any meso-avoidance response to turbines. Large gulls (especially herring gull and great black-backed gull), however, may forage on organisms living on the turbine foundation or use the turbines for roosting (Vanermen *et al.* 2019, Skov & Tjørnløv 2022). As such, these species might show attraction at low altitudes and thus simultaneously avoiding flying at rotor height. Please note, that the presented profiles do not take into account such vertical meso-avoidance behaviour (*i.e.* birds either decreasing or increasing their flight height to avoid entering the collision risk zone of the rotor blades). Therefore, a meso-avoidance rate of 0.50 likely reflects a worst-case meso-avoidance behaviour of large gulls in Luchterduinen.

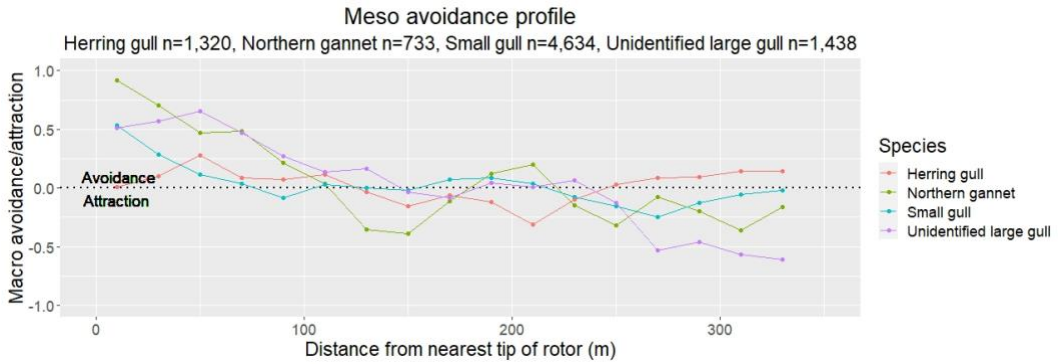

Figure 3.2 *Meso-avoidance/attraction profile of northern gannet, herring gull, small gulls and unidentified large gulls at different distance from the nearest rotor tip of a wind turbines inside the wind farm based on the RWS radar. Sample size (n) shows the number of track points per species.*

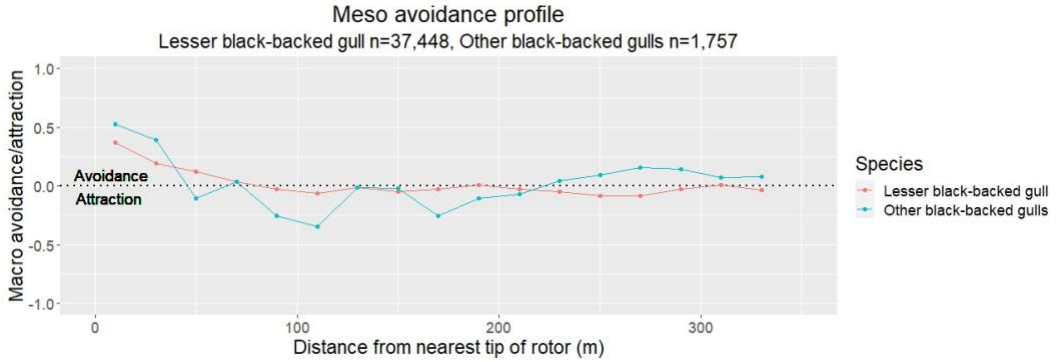

Figure 3.3 *Meso-avoidance/attraction profile of lesser black-backed gulls and unidentified black-backed gulls at different distance from the nearest rotor tip of a wind turbines inside the wind farm based on the RWS radar. Sample size (n) shows the number of track points per species.*

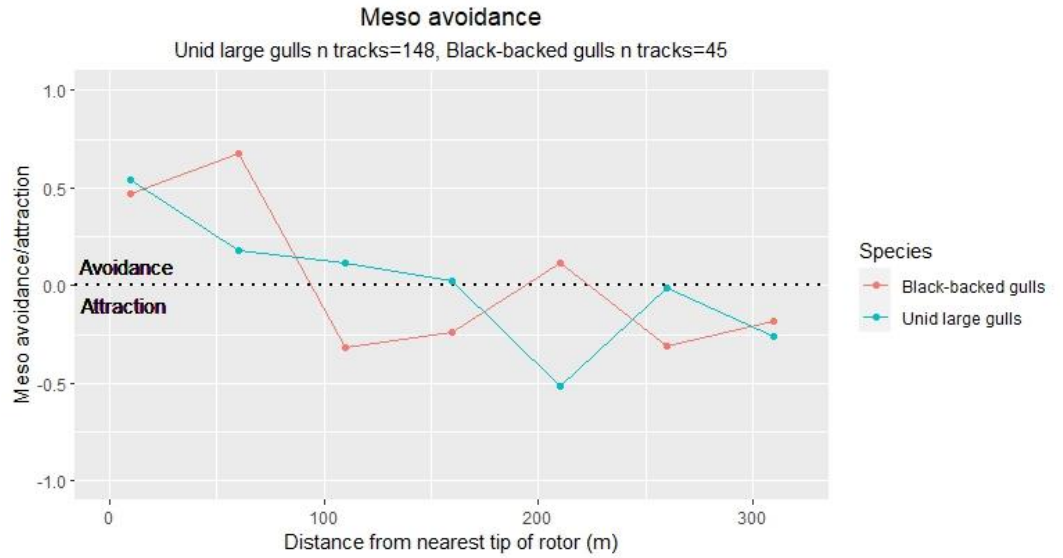

Figure 3.4 *Meso-avoidance/attraction profile of black-backed gulls and unidentified large gulls at different distance from the nearest rotor tip of a wind turbines inside the wind farm based on the ENECO radar. Sample size (n) shows the number of tracks per species. Source: Skov & Tjørnløv (2022).*

3.3 Micro-avoidance

Skov & Tjørnløv (2022) report that large gulls did not show avoidance behaviour on 14% of 108 videos. Two collisions of **large gulls** were recorded (Skov & Tjørnløv 2022). All in all, these results give micro-avoidance rates of respectively 0.950, 0.800 and 0.861 for unidentified large gulls, black-backed gulls and all large gulls (table 3.4). Micro-avoidance rates were not determined by Skov & Tjørnløv (2022) at species level. This considers also **northern gannets**, which were not recorded by the cameras close to the rotor-swept zone, implying a meso-avoidance response of virtually 100% (Skov & Tjørnlov 2022).

Table 3.4 *Species-specific micro-avoidance rate of large gulls based on video data (sample size relates to number of videos) collected between autumn 2019 and summer 2020. Source: Skov & Tjørnløv (2022).*

Species	mean micro-avoidance rate	sample size
unidentified large gulls	0.950	40
black-backed gulls	0.800	45
all large gulls	0.861	108

3.4 Overall avoidance rates

Forwards calculated

Based on the reported macro-, meso- and micro-avoidance rates, we were able to calculate species-specific total avoidance rates for lesser- and great black-backed gull and herring gull (table 3.5). For these gulls, no significant macro-avoidance rate was found, thus no macro-avoidance was assumed in the calculations. This results in a total avoidance rate for black-backed gulls of 0.90 and for herring gull of 0.931.

For northern gannet, the measurements of DHI showed virtually 100% meso-avoidance, meaning that no birds approached the wind turbines to very close distances, and hence no empirical estimate of micro-avoidance could be calculated. A 100% meso-avoidance would lead to a 100% overall avoidance rate, and hence no collisions to occur. Assuming the hypothetical absence of any micro-avoidance by northern gannets would provide a total avoidance rate of 0.937. The actual total avoidance rate will expectedly be higher than this value, but without having an empirical estimate of micro-avoidance the value of 0.937 can be considered as an absolute worst-case avoidance rate. If we assume micro-avoidance of northern gannets to be equal to the average value of large gulls (0.861), the estimated total avoidance rate for northern gannet is 0.991. This latter value is also used in the collision rate modelling in §3.5.

Backwards calculated

Using backwards calculation, we were able to calculate an overall avoidance rate for large gulls (table 3.5). In total, 15 birds flew through the rotor-swept zone without taking any avoidance action (Skov & Tjørnløv 2022), while an average annual within wind farm flux of 120,647 birds per km in Luchterduinen was calculated. With these values, we calculated an overall avoidance rate of 0.989 for large gulls.

Table 3.5 *Summary of species-specific macro-, meso- and micro-avoidance rates, and calculated total avoidance rates found in Luchterduinen. [1] in absence of an empirical estimate of micro-avoidance for northern gannet. [2] assuming micro-avoidance equal to herring gull.*

Species	calculation	macro	meso	micro	total
lesser black-backed gull	forwards	0	0.50	0.80	**0.90**
lesser black-backed gull	backwards				**0.989**
great black-backed gull	forwards	0	0.50	0.80	**0.90**
great black-backed gull	backwards				**0.989**
herring gull	forwards	0	0.50	0.861	**0.931**
herring gull	backwards				**0.989**
northern gannet[1]	forwards	0.3657	0.90	-	**0.937**
northern gannet[2]	forwards	0.3657	0.90	0.861	**0.991**

3.5 Collision Rate Modelling

The estimated numbers of collision victims in Luchterduinen per year for each species in each scenario are shown in table 3.6. The updated values of **forwards calculated avoidance rate** strongly increase the estimated number of collision victims for lesser- and great black-backed gull and herring gull in comparison with earlier KEC estimates (cf. Soudijn *et al.* 2022, Collier *et al.* 2022), while it leads to lower estimates for northern gannet. The **backwards calculated avoidance rates** also lead to increases in the estimated number of collisions among large gulls, although the increases are less strong than when using the forwards calculated rate. Using **fluxes** as calculated by Leemans *et al.* (2022) instead of densities as in the KEC 4.0 study, led to more victims among lesser black-backed gull and herring gull, and less victims among northern gannet and great black-backed gull. The effect of the fluxes on the number of victims is especially strong for lesser black-backed gull (~20x higher) and northern gannet (~10x lower). Note that the fluxes at rotor height only concern daytime fluxes, so any nocturnal activity among the species will even increase the fluxes and hence the number of collisions. In KEC 4.0, respectively 42.5%, 50%, 1% and 8% of nocturnal activity was used for lesser black-backed gull, great black-backed gull, herring gull and northern gannet (Potiek *et al.* 2022). The updated values of **flight speed** do not significantly affect the estimated numbers of collision victims for all species. The combined effect of the updated values with the forwards calculated avoidance rate leads to a very strong increase in the estimated collision victims for lesser black-backed gull (~1000x higher) compared to KEC 4.0.

Table 3.6 *Estimated numbers of collision victims in Luchterduinen per year for each species in each scenario, and the ratio between this number and the number calculated in KEC 4.0 (Potiek et al. 2022: lesser- and great black-backed gull) or additional calculations as part of KEC 4.0 (Soudijn et al. 2022: herring gull, Collier et al. 2022: northern gannet). The second column summarises which parameters are updated in each scenario: 'fs' = flight speed; 'fAv' = forwards calculated avoidance rate; 'bAv' = backwards calculated avoidance rate; 'flx' = flux.*

Scenario	**updated params**	**lesser black-backed gull**		**great black-backed gull**		**herring gull**		**northern gannet**	
		mean	ratio	mean	ratio	mean	ratio	mean	ratio
KEC 4.0	-	3	-	13	-	5	-	29	-
1	fs	4	1.19	14	1.11	5	1.10	29	1.00
2	fAv	176	58	246	20	65	13	23	0.79
3	fAv, fs	175	58	279	22	71	15	24	0.84
4	flx	66	22	7	0.5	8	1.68	3	0.10
5	flx, fs	50	17	8	0.6	8	1.56	3	0.10
6	flx, fAv	3,391	1,122	133	11	113	23	2	0.08
7	flx, fAv, fs	2,514	832	153	12	106	22	2	0.08
8	bAv	21	35	28	16	10	10	-	-
9	bAv, fs	20	11	30	35	11	10	-	-
10	flx, bAv	371	294	15	0.62	18	12	-	-
11	flx, bAv, fs	275	34	17	10	17	11	-	-

4 Discussion

In this report, we combined the macro-, meso- and micro-avoidance rates reported in Leemans *et al.* (2022) and Skov and Tjørnløv (2022) to determine overall avoidance rates for lesser black-backed gull, great black-backed gull, herring gull and northern gannet. Additionally, we carried out a backwards calculation of the overall avoidance rate of large gulls using the number of crossings through the rotor-swept zone in which the birds did not take any avoidance action, together with the annual within wind farm flux in Luchterduinen. With these avoidance rates, together with the fluxes and flight speeds reported in Leemans *et al.* (2022), we calculated the estimated number of collision victims in wind farm Luchterduinen for several scenarios and compared these to the estimations of KEC 4.0 (Potiek *et al.* 2022). In this chapter, we discuss methodological issues how the results of this current study came about and set these results in perspective of earlier studies.

4.1 Comparison to KEC 4.0 results

In the Band model (Band 2012), the flux through the rotor-swept area is multiplied by the risk of collision to get the number of collisions in the absence of any avoidance behaviour. The resulting number is subsequently corrected by multiplication with the avoidance rate. As a result, the ratio between the updated values of (non-)avoidance rates and the values of (non-)avoidance rates used in KEC 4.0 already gives a strong indication of the ratio with which the estimated number of collision victims will change (table 4.1). This argument is confirmed when comparing the ratios presented for scenarios 2 and 8 in table 3.6 (in which only avoidance rate was updated) with the ratios in table 4.1. A similar reasoning holds for the bird density or flux data. For example, twice as high fluxes will also lead to approximately double the number of collision victims. On the contrary, flight speed does not have such a linear relationship with the number of collisions, as flight speed is incorporated in the model in two aspects. First, flight speed is used to calculate the collision risk, which implies that a higher flight speed (through the rotor-swept area) decreases the chance of collision. However, the model transforms (stationary) bird densities into (directional) fluxes through multiplying densities by a time period and flight speed (Band 2012). Hence, a higher flight speed will also lead to higher fluxes and thus to more collisions.

Table 4.1 *Comparison of values for avoidance rate and flight speed (mean ± sd) used in KEC 4.0 (Potiek et al. 2022) and in the current calculations based on measurements in Luchterduinen (LUD). The ratio between avoidance rates is given as the ratio between the non-avoidance rates (1 – avoidance rate), while the ratio between flight speeds is the ratio between the means.*

species	**avoidance rate**			**flight speed**		
	KEC 4.0	this report	ratio	KEC 4.0	LUD	Ratio
lesser black-backed gull	0.998	0.90 / 0.989	50 / 5.5	9.4 ± 3.9	12.3 ± 2.8	1.31
great black-backed gull	0.995	0.90 / 0.989	20 / 2.2	13.7 ± 1.2	13.2 ± 4.9	0.96
herring gull	0.995	0.931 / 0.989	13.8 / 2.2	11.3 ± 3.9	12.8 ± 4.4	1.13
northern gannet	0.989	0.991	0.8	14.9 ± 2.6	14.9 ± 3.4	1

4.2 Methodological issues

Species-specific fluxes used in collision risk models

Due to the linear relationship of both avoidance rate and densities/flux with the estimated number of collisions in Luchterduinen, their combined effect leads to substantially higher collision victims using the updated values compared to the KEC 4.0 values. This holds especially for lesser black-backed gull using the forwards calculated avoidance rate with more than 1000x higher number of estimated collisions than in the KEC 4.0 study. Therefore, it is essential to also understand the uncertainties incorporated in the updated collision risk calculations. For example, the species-specific fluxes are based on radar measurements that may be quickly largely overestimated if clutter due to rain showers enter the radar dataset as bird tracks (Leemans *et al.* 2022), which may be the cause for the high fluxes of lesser black-backed gulls compared to the KEC 4.0 densities. Another possibility is that the relative presence of lesser black-backed gulls at rotor height is overestimated. This may be true if at higher altitudes lesser black-backed gulls are more easily detected by observers than other (smaller) species. For instance, the calculated fluxes only considered seabird species and no migratory landbirds, such as small songbirds. It cannot be excluded that in certain periods of the year large numbers of migratory birds occurred at rotor height. Such large fluxes can peak on a few days during the seasonal migration and may be missed by the 1-2 days of field observations per month and could also be missed by the large-scale radar analyses focussing on seasonal patterns. The fact that for most of the other species the fluxes calculated by Leemans *et al.* (2022) are not higher than in the KEC 4.0 study (see table 4.3.1 in Leemans *et al.* 2022) suggests that an overestimation of lesser black-backed gulls in the species composition at rotor height may be a plausible explanation and it would be worth to investigate whether a further in depth analysis of the radar tracks could confirm this assumption.

On the other hand, the way fluxes are calculated from bird densities in collision risk models, such as the Band model, are also heavily discussed (Masden & Cook 2016). Namely, the model transforms stationary densities into a constant straight flux of birds flying through the wind farm, prone to large overestimations of the actual numbers of birds in flight in the wind farm. Due to the uncertainties both in the radar measurements and in the fluxes based on bird densities, we propose to further investigate through dedicated validation observations the actual fluxes at rotor height in offshore wind farms and corresponding bird densities, and how these relate to measured radar fluxes and flux rates calculated by the Band model.

Pre- and post-construction measurements

The densities used in KEC 4.0 are based on long-term bird surveys and hence are more robust to yearly fluctuations. However, these long-term bird survey data are mainly collected in years before the construction of Luchterduinen and may therefore less accurately reflect the current post-construction densities in the wind farm. Hence, the densities used in KEC 4.0 are most appropriate for use in pre-construction wind farm assessments. For post-construction collision rate modelling it would be advisable to use accurate within wind farm fluxes or post-construction densities. Another option for determining post-construction collision rates is to correct for the pre-construction densities with macro-avoidance rates. However, Leemans *et al.* (2022) did not find any evidence for macro-avoidance among the gull species, and also the results of Krijgsveld *et al.* (2011),

Thaxter *et al.* (2018) and Vanermen *et al.* (2022) do not represent any consistent macro-avoidance response of large gulls either. On the contrary, these gull species may even be attracted to offshore wind farms, although Leemans *et al.* (2022) could not significantly prove that either. All in all, based on the results we cannot conclude that large gulls show either general avoidance- or attraction behaviour to offshore wind farms. Alternatively, it may also be that for large gulls you cannot talk about general species-specific avoidance or attraction, but that *individuals* within a species react in a different way to wind farms: some may avoid these structure, while others may be even attracted to them (cf. Vanermen *et al.* 2022). If no major macro-avoidance occurs, the pre-construction densities used in KEC 4.0 could be fairly representative for the current densities of large gull species (*i.e.* post-construction) occurring inside Luchterduinen. This again may indicate that the high fluxes of lesser black-backed gulls presented in Leemans *et al.* (2022) may be an overestimation of the actual flux. Or alternatively, that the numbers of lesser black-backed gulls have greatly increased in and around Luchterduinen in the most recent years, a hypothesis that could be tested by dedicated analysis of aerial surveys of different periods.

Contrary to the large gull species, Leemans *et al.* (2022) found a significant macro-avoidance response for northern gannet, which is in line with multiple other studies (see Leemans & Gyimesi 2022). As the avoidance rate in Leemans *et al.* (2022) was based on visual observations, this rate merely reflects the avoidance of gannets close to the wind farm perimeters, while northern gannet may show a response to wind farms even at greater distances. Moreover, the macro-avoidance rate of northern gannet as reported in Leemans *et al.* (2022) is measured in an existing wind farm, and hence will only be useful when using post-construction densities in collision rate modelling. In contrast, for future wind farm developments only pre-construction densities of birds are available. In order to be able to model the number of collisions in such future wind farms, we need to better understand whether there is also a fraction of birds that will completely avoid the area where an offshore wind farm is erected. Namely, these birds cannot be measured actively avoiding the wind farm as they may completely abandon the area. Therefore, we generally need more measurements on the fluxes and behaviour of birds in the pre-construction period of offshore windfarms.

The scenarios presented in this study that use the measured within wind farm fluxes as input, are likely underestimates of the number of collisions among northern gannets. This is because in these scenarios the within wind farm fluxes already implicitly incorporate macro-avoidance and are subsequently corrected by an overall avoidance rate that also contains macro-avoidance. On the other hand, the visual observations on macro-avoidance are also likely to be biased by unequal effort of tagging radar tracks. Namely, macro-avoidance can take place at several kilometres from the wind farm, and we cannot reasonably assume that visual detection of birds is equally possible across all distances (*i.e.* tracks close to the observers were more likely to be tagged). Comparably, the numbers of collision victims of northern gannets in scenarios combining KEC 4.0 densities with the updated avoidance rate are likely overestimated, as these densities should ideally be corrected for a macro-avoidance rate that is based on studies examining differences in abundance at greater distances to the wind farm or comparing pre- and post-construction abundances (Leemans & Gyimesi 2022).

The micro-avoidance rates found by Skov and Tjørnløv (2022) are substantially lower than the rates found in similar studies such as Skov *et al.* (2018) and Tjørnløv *et al.* (2021). As a result, also the within wind farm avoidance rates of large gulls are substantially lower than those reported by Cook *et al.* (2018). The latter study reported within wind farm rates for large gulls of more than 0.995 and specifically for lesser black-backed gull a rate of 0.998, while we found within wind farm rates of 0.9 for black-backed gulls and 0.931 for herring gull using the forwards avoidance calculation. This means that we found 13-50 times lower within wind farm avoidance rates for large gulls in offshore wind farms than the rates reported by Cook *et al.* (2018). One major limitation of values presented by Cook *et al.* (2018) is that those were based on data from terrestrial sites along the coast, rather than a truly offshore site as our study. This could mean that large gulls have a lower micro-avoidance rate along the coast offshore, which should be further investigated. However, improvements of the quality of the cameras used offshore in a follow-up study will also shed a light on how reliable our currently reported micro-avoidance rates are.

We have determined overall avoidance rates in two different ways: by forward- (*i.e*. based on the measured micro-, meso- or macro-avoidance) and backward calculations (*i.e*. based on the number of birds entering the rotor-swept zone and the recorded collisions). When using the forward method, the calculations resulted in an overall avoidance rate of 0.90 for large gulls, while by using the backwards calculation method in an overall avoidance rate of 0.989. Our results generally supported the theory that large gulls do not seem to show macro-avoidance behaviour of offshore wind farms. Consequently, their within wind farm avoidance should be considered equal to the overall avoidance rate. Of our two calculated overall avoidance rates, 0.989 is more in line (although still lower) with the rates reported in earlier studies and summarized by Cook *et al.* (2018) as 0.995 and 0.992, respectively for the lesser black-backed gull and the herring gull.

The measured within wind farm avoidance rates comprised of the components of meso- and micro-avoidance. Due to the small sample size and quality of videos, the measured micro-avoidance rates are thought to be less reliable than the measured meso-avoidance rate that we found for large gulls (0.5). In combination with the expectedly more reliable (see previous paragraph) backwards calculated overall avoidance rate of 0.989, results in a calculated micro-avoidance rate of 0.978. This micro-avoidance rate better resembles the rates found in similar studies of 0.9565 (Skov *et al.* 2018) and 0.938-0.944 (Tjørnløv *et al.* 2021) Therefore, we believe that backwards calculated micro-avoidance rate of 0.978 might be more reliable for large gulls than the measured micro-avoidance rates of 0.8 and 0.861 reported in table 3.5 respectively for the black-backed gulls and the herring gull. Moreover, if we assume that the micro-avoidance behaviour of northern gannet should be at least similar to that of large gulls, the overall avoidance rate of northern gannet would also be higher than 0.991. Using better cameras would enable improving both sample size and quality of videos in future studies aiming to monitor bird behaviour within wind farms, based on which more reliable estimates of micro-avoidance- and collision rates can be established.

5 Conclusion

The current report integrates the results of two bird radar studies in offshore wind farm Luchterduinen to determine overall species-specific avoidance rates for four species. Generally, macro-avoidance responses found in this study are in line with other studies. However, the micro-avoidance rates of large gulls observed in Luchterduinen are substantially lower than the rates found in similar studies, and hence also the within wind farm rates of large gulls are substantially lower than those recommended for use by Cook *et al.* (2018). This may be caused by differences in the circumstances under which the avoidance rates were measured, such as location -specific (*e.g.* distance of the wind farm to the coast or breeding colonies) or time-specific (*e.g.* breeding vs. non-breeding period, number of birds present in a certain year) differences. However, quantifying exact levels of avoidance is notoriously difficult, and hence the results of different studies on avoidance rates of seabirds show also substantial variation. Nevertheless, our lower levels of micro-avoidance compared to such reviews relying on multiple studies could also indicate that the overall avoidance rates (of large gulls) presented in this report are an underestimation. This statement is supported by the backwards calculated overall avoidance rate, which resulted in micro-avoidance rates that are more in line with previous studies. Based on this, we recommend the use of the backward calculated avoidance rates of this study, which could be representative to an offshore wind farm relatively close to the coast (25 km) and breeding colonies. In the case of Luchterduinen this latter holds for lesser black-backed gulls and herring gulls, but not for great black-backed gulls and northern gannets, which may show different avoidance rates close to colonies (cf. Leemans & Gyimesi 2022).

Subsequently, the overall avoidance rates found in this study were used, together with updated values of fluxes and flight speed, to calculate the number of collision victims in Luchterduinen using the stochastic Band model. The results show that variation in the densities/fluxes and avoidance rates as input parameters for the model may lead to significant variation in the estimated yearly collision figures. This variation is of such extent that for some species it would lead to different conclusions on the population impacts of collision mortality. As avoidance rates have a significant effect on the outcomes of collision risk models but are extremely difficult to measure, we stress the importance of using locally-measured avoidance rates, or in the absence of those, studies that are based on the results of multiple studies (like is done in Cook *et al.* 2018 and Leemans & Gyimesi 2022) in order to account for the large variation that exists in measured avoidance rates. Furthermore, we argue that while using location-specific bird numbers remains evident, it is particularly important to measure these bird numbers both in the pre- and post-construction period, in order to better understand how macro-avoidance influences the bird fluxes entering a wind farm. Namely, our study indicates that measured macro-avoidance rates in the post-construction period do not comply with the use of collision risk models. Furthermore, our results also show that using different combinations of pre-and post-construction bird numbers (*i.e.* fluxes or densities) with avoidance rates can provide extraordinary variation in the outcome of the collision risk models. In addition, if pre-construction densities are available, future work should concentrate on how these translate into bird fluxes (numbers of birds passing through a wind farm) that are used in collision rate estimates.

References

Band, W., 2012. Using a collision risk model to assess bird collision risks for offshore windfarms. SOSS, The Crown Estate, London, UK.

Collier, M.P., A. Potiek, V. Hin, J.J. Leemans, F.H. Soudijn, R.P. Middelveld & A. Gyimesi, 2022. Northern gannet collision risk with wind turbines at the southern North Sea: Extension of the impact assessment for KEC 4.0, additional analyses of the assessment framework. Bureau Waardenburg Rapportnr. 22- 052. Bureau Waardenburg, Culemborg.

Cook, A.S.C.P., E.M. Humphreys, F. Bennet, E.A. Masden & N.H.K. Burton, 2018. Quantifying avian avoidance of offshore wind turbines: Current evidence and key knowledge gaps. Marine Environmental Research 140: 278-288.

Cook, A.S.C.P., 2021. Additional analysis to inform SNCB recommendations regarding collision risk modelling. BTO Research Report 739. British Trust for Ornithology, The Nunnery, Thetford, Norfolk.

Rijkswaterstaat, 2015. Kader Ecologie en Cumulatie t.b.v. uitrol windenergie op zee Deelrapport B - Bijlage Imares onderzoek Cumulatieve effecten op vogels en vleermuizen. Ministerie van Economische Zaken en Ministerie van Infrastructuur en Milieu, Den Haag.Rijkswaterstaat, 2019. Kader Ecologie en Cumulatie t.b.v. uitrol windenergie op zee, KEC 3.0. Rijkswaterstaat in opdracht van het Ministerie van Landbouw, Natuur en Voedselkwaliteit, Den Haag.Krijgsveld, K.L., R.C. Fijn, M. Japink, P.W. van Horssen, C. Heunks, M.P. Collier, M.J.M. Poot, D. Beuker & S. Dirksen, 2011. Effect Studies Offshore Wind Farm Egmond aan Zee. Final report on fluxes, flight altitudes and behaviour of flying birds, Rapport 10-219. Bureau Waardenburg, Culemborg.

Leemans, J.J. & A. Gyimesi, 2022. Avoidance rates of northern gannet in offshore wind farms in the southern North Sea, Rapport 18-0178/22.06209/AbeGy. Bureau Waardenburg, Culemborg.

Leemans, J.J., R.S.A. van Bemmelen, R.P. Middelveld, J. Kraal, E.L. Bravo Rebolledo, D. Beuker, K. Kuiper & A. Gyimesi, 2022. Bird fluxes, flight- and avoidance behaviour of birds in offshore wind farm Luchterduinen. Bureau Waardenburg Report 22-078. Bureau Waardenburg, Culemborg.

Masden, E.A. & A.S.C.P. Cook, 2016. Avian collision risk models for wind energy impact assessments. Environmental Impact Assessment Review 56: 43-49.

Potiek, A., J.J. Leemans, R.P. Middelveld & A. Gyimesi, 2022. Cumulative impact assessment of collisions with existing and planned offshore wind turbines in the southern North Sea. Analysis of additional mortality using collision rate modelling and impact assessment based on population modelling for the KEC 4.0. Report 21-205. Bureau Waardenburg, Culemborg.

Skov, H. & R.S. Tjørnløv, 2022. Monitoring bird collisions – meso and micro avoidance at offshore wind farm Eneco Luchterduinen. Final report. DHI.

Skov, H., S. Heinänen, T. Norman, R.M. Ward, S. Méndez-Roldán & I. Ellis, 2018. ORJIP Bird Collision and Avoidance Study. Final report - April 2018. The Carbon Trust, United Kingdom.

Soudijn, F.H., C. Chen, A. Potiek & S. van Donk, 2022. Density maps of the herring gull for the Dutch continental shelf. Memo to supplement the seabird assessment reports within KEC (“Kader Ecologie en Cumulatie”) 4.0. Wageningen Marine Research, IJmuiden.

Thaxter, C.B., V.H. Ross-Smith, W. Bouten, E.A. Masden, N.A. Clark, G.J. Conway, L. Barber, G.D. Clewley & N.H.K. Burton, 2018. Dodging the blades: new insights into three-dimensional space use of offshore wind farms by Lesser Black-backed Gulls *Larus fuscus*. Marine Ecology Progress Series 587: 247-253.

Tjørnløv, R.S., H. Skov, M. Armitage, M. Barker, F. Cuttat & K. Thomas, 2021. Resolving Key Uncertainties of Seabird Flight and Avoidance Behaviours at Offshore Wind Farms. Annual report for April 2020 – October 2020. AOWFL.

Vanermen, N., W. Courtens, R. Daelemans, L. Lens, W. Müller, M. Van de walle, H. Verstraete, E.W.M. Stienen & S. Votier, 2019. Attracted to the outside: a meso-scale response pattern of lesser black-backed gulls at an offshore wind farm revealed by GPS telemetry. ICES Journal of Marine Science 77(2): 701-710.

Vanermen, N., R.C. Fijn, E.B. Rebolledo, R.J. Buijs, W. Courtens, S. Duijns, S. Lilipaly, H. Verstraete & E.W.M. Stienen, 2022. Tracking lesser black-backed and herring gulls in the Dutch Delta. Distribution, behaviour, breeding success and diet in relation to (future) offshore wind farms, Rapport 21-318. Bureau Waardenburg, Culemborg.

Bureau Waardenburg bv
Onderzoek en advies voor ecologie en landschap